

TECHNISCHE UNIVERSITÄT MÜNCHEN

DEPARTMENT CHEMIE

LEHRSTUHL FÜR BIOCHEMIE

Structural and functional characterization of the non-mevalonate pathway  
enzymes IspC and IspD in complex with natural and synthetic ligands

**Andrea Christiana Kunfermann**

Vollständiger Abdruck der von der Fakultät für Chemie der Technischen Universität München zur  
Erlangung des akademischen Grades eines

**Doktors der Naturwissenschaften**

genehmigten Dissertation.

Vorsitzender: Univ.-Prof. Dr. Aymelt Itzen

Prüfer der Dissertation: 1. Univ.-Prof. Dr. Michael Groll

2. Univ.-Prof. Dr. Thomas Kiefhaber

Die Dissertation wurde am 03.12.2013 bei der Technischen Universität München eingereicht und  
durch die Fakultät für Chemie am 17.02.2014 angenommen.



*FÜR MEINE ELTERN*



## LIST OF PUBLICATIONS

- “Pseudilins: halogenated, allosteric inhibitors of the non-mevalonate pathway enzyme IspD”  
**Andrea Kunfermann**,\* Matthias Witschel,\* Boris Illarionov, René Martin, Matthias Rottmann, H. Wolfgang Höffken, Michael Seet, Wolfgang Eisenreich, Hans-Joachim Knölker, Markus Fischer, Adelbert Bacher, Michael Groll, and François Diederich.  
*Angew. Chem., Int. Ed.* **2014**, *53* (8), 2235-2239.  
*Angew. Chem.* **2014**, *126* (8), 2267-2272.
- “IspC as target for antiinfective drug discovery: synthesis, enantiomeric separation, and structural biology of fosmidomycin thia isosteres”  
**Andrea Kunfermann**,\* Claudia Lienau,\* Boris Illarionov, Jana Held, Tobias Gräwert, Christoph T. Behrendt, Philipp Werner, Saskia Hähn, Wolfgang Eisenreich, Ulrich Riederer, Benjamin Mordmüller, Adelbert Bacher, Markus Fischer, Michael Groll, and Thomas Kurz.  
*J. Med. Chem.* **2013**, *56* (20), 8151–8162.
- “ $\alpha$ -Substituted  $\beta$ -oxa isosteres of fosmidomycin: synthesis and biological evaluation”  
Karin Brücher, Boris Illarionov, Jana Held, Serena Tschan, **Andrea Kunfermann**, Miriam K. Pein, Adelbert Bacher, Tobias Gräwert, Louis Maes, Benjamin Mordmüller, Markus Fischer, and Thomas Kurz.  
*J. Med. Chem.* **2012**, *55* (14), 6566-6575.
- “Reverse fosmidomycin derivatives against the antimalarial drug target IspC (Dxr)”  
Christoph T. Behrendt,\* **Andrea Kunfermann**,\* Victoriya Illarionova, An Matheussen, Miriam K. Pein, Tobias Gräwert, Johannes Kaiser, Adelbert Bacher, Wolfgang Eisenreich, Boris Illarionov, Markus Fischer, Louis Maes, Michael Groll, and Thomas Kurz.  
*J. Med. Chem.* **2011**, *54* (19), 6796-6802.
- “Synthesis and antiplasmodial activity of highly active reverse analogs of the antimalarial drug candidate fosmidomycin”  
Christoph T. Behrendt, **Andrea Kunfermann**, Victoriya Illarionova, An Matheussen, Tobias Gräwert, Michael Groll, Felix Rohdich, Adelbert Bacher, Wolfgang Eisenreich, Markus Fischer, Louis Maes, and Thomas Kurz.  
*ChemMedChem* **2010**, *5* (10), 1673-1676.

\*Equal contribution of authors.



## TABLE OF CONTENTS

<b>1 INTRODUCTION</b>	<b>1</b>
1.1 The biological role of isoprenoids	1
1.2 The terpene biosynthesis	3
1.2.1 <i>The mevalonate pathway</i>	4
1.2.2 <i>The non-mevalonate pathway</i>	6
1.3 1-Deoxy-D-xylulose-5-phosphate reductoisomerase (IspC)	9
1.3.1 <i>The catalytic mechanism of IspC</i>	9
1.3.2 <i>Fosmidomycin as a natural inhibitor of IspC</i>	12
1.3.3 <i>The crystal structure of IspC</i>	13
1.4 2C-methyl-D-erythritol-4-phosphate cytidylyl transferase (IspD)	15
1.4.1 <i>The catalytic mechanism of IspD</i>	15
1.4.2 <i>The biological importance as herbicidal drug target</i>	16
1.4.3 <i>The crystal structure of IspD</i>	17
1.5 Objectives	20
1.6 References	21
<b>2 SYNTHESIS AND ANTIPLASMODIAL ACTIVITY OF HIGHLY ACTIVE REVERSE ANALOGS OF FOSMIDOMYCIN</b>	<b>31</b>
2.1 Summary	32
2.2 Zusammenfassung	33
2.3 Background	34
2.4 Results and discussion	35
2.4.1 <i>Synthesis of the compounds</i>	35
2.4.2 <i>Photometric activity assays</i>	37
2.4.3 <i>Conclusion</i>	39
2.5 Experimental procedures	39
2.5.1 <i>Enzyme assays</i>	39
2.5.2 <i>Biological evaluation of antiplasmodial activity and cytotoxicity</i>	40
2.5.3 <i>Supporting Information</i>	41
2.6 References	42

<b>3 REVERSE FOSMIDOMYCIN DERIVATIVES AGAINST THE ANTIMALARIAL DRUG TARGET ISPC</b>	<b>45</b>
3.1 Summary	46
3.2 Zusammenfassung	47
3.3 Background	48
3.4 Results and discussion	49
3.4.1 <i>Synthesis of the compounds</i>	49
3.4.2 <i>Photometric in vitro activity assay</i>	50
3.4.3 <i>Structure elucidation</i>	51
3.4.4 <i>In vivo activity assay</i>	54
3.4.5 <i>Conclusion</i>	55
3.5 Experimental section	56
3.5.1 <i>General procedures in synthesis</i>	56
3.5.2 <i>Experimental data for the compounds</i>	56
3.5.3 <i>Crystallization and structure determination</i>	59
3.5.4 <i>Supporting Information</i>	60
3.6 References	61
<b>4 ISPC AS TARGET FOR ANTIINFECTIVE DRUG DISCOVERY</b>	<b>64</b>
4.1 Summary	65
4.2 Zusammenfassung	66
4.3 Background	67
4.4 Results and discussion	68
4.4.1 <i>Synthesis of the compounds</i>	68
4.4.2 <i>Photometric activity assay</i>	68
4.4.3 <i>Crystal structure elucidation of PflspC in complex with 5a</i>	73
4.4.4 <i>Enantiomeric separation of the racemic mixture of 5a</i>	75
4.4.5 <i>Conclusion</i>	76
4.5 Experimental section	77
4.5.1 <i>General procedures in synthesis</i>	77
4.5.2 <i>Gene expression and protein purification</i>	78
4.5.3 <i>Crystallization and structure determination</i>	78
4.5.4 <i>Supporting Information</i>	80
4.6 References	81



<b>5 PSEUDILINS: HALOGENATED, ALLOSTERIC INHIBITORS OF THE NON-MEVALONATE PATHWAY ENZYME ISPD</b>	<b>84</b>
5.1 Summary	85
5.2 Zusammenfassung	86
5.3 Background	87
5.4 Results and discussion	88
5.4.1 <i>In vitro</i> activity assays	88
5.4.2 Crystallization of AthIspD apo and in complex with ligands	90
5.4.3 Halogen bond interaction of the ligands with the enzyme backbone	94
5.4.4 Conclusion	95
5.5 Experimental section	96
5.5.1 <i>In vitro</i> antimalarial activity and cytotoxicity	96
5.5.2 Herbicidal activity of pseudilins	97
5.5.3 Cloning and gene expression of AthIspD protein	97
5.5.4 Purification of the recombinant AthIspD protein	98
5.5.5 Crystallization of AthIspD	98
5.5.6 X-ray structure determination	99
5.5.7 $IC_{50}$ determination	101
5.5.8 Supporting Information	103
5.6 References	103
<b>6 ACKNOWLEDGMENTS</b>	<b>107</b>

## ABBREVIATIONS

3OA	6-Benzyl-5-chloro-7-hydroxypyrazolo[1,5- $\alpha$ ]pyrimidine-3-carboxylic acid
6BC	5-Chloro-7-hydroxy-6-(phenylmethyl)pyrazolo[1,5- $\alpha$ ]pyrimidine-3-carbonitrile
Ac	Acetyl
Acat	Acetoacetyl-CoA thiolase
AMP-PNP	Adenosine 5'-( $\beta,\gamma$ -imido)triphosphate
ATP	Adenosine triphosphate
Bn	Benzyl
calc.	Calculated
CDI	1,1'-Carbonyldiimidazole
CDP-ME	4-Diphosphocytidyl-2C-methyl-D-erythritol
CDP-MEP	4-Diphosphocytidyl-2C-methyl-D-erythritol-2-phosphate
CMP	Cytidine monophosphate
CoA	Coenzyme A
CTP	Cytidine triphosphate
DCC	<i>N,N'</i> -Dicyclohexylcarbodiimide
DMAPP	Dimethylallyl diphosphate
DMF	Dimethyl fumarate
DMSO	Dimethyl sulfoxide
DTT	Dithiothreitol
DXP	1-Deoxy-D-xylulose-5-phosphate
Dxs	1-Deoxy-D-xylulose-5-phosphate synthase
EC	Enzyme commission numbers
EC <sub>50</sub>	Half maximal effective concentration
<i>EclspC</i>	<i>IspC</i> from <i>Escherichia coli</i>
<i>EclspD</i>	<i>IspD</i> from <i>Escherichia coli</i>
EDTA	Ethylenediaminetetraacetic acid
ee	Enantiomeric excess
equiv.	Equivalent
Et	Ethyl
G3P	D-Glyceraldehyde-3-phosphate
GAP	Glycerinaldehyde-3-phosphate
EoH	Enol of hydroxyacetone
EtOAc	Ethyl acetate
FID	Free induction decay
Fd <sub>ox</sub>	Oxidized ferredoxin/ferredoxin
Fd <sub>red</sub>	Reduced ferredoxin/ferredoxin
HEPES	4-(2-Hydroxyethyl)-1-piperazineethanesulfonic acid
HMBPP	1-Hydroxy-2-methyl-2-( <i>E</i> )-butenyl-4-diphosphate
HMG-CoA	3-Hydroxy-3-methylglutaryl-CoA
Hmgr	HMG-CoA reductase

Hmgs	HMG-CoA synthase
HPLC	High performance liquid chromatography
HRMS	High resolution mass spectrometry
HTP	7-Hydroxy[1,2,4]triazolo[1,5- $\alpha$ ]pyrimidine
IC <sub>50</sub>	Half maximal inhibitory concentration
Idi	Isopentenyl diphosphate isomerase
IPP	Isopentenyl diphosphate
IR	Infrared
IPTG	Isopropylthiogalactoside
IspC	1-Deoxy-D-xylulose-5-phosphate reductoisomerase; also Dxr or YaeM
IspD	4-Diphosphocytidyl-2C-methyl-D-erythritol synthase; also YgbP
IspE	4-Diphosphocytidyl-2C-methyl-D-erythritol kinase; also YchB
IspF	2C-methyl-D-erythritol-2,4-cyclodiphosphate synthase; also YgbB
IspG	2C-Methyl-D-erythritol-2,4-cyclodiphosphate reductase; also GcpE
IspH	4-Hydroxy-3-methylbut-2-enyl diphosphate reductase; also LytB
K	Kelvin
KOAc	Potassium acetate
LDH	Lactate dehydrogenase
LB	Lysogeny broth
MEcPP	2C-methyl-D-erythritol-2,4-cyclodiphosphate
Me	Methyl
MeOH	Methanol
MEP	2C-methyl-D-erythritol-4-phosphate
Mdpd	Mevalonate diphosphate decarboxylase
MHz	Megahertz
Mk	Mevalonate kinase
mp	Melting point
MRC-5	Human diploid cell cultures
MtIspC	IspC from <i>Mycobacterium tuberculosis</i>
NADP <sup>+</sup> /NADPH	Nicotinamide adenine dinucleotide phosphate (oxidized/reduced)
NaOAc	Sodium acetate
<i>n</i> -BuLi	<i>n</i> -Butyllithium
NMR	Nuclear magnetic resonance
PDB	Protein Data Bank
<i>Pf</i> IspC	IspC from <i>Plasmodium falciparum</i>
Ph	Phenyl
Pk	Pyruvate kinase
Pmk	Phosphomevalonate kinase
ppm	Parts per million
<i>Pv</i> IspD	IspD from <i>Plasmodium vivax</i>
rt	Room temperature

r.m.s.d.	Root-mean-square deviation
rpm	Rounds per minute
RPMI-1640	Roswell Park Memorial Institute medium
SD	Standard deviation
spp.	<i>Species pluralis</i>
THF	Tetrahydrofuran
TMSBr	Trimethylsilyl bromide
TPP	Thiamine diphosphate
Tris	2-Amino-2-hydroxymethyl-propane-1,3-diol

# 1 INTRODUCTION

## 1.1 The biological role of isoprenoids

Isoprenoids or terpenes are ubiquitous natural products that are present in all living organisms. As common ground, all isoprenoids are based on a branched C<sub>5</sub> skeleton. Due to variable numbers of isoprenoid units as well as rearrangements, cyclizations and/or oxidation of the carbon skeleton, the diversity of the resulting structures is tremendous. The family of terpenes contains more than 30,000 molecular species with a wide variety of functions.<sup>[1,2]</sup> The most studied ones are sterols, e.g. cholesterol (Figure 1.1), which are omnipresent in most eukaryotes, where they act as membrane stabilizers and moreover constitute biosynthetic precursors for bile acids and steroid hormones (e.g. glucocorticoids, estrogens, insect hormones, etc.). Besides the naturally occurring cholesterol, a variety of synthetic analogs are used as contraceptives and for therapeutic reasons. Remarkably, bacteria, beside some exceptions, do not synthesize sterols. However, triterpenoids of the hopane series are comparable molecules that are found in a fair number of eubacteria (Figure 1.1). Due to the structural similarities of eukaryotic sterols and bacterial hopanoids, similar functional roles are denoted. Other terpenoids are carotenoids (Figure 1.1, zeaxanthin), which are present in photosynthesizing organisms, and long acyclic isoprenic chains such as menaquinone, ubiquinone (Figure 1.1), plastoquinone or polyprenols (quinones of the electron transport chains). Actually, the carotenoids lutein and lycopene are listed as oncopreventive agents.<sup>[3,4]</sup> Further terpenoids that fulfill an important role in the metabolism are the lipid-soluble vitamins A, D, E and K. Vitamin A interferes in many processes of the body, such as vision, skin and cellular health, bone metabolism and many more. Vitamin D is involved in the regulation of the calcium and phosphate levels, vitamin E acts as antioxidant and vitamin K is necessary in the blood coagulation and posttranslational modification. However, the most known representatives are the mono-, di- and sesquiterpenes from plant essential oils and resins. Those secondary plant compounds support the plant in attracting insects for pollination and prevent damage by predators. Common examples are linalool, citronellol and geraniol for monoterpenes, taxadiene (precursor of taxol), phytol (Figure 1.1) and abietic acid for diterpenes and finally farnesol and patchoulol for sesquiterpenes. Taxol, a yew toxin, has become one of the most important cytostatic agents for the treatment of malignant tumors such as ovarian and mammary carcinoma.<sup>[5]</sup>

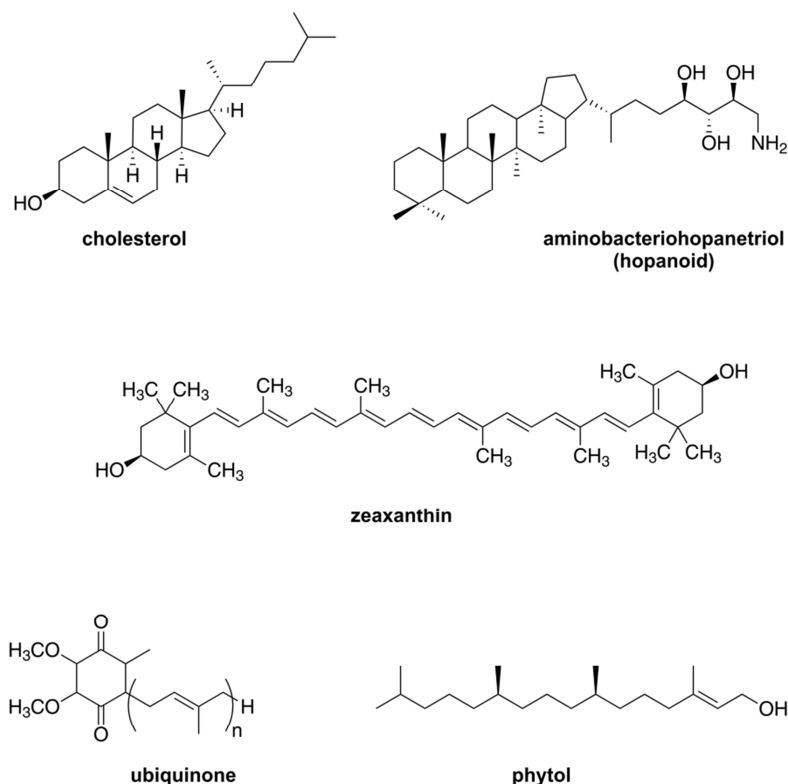


**Figure 1.1** Examples of different terpenes. Eukaryotic steroid: cholesterol, bacterial isoprenoids: aminobacteriohopanetriol and ubiquinone, carotenoids: zeaxanthin (responsible for the yellow color in maize; also present in the retina of animals) and phytol (natural flavor, used for synthesis of vitamin K and E).

The precursors of isoprenoids are the C5-molecules isopentenyl diphosphate (IPP) and its isomer dimethylallyl diphosphate (DMAPP). They can be synthesized via two different pathways (mevalonate/non-mevalonate pathway) that will be discussed in more detail in chapter 1.2. The higher isoprenoid homologues are obtained by condensation of IPP with DMAPP or with other prenyl diphosphates, catalyzed by prenyltransferases (Scheme 1.1). The first condensation reaction of IPP (C5) with DMAPP (C5) leads to a monoterpene (C10). Further condensation of IPP with the monoterpene results in a sesquiterpene (C15) and so forth (Scheme 1.1).



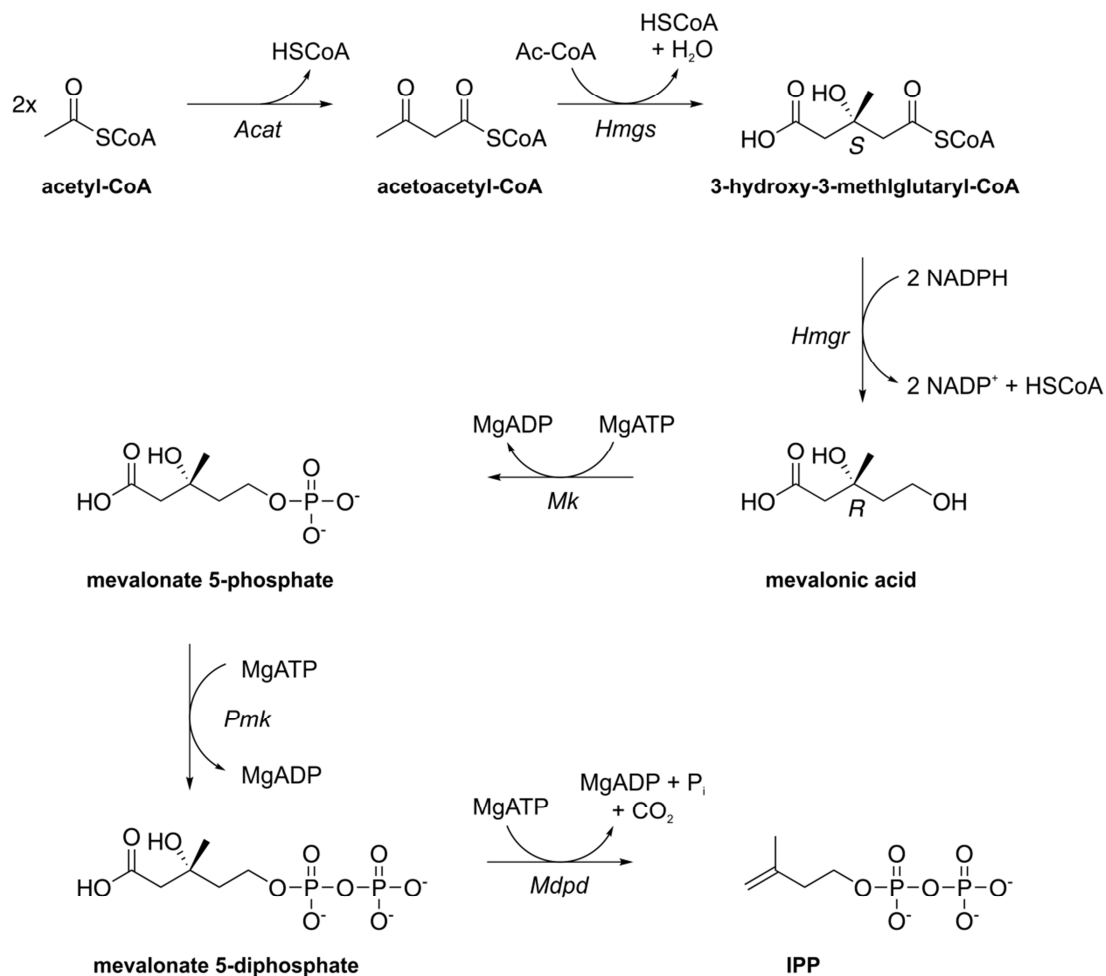
For more than 40 years it was believed that the mevalonate pathway is the unique way for the production of IPP and DMAPP.<sup>[9,11,12,14]</sup> Finally, a mevalonate-independent pathway called non-mevalonate pathway was discovered at the end of the 20<sup>th</sup> century.<sup>[6,15,16]</sup> Alternatively, it is also termed 1-deoxy-D-xylulose-5-phosphate (DXP) or 2C-methyl-D-erythritol-4-phosphate (MEP) pathway (Scheme 1.4). This pathway was first found in eubacteria<sup>[17]</sup> and later also in higher plants<sup>[18,19]</sup> and algae,<sup>[20-23]</sup> as well as in cyanobacteria and diatoms.<sup>[24]</sup> Whereas e.g. plants harbor both pathways, this alternative route of IPP production was found as the unique source in the malarial parasite *Plasmodium falciparum*<sup>[25-27]</sup> and most of the common human pathogens.<sup>[28,29]</sup> Contrarily, in mammals and archaeobacteria as well as e.g. the Gram-positive bacterium *Streptococcus* spp., only the mevalonate pathway is present.<sup>[30-33]</sup> Therefore, the enzymes of the alternative pathway are ideal targets for the development of anti-infective and antimalarial drugs since there are minimal cross-reactions with enzymes of the human body.<sup>[34,35]</sup>

### **1.2.1 The mevalonate pathway**

The mevalonate pathway (Scheme 1.2) begins with a condensation reaction of two molecules of acetyl-CoA leading to acetoacetyl-CoA. The carbon-carbon bond formation of two units of acetyl-CoA is catalyzed by the acetoacetyl-CoA thiolase (Acat, EC 2.3.1.9). Acat is present in the cytoplasm and the peroxisomes.<sup>[36]</sup> There exists a second isoform, which is located in the mitochondria.<sup>[37]</sup> Acetoacetyl-CoA then condenses with the help of the HMG-CoA synthase (Hmgs, EC 2.3.3.10) with another acetyl-CoA to the six-carbon intermediate 3-hydroxy-3-methylglutaryl-CoA (HMG-CoA). The HMG-CoA synthase has also two isoforms. The synthase responsible for HMG-CoA production is localized in the cytoplasm.<sup>[38]</sup> The subsequent reduction step is catalyzed by the HMG-CoA reductase (Hmgr, EC 1.1.1.34) and is the rate-limiting step of the IPP synthesis. HMG-CoA is reduced by two molecules of NADPH to mevalonic acid.<sup>[39,40]</sup> Regulation of this reaction step can influence the downstream products of the terpene biosynthesis as for example cholesterol.<sup>[41,42]</sup> Statins inhibit Hmgr whereby the cholesterol levels in the blood are lowered and they are therefore used for the prevention and therapy of cardiovascular disease.<sup>[41,42]</sup> Atorvastatin, whose active part has structural similarity to mevalonate, is the most successful example of available statins on the international market. Hmgr is transported to the membrane of the endoplasmic reticulum and anchored into the membrane.<sup>[39,40]</sup> Subsequent to the Hmgr reaction, two ATP-dependent phosphorylations take place, catalyzed by the mevalonate kinase (Mk, EC 2.7.1.36) and the phosphomevalonate kinase (Pmk, EC 2.7.4.2), yielding mevalonate 5-phosphate and mevalonate 5-diphosphate,



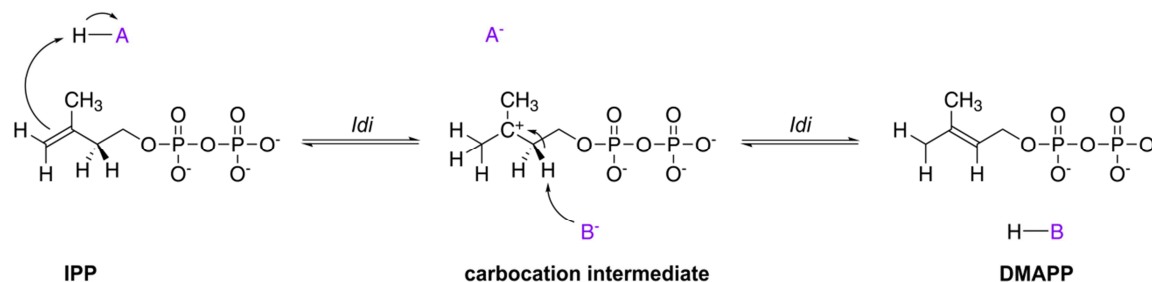
respectively. *Mk* and *Pmk* are cytosolic enzymes, the latter one is also found in the peroxisomes, if the protein has a targeting sequence.<sup>[43,44]</sup> The final step of this pathway is the decarboxylation of mevalonate 5-diphosphate to IPP by the ATP-dependent mevalonate diphosphate decarboxylase (*Mdpd*, EC 4.1.1.33). *Mdpd* is predominantly present in the cytosol, some exceptions are also in the peroxisomes.<sup>[45]</sup>



**Scheme 1.2** Mevalonate pathway for IPP synthesis. *Acat*, acetoacetyl-CoA thiolase; *Hmgs*, HMG-CoA synthase; *Hmgr*, HMG-CoA reductase; *Mk*, mevalonate kinase; *Pmk*, phosphomevalonate kinase; *Mdpd*, mevalonate diphosphate decarboxylase. Modified after Miziorko et al. 2011.<sup>[46]</sup>

The product of the mevalonate pathway, IPP, itself is fairly unreactive. The condensation reaction to form higher isoprenoid homologues would not take place only with IPP. Therefore, IPP must be interconverted to some extent to the more reactive form, its isomer DMAPP.<sup>[47]</sup> This reaction is catalyzed by the isopentenyl diphosphate isomerase (*Idi*, EC 5.3.3.2).<sup>[48]</sup> The proposed

mechanism proceeds by protonation/deprotonation (Scheme 1.3). A proton is added to the inactivated C3-C4 double bond of IPP leading to a transient carbocation intermediate. The removal of the proton from C2 of the intermediate results in the C2-C3 double bond formation and thereby in DMAPP.<sup>[48,49]</sup> As soon as both isoforms are present, the condensation reactions to form higher isoprenoids can be conducted (see also Scheme 1.1).



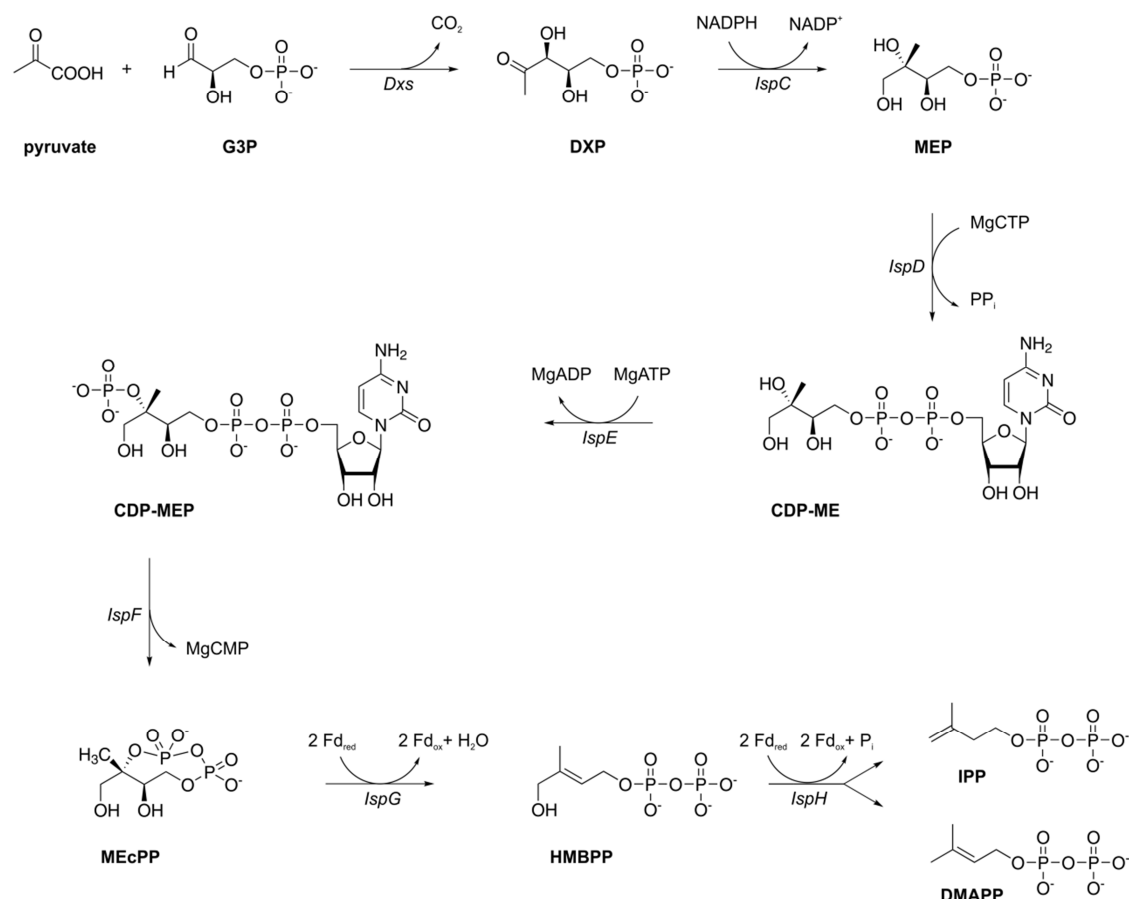
**Scheme 1.3** Isomerization of IPP to DMAPP via the carbocation intermediate catalyzed by the isopentenyl diphosphate isomerase (*Idi*). Modified after Cornforth et al. 1966.<sup>[50]</sup>

### 1.2.2 The non-mevalonate pathway

The first reaction of the non-mevalonate pathway (Scheme 1.4) is catalyzed by the 1-deoxy-D-xylulose-5-phosphate synthase (*Dxs*, EC 2.2.1.7). Hereby, an acetaldehyde moiety derived from pyruvate is transferred to the acceptor D-glyceraldehyde-3-phosphate (G3P).<sup>[51,52]</sup> *Dxs* is a member of the transketolase family and in analogy to those enzymes, *Dxs* uses thiamine diphosphate (TPP) as cosubstrate for the group transfer reaction. Up to now, only two crystal structures of the enzyme from *Escherichia coli* (PDB code 2OIS) and *Deinococcus radiodurans* (PDB code 2OIX) are reported.<sup>[53]</sup> The structures exhibit that *Dxs* forms a homo-dimer, where each monomeric subunit binds TPP and a divalent metal ion (magnesium or manganese).<sup>[53]</sup> The reaction was shown to involve a ping-pong mechanism: pyruvate binds first to the enzyme, CO<sub>2</sub> is released, G3P binds, and finally the product 1-deoxy-D-xylulose-5-phosphate (DXP) is released after conversion.<sup>[54]</sup> Compared to the subsequent enzymes of the non-mevalonate pathway, the catalytic activity of *Dxs* is relatively high with 300–500 μmol mg<sup>-1</sup> min<sup>-1</sup>.<sup>[16,54]</sup> Notably, DXP can also serve as a precursor for the biosynthesis of the vitamins B<sub>1</sub> and B<sub>6</sub>.<sup>[55-57]</sup> Ketoclozazole is a known inhibitor of *Dxs* and acts as an antifungal agent.<sup>[58]</sup>

The subsequent conversion of DXP to 2C-methylerythritol-4-phosphate MEP is catalyzed by the DXP reductoisomerase (*IspC*, *Dxr* or *YaeM*, EC 1.1.1.267) and is the first committed step of the

non-mevalonate pathway. IspC requires a divalent metal ion, preferably magnesium or manganese, and NADPH as cosubstrate. The catalytic reaction involves a skeletal rearrangement of DXP and consecutive reduction step, utilizing NADPH. More details on the reaction mechanism and the enzyme itself will be provided in chapter 1.3.



**Scheme 1.4** Schematic representation of the non-mevalonate pathway. G3P, glyceraldehyde-3-phosphate; DXP, 1-deoxy-D-xylulose-5-phosphate; MEP, 2C-methylerythritol-4-phosphate; CDP-ME, 4-diphosphocytidyl-2C-methylerythritol; CDP-MEP, 4-diphosphocytidyl-2C-methyl-D-erythritol-2-phosphate; MEcPP, 2C-methyl-D-erythritol-2,4-cyclodiphosphate; HMBPP, 1-Hydroxy-2-methyl-2-(E)-butenyl-4-diphosphate; IPP, isopentenyl diphosphate; DMAPP, dimethylallyl diphosphate; Fd<sub>red</sub>, reduced ferredoxin/ flavodoxin; Fd<sub>ox</sub>, oxidized ferredoxin/ flavodoxin. Modified after Eisenreich et al. 2004.<sup>[16]</sup>

In the next step, MEP is converted to 4-diphosphocytidyl-2C-methyl-D-erythritol (CDP-ME) by the 4-diphosphocytidyl-2C-methyl-D-erythritol synthase (IspD or YgbP, EC 2.7.7.60). During the reaction, a phosphocytidyl moiety of CTP is transferred to MEP under formation of CDP-ME and

inorganic diphosphate.<sup>[59]</sup> Depending on the organism, different metal ions are used as cofactor:  $Mg^{2+}$ ,  $Mn^{2+}$  and  $Co^{2+}$  in case of IspD from *E. coli* and additionally  $Ni^{2+}$  ions in case of the plant enzyme. The second cosubstrate, CTP, can be replaced by one of the other nucleotide triphosphates, although the reaction rates are considerably lower.<sup>[59]</sup> More details on IspD can be found in chapter 1.4.

CDP-ME is then phosphorylated at the position 2-hydroxy group by the 4-diphosphocytidyl-2C-methyl-D-erythritol kinase (IspE or YchB, EC 2.7.1.148) under formation of 4-diphosphocytidyl-2C-methyl-D-erythritol-2-phosphate (CDP-MEP) using ATP and  $Mg^{2+}$  as cosubstrate and cofactor.<sup>[60]</sup> The first crystal structure of IspE from *E. coli* in complex with CDP-MEP and the non-hydrolysable ATP analog AMP-PNP was solved in 2003 (PDB code 1OJ4).<sup>[61]</sup> Since the sequence of the enzyme reveals similarities to other ATP-dependent kinases, it is not surprising that the enzyme subunits exhibit an  $\alpha/\beta$ -fold characteristic of the GHMP kinase superfamily (named after four of its members: galactokinase, homoserine kinase, mevalonate kinase and phosphomevalonate kinase).<sup>[16]</sup> The active site of IspE is located at the domain interface in a deep cleft.

The next reaction step is the conversion of CDP-MEP to 2C-methyl-D-erythritol-2,4-cyclodiphosphate (MEcPP) by the 2C-methyl-D-erythritol-2,4-cyclodiphosphate synthase (IspF or YgbB, EC 4.6.1.12) under release of CMP.<sup>[62,63]</sup> The enzyme requires  $Zn^{2+}$ ,  $Mn^{2+}$  or  $Mg^{2+}$  for catalysis. Crystal structures of IspF from *E. coli* in complex with various ligands (PDB codes 1JY8, 1GX1, 1KNJ and 1KNK),<sup>[64-66]</sup> IspF from *Haemophilus influenzae* (PDB code 1JN1)<sup>[67]</sup> and additionally IspF from *Thermus thermophilus* (PDB codes 1V1-4)<sup>[68]</sup> were solved showing that the enzyme forms a homo-trimer. A  $Zn^{2+}$  ion at the active site is coordinated by two conserved histidine residues and one aspartate residue.<sup>[64]</sup> The comparison of various structures with bound substrate and product suggests that the zinc ion controls the position of the substrate at the active site and facilitates the nucleophilic attack of the 2-phosphate group.<sup>[16]</sup> The  $Mg^{2+}$  or  $Mn^{2+}$  ion is responsible for the coordination of the phosphate groups of the cytidine phosphate moiety.

2C-Methyl-D-erythritol-2,4-cyclodiphosphate reductase (IspG or GcpE, EC 1.17.7.1) catalyzes the penultimate step of the non-mevalonate pathway, initiating the reductive ring opening of MEcPP. IspG generates 1-hydroxy-2-methyl-2-(E)-butenyl-4-diphosphate (HMBPP) using a photoreduced deazaflavin derivative as an electron donor.<sup>[69,70]</sup> As cofactor, the enzyme harbors a  $[4Fe-4S]^{2+}$  cluster<sup>[69-71]</sup> that is coordinated by three strictly conserved cysteine residues and a glutamate residue as shown by the crystal structures of IspG from *Aquifex aeolicus* (PDB code

3NOY)<sup>[72]</sup> and from *T. thermophilus* (PDB codes 2Y0F<sup>[73]</sup> and 4G9P)<sup>[74]</sup> published between 2010 and 2012. These structures also exhibited that IspG, apart from herbal origin, forms a homodimer whose monomers consist of a substrate binding domain as well as an additional domain harboring the iron-sulfur cluster.

The final reaction step of the non-mevalonate pathway is the conversion of HMBPP to IPP and DMAPP by the 4-Hydroxy-3-methylbut-2-enyl-diphosphate reductase (IspH or LytB, EC 1.17.1.2). The enzyme generates both IPP and DMAPP at an approximate ratio of 6:1.<sup>[75,76]</sup> Photometric analysis on IspH from *E. coli*<sup>[70,77]</sup> and *A. aeolicus*,<sup>[78]</sup> as well as electron paramagnetic resonance studies on IspH from *E. coli*<sup>[77]</sup> suggested the presence of a [4Fe-4S]<sup>2+</sup> cluster. The first released crystal structure of IspH from *A. aeolicus* (PDB code 3DNF) exhibited a [3Fe-4S]<sup>+</sup> cluster and represented the open conformation of the enzyme.<sup>[79]</sup> In 2009 and 2010 two novelties could be shown in the *E. coli* enzyme: first the closed conformation of IspH displaying an [3Fe-4S]<sup>+</sup> cluster (PDB code 3F7T)<sup>[80]</sup> and second an intact [4Fe-4S]<sup>2+</sup> cluster in IspH (PDB code 3KE8).<sup>[81]</sup>

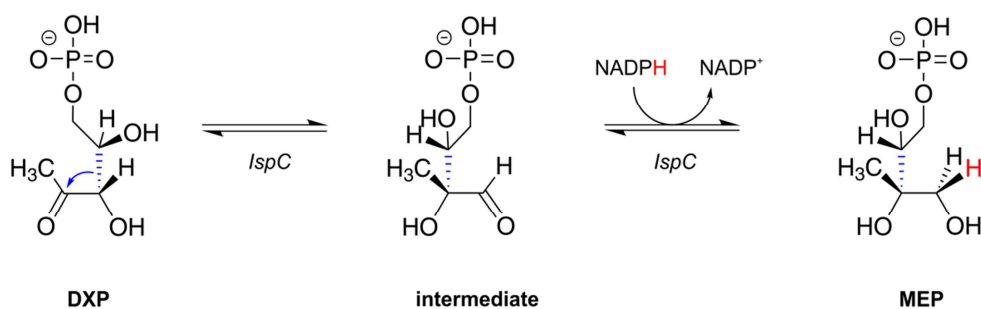
The non-mevalonate pathway genes of plant origin are expressed with N-terminal chloroplast transit peptide sequences, which enable the translocation of the proteins from the cytosol into the chloroplasts.<sup>[82]</sup> In the protozoan *P. falciparum*, the pathway is located at the apicoplast that is equivalent to plant chloroplasts. This compartment was revealed as a stripped down version of a chloroplast, where the photosynthetic pathways had been lost.<sup>[83,84]</sup>

### 1.3 1-Deoxy-D-xylulose-5-phosphate reductoisomerase (IspC)

#### 1.3.1 The catalytic mechanism of IspC

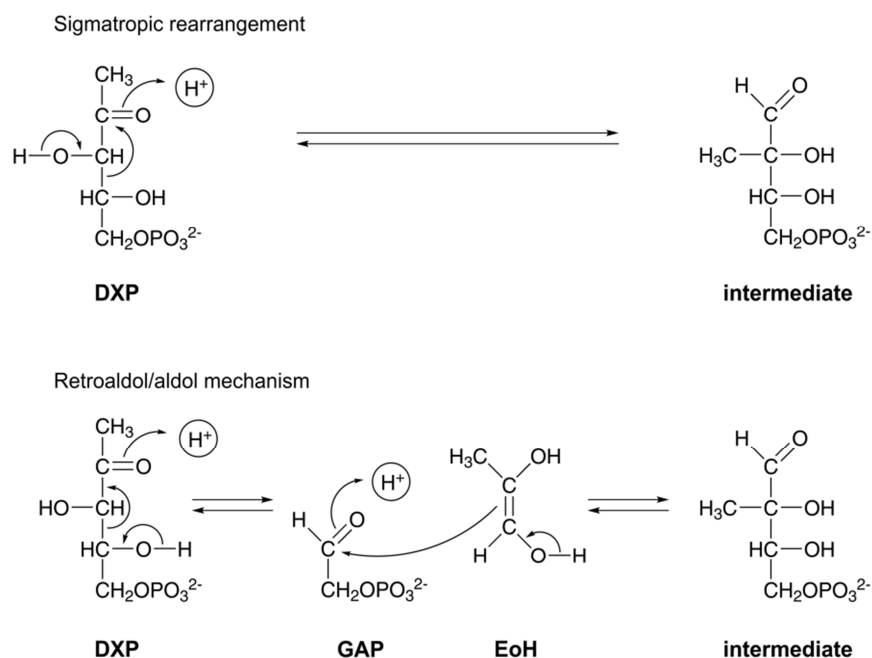
As implied by the systematic name of IspC, the catalytic reaction involves an isomerization and reduction step. IspC requires for its activity a bivalent metal ion (Mn<sup>2+</sup> or Mg<sup>2+</sup>) as well as NADPH for the reduction step.<sup>[85,86]</sup> In the reaction, the enzyme first catalyzes the conversion of the substrate DXP into an intermediate, 2C-methyl-D-erythrose-4-phosphate, a branched aldose.<sup>[86,87]</sup> This intermediate is subsequently reduced to the final product, MEP (Scheme 1.5), while the cosubstrate is oxidized to NADP<sup>+</sup>.<sup>[86]</sup> To confirm that this intermediate aldose is an accepted substrate for IspC, it was synthesized and the turnover was monitored in a <sup>1</sup>H-NMR based activity assay.<sup>[88]</sup> The reaction could be experimentally observed in the forward and the reverse direction.<sup>[88,89]</sup> Compared to Dxs, the catalytic activities of IspC that are in the range of

12  $\mu\text{mol mg}^{-1} \text{min}^{-1}$  seem to be quite low, but they are still higher than some of the activities for the other non-mevalonate enzymes.<sup>[16]</sup>



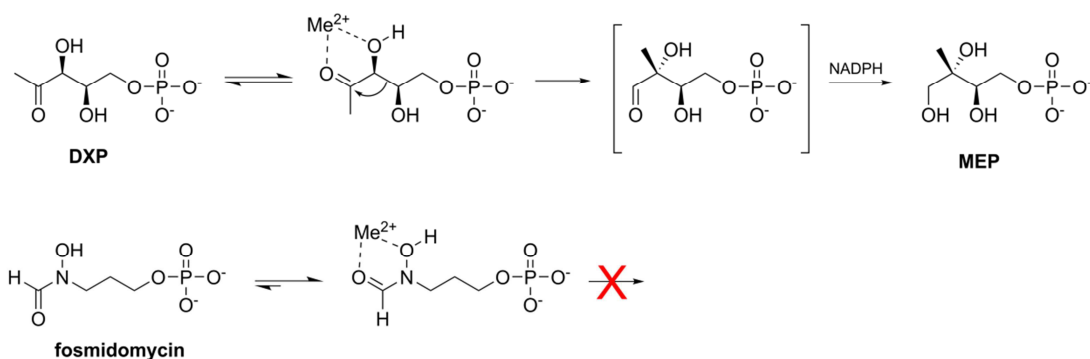
**Scheme 1.5** Schematic representation of the catalytic *IspC* reaction via an intermediate.

*IspC* is categorized as a class B dehydrogenase since it uses the pro-*S* hydride of NADPH.<sup>[90]</sup> The reductive reaction step to form the intermediate was shown to involve a hydride ion attack from the pro-*S* position at C4 of NADPH on the *re*-position of C1 of the reaction intermediate aldehyde.<sup>[90,91]</sup> For the skeletal reorganization catalyzed by *IspC*, two different pathways have been proposed, i.e. a intramolecular sigmatropic/acyloin rearrangement,<sup>[22,92]</sup> vs. a retroaldol/aldol reaction sequence (Scheme 1.6).<sup>[22,93]</sup> The hypothetical retroaldol fragments would fail to exchange with the bulk solvent, requiring extremely strict containment of the cleavage product for the retroaldol mechanism.<sup>[92,94]</sup> However, the retroaldol/aldol hypothesis has been supported by kinetic isotope effect arguments.<sup>[95,96]</sup> Up to now, both, the sigmatropic rearrangement, as well as the retroaldol/aldol reaction sequence are compatible with the available data.<sup>[22,88,92,93,97,98]</sup>



**Scheme 1.6** GAP, glyceraldehyde-3-phosphate; EoH, enol of hydroxyacetone. Modified after Lauw et al. 2008.<sup>[92]</sup>

The catalytic reaction explains the blocking mode of the natural inhibitor fosmidomycin. In the beginning of the IspC catalyzed reaction, the substrate binds very weakly to the active site of the enzyme. Subsequently, the structural rearrangement occurs supported by the metal ion chelation, thereby increasing the binding affinity of the ligand to the active site. In case of DXP, the chelation facilitates the forward reaction and the release of the product, MEP, from the active site. The structural similarity between fosmidomycin and DXP is hereby the basic requirement of the inhibition mechanism by the inhibitor. However, fosmidomycin stays bound to the active site after the isomerization reaction due to its hydroxamic acid moiety (Scheme 1.7).<sup>[99-101]</sup>



**Scheme 1.7** Reaction mechanism of DXP and fosmidomycin at the active site of IspC.  $Me^{2+}$ , divalent metal ion.

### 1.3.2 Fosmidomycin as a natural inhibitor of IspC

Fosmidomycin is a natural inhibitor originating from *Streptomyces lavendulae*.<sup>[102-106]</sup> It has been shown in the late 1990s that IspC is a molecular target for fosmidomycin and its derivative FR-900098.<sup>[25,85,99,107]</sup> It blocks IspC from *E. coli*, *Mycobacterium tuberculosis* and *P. falciparum* *in vitro* and has also an inhibitory effect on these organisms *in vivo*.<sup>[25,108]</sup> Fosmidomycin has been used successfully for the treatment of malaria in small clinical studies, but the relatively high recrudescence rate would not permit its use as a single agent therapy.<sup>[27,109-112]</sup> Hence, fosmidomycin is now under study in combination with artesunate<sup>[113]</sup> or clindamycin.<sup>[26,114,115]</sup> In *M. tuberculosis*, fosmidomycin is inactive at the cellular level due to the lack of uptake.<sup>[116,117]</sup> In contrast, in *P. falciparum*, the inhibitor seems to successfully penetrate several membranes in order to reach the active site of IspC in the apicoplast assuming that IspC is the unique target of fosmidomycin.<sup>[118]</sup>

In recent years, several laboratories worked on analogs of fosmidomycin, thereby trying to further improve its inhibitory potency *in vitro* and *in vivo* as well as its pharmacokinetic properties. Modifications have been made to different parts of fosmidomycin: the carbon linker,<sup>[119-124]</sup> the phosphonate part<sup>[119,125-127]</sup> as well as the hydroxamic acid part.<sup>[119,120,125,126,128-131]</sup> Fosmidomycin has been modified by substituents at the  $\alpha$ -position<sup>[123,124,132-136]</sup> and at the  $\gamma$ -position.<sup>[137]</sup> Crystal structures with such inhibitors were e.g. solved for IspC from *M. tuberculosis* (MtIspC; PDB code 2Y1D).<sup>[136]</sup> Also, in order to disguise the phosphonate group, ester prodrugs have been evaluated.<sup>[120,121,132,133,137-140]</sup> Those inhibitors exhibited improved efficacy *in vivo*.<sup>[139]</sup> In addition, arylphosphonates missing a hydroxamic acid part have been found as IspC



inhibitors.<sup>[141-143]</sup> The mode of action is the same as for fosmidomycin, namely the phosphonate group binds to the phosphonate binding site (PDB codes 3ANL, 3ANM, 3ANN and 3RAS).<sup>[142,143]</sup> It was shown that the analogs of fosmidomycin with the regular hydroxamic acid,<sup>[119,128]</sup> an  $\alpha$ -fluorine<sup>[130]</sup> or a restricted cyclopropyl carbon chain<sup>[124]</sup> possess similar or improved activity compared to fosmidomycin or FR-900098.<sup>[144]</sup> Studies with analogs of fosmidomycin with a “reverse” hydroxamic acid moiety will be provided in chapters 2-4.

### 1.3.3 The crystal structure of *IspC*

The first *IspC* structure was published in 2002 from *E. coli* (*EclspC*) as apo structure (PDB code 1K5H).<sup>[145]</sup> In the same year, the complex structure NAPDH:*EclspC* was determined (PDB code 1JVS).<sup>[100]</sup> One year later, the structure of *EclspC* in complex with  $Mn^{2+}$  and fosmidomycin (PDB codes 1ONO and 1ONP) followed.<sup>[101]</sup> Then, *EclspC* in complex with DXP (PDB code 1Q0Q),<sup>[146]</sup> *IspC* from *Zymomonas mobilis* in complex with NADPH (PDB code 1ROL)<sup>[147]</sup> and *EclspC* in complex with bisphosphonates (PDB codes 1T1R and 1T1S),<sup>[148]</sup> *MtIspC* as apo structure (PDB code 2C82)<sup>[149]</sup> and in complex with fosmidomycin or FR900098 and NAPDH (e. g. PDB codes 2JCV and 4A03)<sup>[150,151]</sup> were published. In 2007, *EclspC* in complex with fosmidomycin and NADPH was also available (PDB code 2EGH).<sup>[152]</sup> Further organisms were published: *Thermotoga maritima* (e.g. PDB code 3A06),<sup>[153]</sup> *P. falciparum* (*PfIspC*; e.g. PDB codes 3AU9 and 4GAE)<sup>[127,154]</sup> and *Yersinia pestis* (PDB code 3IIE, to be published by Osipiuk *et al.*). To date, over 40 *IspC* structures were deposited at the Protein Data Bank (PDB).

### Overall structure of *IspC*

*IspC* forms an elongated homo-dimer with a V-shaped structure in every subunit (Figure 1.2). Each monomer is comprised of three domains. The N-terminal domain binds NADPH and shows a dinucleotide binding motif, also known as Rossmann fold.<sup>[155]</sup> The N-terminal domain of *IspC* contains a seven-stranded parallel  $\beta$ -sheet due to an insertion of an additional  $\alpha$ - $\beta$  motif into its N-terminal Rossmann fold. This N-terminal domain represents the one arm of the V. The central catalytic domain includes the binding site for the divalent metal ion, the binding site for the phosphate of the substrate, as well as a flexible loop. The substrate binding site is covered by the catalytic loop region that is disordered in some crystal structures. The catalytic domain acts as the linker between the two V arms. The C-terminal domain is a four-helix bundle and is connected to the catalytic domain via a linker region that spans the whole monomer. This

domain represents the other arm of the V. Dimer formation is mediated via the catalytic connecting domain.<sup>[145]</sup>

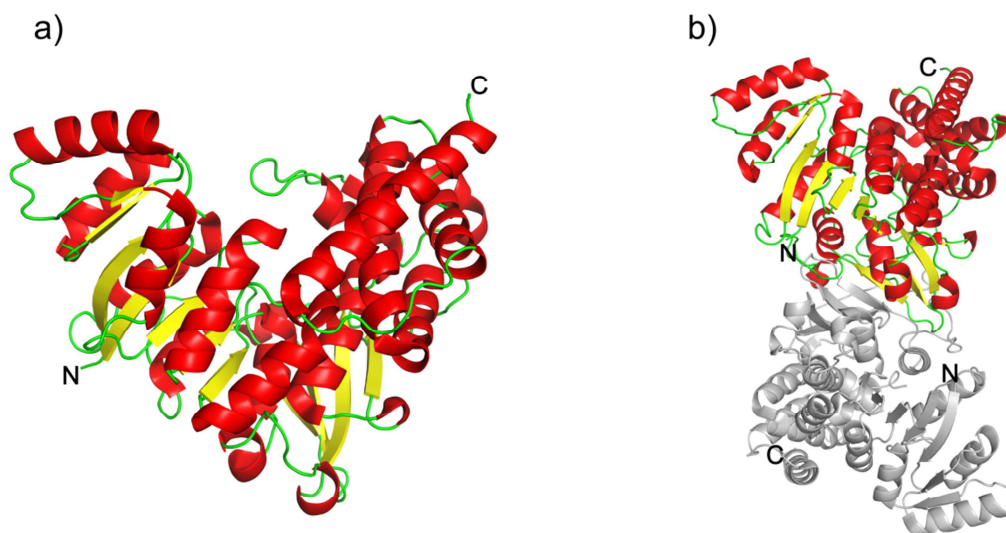


**Figure 1.2** Ribbon plot of *EclspC* (PDB code 1K5H).<sup>[145]</sup> a) Monomer with the typical V-shaped structure. b) Dimer. N- and C-termini are labeled with N and C, respectively.

### Active site

DXP and fosmidomycin show a similar binding mode inside the active site cavity. Since the published substrate-complex structure lacks a divalent metal ion (PDB code 1Q0Q),<sup>[146]</sup> the fosmidomycin-complex structure will be used here for the description of the active site cavity (Figure 1.3). In the apo structure of the enzyme, the metal ion is coordinated by interactions with Asp150, Glu152, Glu231 (*EclspC* numbering for the amino acids) and three additional water molecules in order to form its preferred octahedral coordination.<sup>[145]</sup> However, in the complex structure with fosmidomycin, the oxygen atoms of the hydroxamic acid replace two of the water molecules and thereby further stabilize the metal chelate complex.<sup>[101]</sup> The phosphonate group of DXP as well as fosmidomycin is anchored to a specific pocket by a network of hydrogen bonds including Ser186, Ser222, Asn227 and Lys228 (Figure 1.3). The carbon linker between the hydroxamic acid and phosphonate moiety is stabilized by hydrophobic interactions with the side chain residues of the catalytic loop, e.g. Trp212.

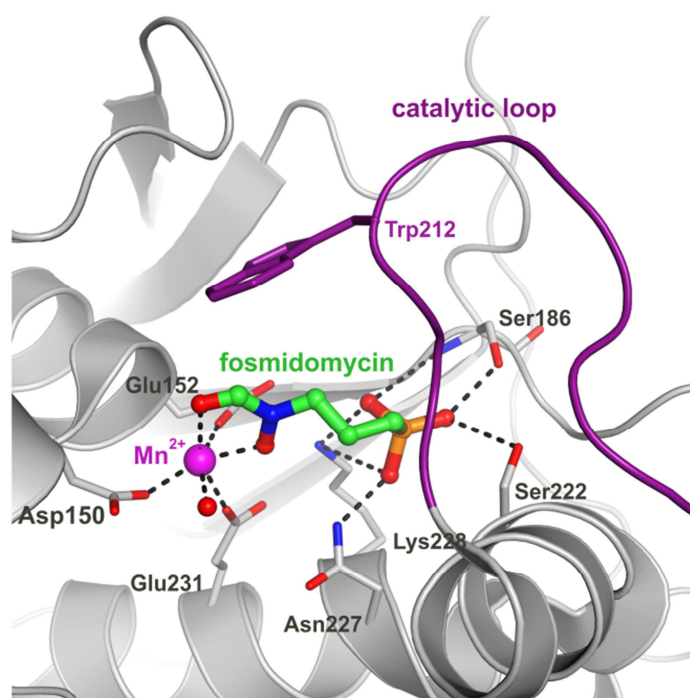
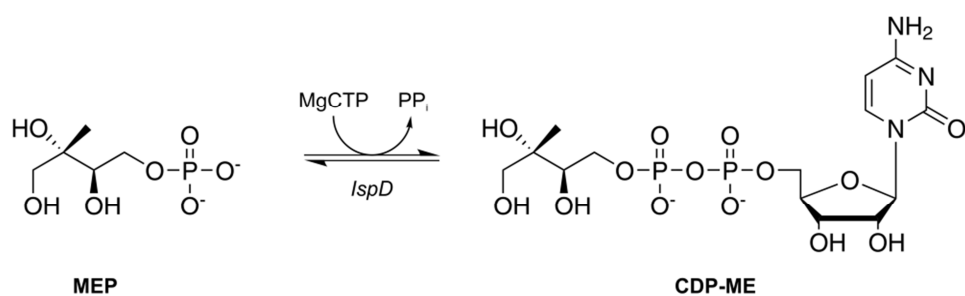


**Figure 1.3** Active site of *EclspC* in complex with fosmidomycin and  $Mn^{2+}$  (PDB code 1ONP).<sup>[101]</sup> Interactions are indicated by dashed lines. Fosmidomycin is presented in green,  $Mn^{2+}$  in magenta, the catalytic loop in purple. The residues in contact with the ligand as well as fosmidomycin are presented as stick model.

## 1.4 2C-methyl-D-erythritol-4-phosphate cytidyltransferase (IspD)

### 1.4.1 The catalytic mechanism of IspD

In the catalytic reaction of IspD, a cytidyl phosphate moiety from CTP is transferred to MEP yielding the product CDP-ME and diphosphate (Scheme 1.8).<sup>[59]</sup> CTP and preferably  $Mg^{2+}$  are necessary cosubstrate/cofactor. It was shown by pulse chase experiments that the IspD reaction involves an ordered sequential mechanism.<sup>[156]</sup> The catalytic activity, studied in *E. coli*, *Streptomyces coelicolor* and *Arabidopsis thaliana*, is in the range of 20-70  $\mu\text{mol mg}^{-1} \text{min}^{-1}$  and is therefore relatively low compared to Dxs.<sup>[59,157-159]</sup> IspD from *E. coli* (*EclspD*) can be inhibited by D-erythritol-4-phosphate, the 2-desmethyl analog of MEP, with an  $IC_{50}$  value in the single-digit nanomolar range ( $IC_{50}=1.4 \text{ nM}$ ).<sup>[160,161]</sup>



**Scheme 1.8** Schematic representation of the catalytic *IspD* reaction.

#### 1.4.2 The biological importance as drug target

Emerging resistance is not only a big problem for anti-infectives, but also for herbicides. The resistance of weeds to almost all available herbicides is increasing, especially to the most important herbicide glyphosate.<sup>[162]</sup> Therefore, new modes of action in the lead compound discovery for herbicides are crucial for the future world food production. Antisense experiments showed that *IspD* is essential in plants and thus, inhibitors against *IspD* are potential herbicides.<sup>[158,163,164]</sup> Based on those findings, the chemical company BASF SE (Ludwigshafen, Germany) tested in a high throughput screening a proprietary library of about 100,000 diverse compounds for the inhibition of *IspD* from *A. thaliana* (*AthIspD*).<sup>[35,165,166]</sup> Only few inhibitors were identified, the best of them, 7-hydroxy[1,2,4]triazolo[1,5- $\alpha$ ]pyrimidine (HTP), with an  $IC_{50}$  value of 140 nM. However, computational docking experiments with the published *AthIspD* structure (PDB code 1W77)<sup>[167]</sup> exhibited no reasonable binding mode to the active site. The subsequent complex structure of *AthIspD* with the ligand (PDB code 2YC3)<sup>[166]</sup> surprisingly showed the formation of an allosteric pocket upon ligand binding (Figure 1.4). This pocket is in close proximity to the substrate and CTP binding site and its formation reduces the size of the active site cavity.<sup>[166]</sup> Those findings were used to introduce further alterations of HTP resulting in a variety of new inhibitors. Two of the best azolopyrimidine derivatives were 5-chloro-7-hydroxy-6-(phenylmethyl)pyrazolo[1,5- $\alpha$ ]pyrimidine-3-carbonitrile (6BC) with an  $IC_{50}$  value of 35 nM and 6-benzyl-5-chloro-7-hydroxypyrazolo[1,5- $\alpha$ ]pyrimidine-3-carboxylic acid (3OA) with an  $IC_{50}$  value of 274 nM. Cocrystallization of those compounds with *AthIspD* led to two complex structures with the PDB codes 2YC5 (6BC) and 2YCM (3OA).<sup>[166]</sup> Notably, those azolopyrimidine derivatives showed very good herbicidal activity in a greenhouse experiment.<sup>[166]</sup> The binding mode in this newly discovered allosteric pocket raises the question whether this pocket would also accept other ligands.

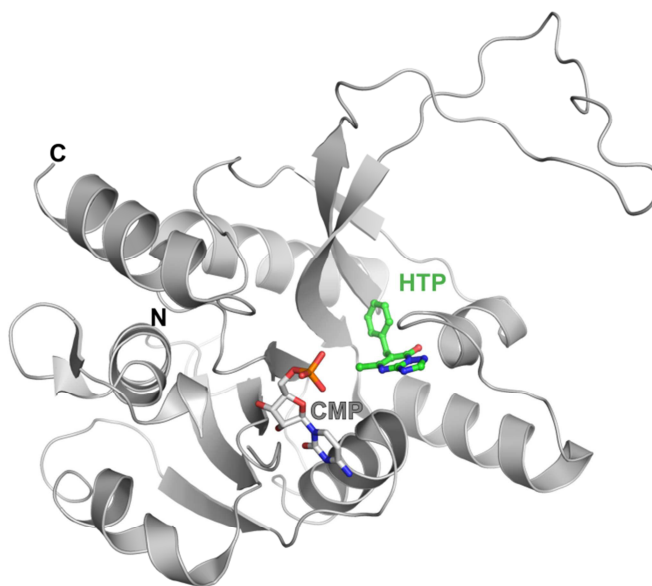


**Figure 1.4** Overall structure of *AthIspD* in complex with HTP (PDB code 2YC3)<sup>[166]</sup> and CMP (from PDB code 1W77).<sup>[167]</sup> N- and C-terminus are labeled with N and C, respectively.

### 1.4.3 The crystal structure of *IspD*

In 2001, the first complex structures from *EclspD* with CTP (PDB code 1I52) and with CDP-ME (PDB code 1INI) were published.<sup>[168]</sup> Next, the apo structure of *EclspD* (PDB code 1VGT)<sup>[169]</sup> and *EclspD* in complex with buffer components (PDB code 1H3M) followed.<sup>[170]</sup> In the same publication *IspD* from *Neisseria gonorrhoeae* (PDB code 1VGW) was released.<sup>[169]</sup> Then, the *IspD* structure from *Thermotoga maritima* in complex with CTP (PDB code 1VPA; no PubMed ID available) was solved. In 2006, the first structure from *A. thaliana* in complex with CMP was published (PDB code 1W77).<sup>[167]</sup> The following released structures were from *T. thermophilus* (PDB code 2PX7), *Listeria monocytogenes* (PDB code 3F1C), *M. tuberculosis* (PDB codes 3OKR, 2XWN, 3Q7U and 3Q80), *Mycobacterium smegmatis* (PDB codes 2XWL and 2XWM), and *Anaerococcus prevotii* (PDB code 4KT7), etc. The last published structures were *EclspD* in complex with buffer components (PDB code 3N9W)<sup>[171]</sup> and *AthIspD* in complex with the before discussed azolopyrimidine derivatives (PDB codes 2YC3, 2YC5, 2YCM).<sup>[166]</sup> To date, there are already 25 *IspD* structures deposited.

### Overall structure of *IspD*

*AthIspD* forms a homo-dimer in which each subunit is related by a crystallographic two-fold axis. The enzyme originally consists of 302 amino acids including an N-terminal plastid targeting sequence followed by the catalytic domain.<sup>[59]</sup> The catalytic part of the enzyme (amino acids 75–302) crystallized in the space group H32 and comprises one subunit in the asymmetric unit. The overall structure exhibits a Rossmann fold-like domain where the core of *AthIspD* consists of a seven-stranded twisted  $\beta$ -sheet ( $\beta$ 11,  $\beta$ 7,  $\beta$ 10,  $\beta$ 6,  $\beta$ 1,  $\beta$ 4,  $\beta$ 5). Apart from  $\beta$ 10, all strands are parallel. In agreement with the *IspD* structures of *E. coli* and *Campylobacter jejuni*, *AthIspD* carries a  $\beta$ -arm that is involved in dimerization of the protein (Figure 1.5). This dimer interface constructed by two  $\beta$ -arms is mainly composed of hydrophobic as well as hydrogen bond interactions.

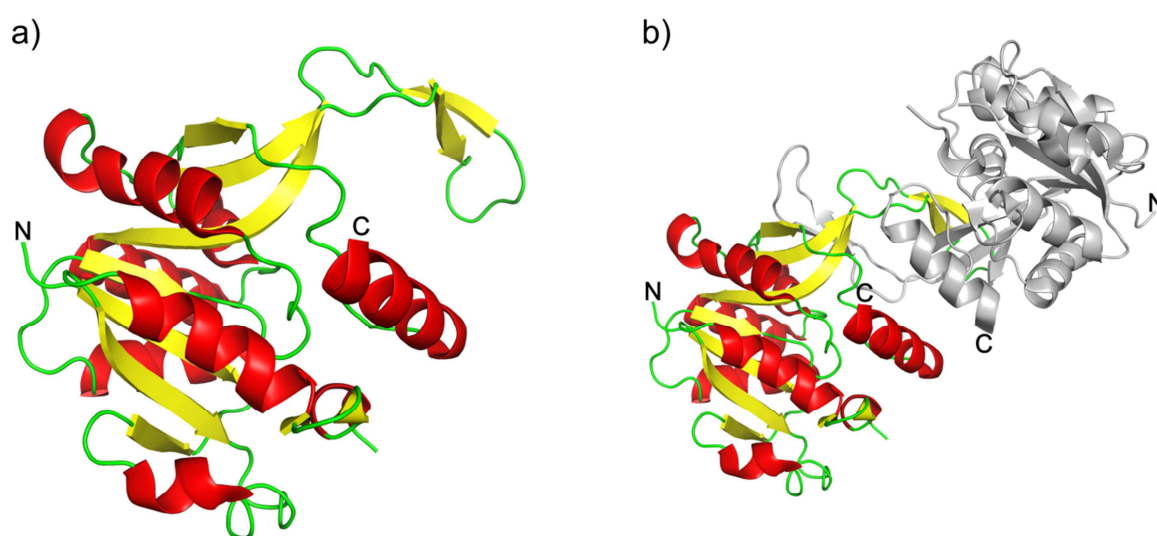


**Figure 1.5** Ribbon plot of *EclspD* (PDB code 1H3M).<sup>[170]</sup> a) Monomer b) Dimer. N- and C-termini are labeled with N and C, respectively.

### Active site

The crystal structure of *AthIspD* in complex with CMP (PDB code 1W77)<sup>[167]</sup> revealed that the cosubstrate is stabilized by hydrogen bond interactions of Lys284 with the phosphate moiety of CMP and of Ser160 with the nitrogen atom of the cytidine moiety (Figure 1.6a). The complex structure of *EclspD* and CDP-ME (PDB code 1INI)<sup>[168]</sup> shows that the hydrogen bond of the

phosphate moiety of CDP-ME with the mentioned lysine side chain (Lys213, Figure 1.6b) is abolished due to sterical reasons, whereas the substrate is further stabilized by interactions with Arg20 and Lys20 (Figure 1.6b). Usually, an arginine residue (Arg157 in *AthIspD*, Arg85 in *EclspD*; Figure 1.6) interacts with an acidic residue (Asp262 in *AthIspD*, Glu191 in *EclspD*; Figure 1.6) and points away from the CTP/CMP binding site. The loop harboring Asp262 in Figure 1.6a is distorted and therefore the interaction is not depicted. However, the determination of the apo *AthIspD* structure during this thesis confirmed this interaction (see chapter 5). Interestingly, binding of HTP (see chapter 1.4.2) to an allosteric pocket near the active site leads to a structural rearrangement of Asp262. The interaction to Arg157 is abolished and Asp262 turns into the MEP binding site, thereby preventing the binding of the substrate and blocking the reaction. Notably, it was found that CTP<sup>[156]</sup> as well as CMP<sup>[167]</sup> can be inhibitors of IspD, which seems to be a feedback regulation of the protein activity.

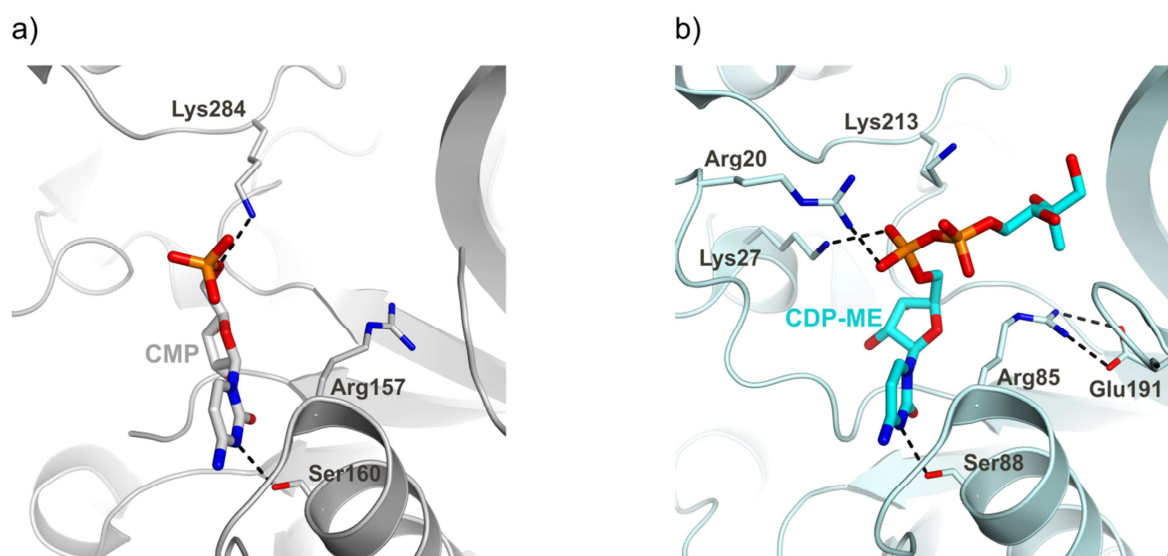


**Figure 1.6** a) Active site of *AthIspD* (PDB code 1W77)<sup>[167]</sup> in complex with CMP. Interactions of Ser160 and Lys284 (*AthIspD* numbering) are indicated by dashed lines. b) Active site of *EclspD* in complex with CDP-ME (PDB code 1INI)<sup>[168]</sup> Interactions of side chains (*EclspD* numbering) with CDP-ME are indicated by dashed lines. N- and C-termini are labeled with N and C, respectively. The active site in a) and b) are represented in the same orientation.

## 1.5 Objectives

Major efforts were performed to identify novel antiinfectives, antimalarials and herbicides against the enzymes of the non-mevalonate pathway.<sup>[25]</sup> However, only few new chemical entities could be discovered that are actually on the market nowadays. Thus, there is still an urgent need for further input in this research area.

Fosmidomycin was shown to have antibacterial as well as antimalarial activity with IC<sub>50</sub> values in the low nanomolar range *in vitro*. Nevertheless, at the cellular level, the inhibition level is decreased due to the lack of uptake e.g. in case of *M. tuberculosis*. In clinical studies, fosmidomycin was a moderate inhibitor against uncomplicated malaria. Therefore, combinational approaches with artesunate and clindamycin are currently tested to enhance its efficiency. Since the molecular structure of the natural compound seems to be a promising lead structure, analogs of fosmidomycin are in the focus of many research institutes. The group of Prof. Dr. Thomas Kurz from the Heinrich Heine Universität in Düsseldorf (Germany) is designing and synthesizing new ligands with a “reverse” hydroxamic acid moiety. In a joint collaboration, the aim of this thesis was the expression of the *ispC* gene from *E. coli* and *P. falciparum* and subsequent purification of the resulting his-tagged proteins using Ni<sup>2+</sup>-chelating sepharose columns. The inhibitory potency of the new compounds should then be determined using photometric activity assays by monitoring the decrease in absorption at 340 nm caused by oxidation of NADPH. In addition, the crystal structures of IspC from different organisms in complex with the ligands should yield insights into the binding and therefore the mode of action of the compounds. Preliminary experiments of the Kurz group showed that small alterations of the natural product scaffold lead to promising new ligands. To date, only racemic mixtures of IspC inhibitors were tested in activity assays and in crystallographic studies. It is unclear, which enantiomer of diverse ligands is preferred by the enzyme. This long pending question on the stereochemistry of chiral inhibitors should be addressed in the present work.

The research group of Prof. Dr. François Diederich from the ETH Zürich (Switzerland) as well as Dr. Matthias Witschel and Dr. Wolfgang Höffken from the chemical company BASF SE in Ludwigshafen (Germany) extensively studied the second enzyme of the non-mevalonate pathway, namely IspD. Their research in the field of herbicides led to the finding of potent azolopyrimidine derivatives. As preliminary work, the BASF SE performed high throughput screenings of compound libraries in order to find new inhibitors of IspD. In both research units, design and synthesis of ligands is approached. In this collaboration project, my aim was the expression of the *ispd* gene and subsequent purification of *AthIspD*. To facilitate the



crystallization, the protein should lack an affinity tag, and therefore, separation of the protein of interest would be performed natively utilizing different strategies, namely application of *Ath1spD* on anion exchange columns as well as on gel filtration columns. NMR based activity assays should be performed with the purified protein to test new ligands. Hereby, the turnover of substrate to products will be detected by the shifts in  $^{31}\text{P}$ -signals. Crystallographic studies have been designed to answer the question whether new, active inhibitors address the same allosteric binding site as the published azolopyrimidine derivatives, or whether a new mode of action plays a role for these compounds. Based on these results, further improvement of the ligands can be aspired by drug design.

## 1.6 References

- (1) V. De Luca, B. St Pierre, *Trends in Plant Sci.* **2000**, *5*, 168-173.
- (2) J. C. Sacchettini, C. D. Poulter, *Science* **1997**, *277*, 1788-1789.
- (3) F. Khachik, G. R. Beecher, J. C. Smith Jr., *J. Cell. Biochem. Suppl.* **1995**, *22*, 236-246.
- (4) B. Demmig-Adams, W. W. Adams, *Science* **2002**, *298*, 2149-2153.
- (5) R. T. Skeel, *Handbook of cancer chemotherapy*; Lipincott Williams and Wilkins, **1999**; 5<sup>th</sup> edition.
- (6) M. Rohmer, *Nat. Prod. Rep.* **1999**, *16*, 565-574.
- (7) L. D. Wright, E. L. Cresson, H. R. Skeggs, G. D. E. Macrae, C. H. Hoffman, D. E. Wolf, K. Folkers, *J. Am. Chem. Soc.* **1956**, *78*, 5273-5275.
- (8) P. A. Tavormina, M. H. Gibbs, J. W. Huff, *J. Am. Chem. Soc.* **1956**, *78*, 4498-4499.
- (9) N. Qureshi, J. W. Porter, In *Biosynthesis of isoprenoid compounds*; J. W. Porter & S. L. Spurgeon: John Wiley & Sons, New York, **1981**; Vol. 1.
- (10) D. V. Banthorpe, B. V. Charlwood, M. J. O. Francis, *Chem. Rev.* **1972**, *72*, 115-155.
- (11) K. Bloch, *Steroids* **1992**, *57*, 378-383.
- (12) T. J. Bach, *Lipids* **1995**, *30*, 191-202.
- (13) F. Lynen, K. Bloch,  
[http://www.nobelprize.org/nobel\\_prizes/medicine/laureates/1964/press.html](http://www.nobelprize.org/nobel_prizes/medicine/laureates/1964/press.html);  
12.11.2013.
- (14) N. Qureshi, S. Nimmannit, J. W. Porter, *Methods Enzymol.* **1981**, *71* (pt. c), 455-461.
- (15) M. Rodriguez-Concepcion, A. Boronat, *Plant Physiol.* **2002**, *130*, 1079-1089.
- (16) W. Eisenreich, A. Bacher, D. Arigoni, F. Rohdich, *Cell. Mol. Life Sci.* **2004**, *61*, 1401-1426.

- (17) M. Rohmer, M. Knani, P. Simonin, B. Sutter, H. Sahm, *Biochem. J.* **1993**, *295*, 517-524.
- (18) H. K. Lichtenthaler, M. Rohmer, J. Schwender, *Physiol. Plant.* **1997**, *101*, 643-652.
- (19) J. Schwender, M. Seemann, H. K. Lichtenthaler, M. Rohmer, *Biochem. J.* **1996**, *316*, 73-80.
- (20) A. Disch, J. Schwender, C. Müller, H. K. Lichtenthaler, M. Rohmer, *Biochem. J.* **1998**, *333*, 381-388.
- (21) H. K. Lichtenthaler, J. Schwender, A. Disch, M. Rohmer, *FEBS Lett.* **1997**, *400*, 271-274.
- (22) D. Arigoni, S. Sagner, C. Latzel, W. Eisenreich, A. Bacher, M. H. Zenk, *Proc. Natl. Acad. Sci. USA* **1997**, *94*, 10600-10605.
- (23) J. Schwender, J. Zeidler, R. Groner, C. Müller, M. Focke, S. Braun, F. W. Lichtenthaler, H. K. Lichtenthaler, *FEBS Lett.* **1997**, *414*, 129-134.
- (24) J. H. Cvejic, M. Rohmer, *Phytochemistry* **2000**, *53*, 21-28.
- (25) H. Jomaa, J. Wiesner, S. Sanderbrand, B. Altincicek, C. Weidemeyer, M. Hintz, I. Turbachova, M. Eberl, J. Zeidler, H. K. Lichtenthaler, D. Soldati, E. Beck, *Science* **1999**, *285*, 1573-1576.
- (26) S. Borrmann, S. Issifou, G. Esser, A. A. Adegnika, M. Ramharter, P. B. Matsiegui, S. Oyakhirome, D. P. Mawili-Mboumba, M. A. Missinou, J. F. J. Kun, H. Jomaa, P. G. Kreamsner, *J. Infect. Dis.* **2004**, *190*, 1534-1540.
- (27) M. A. Missinou, S. Borrmann, A. Schindler, S. Issifou, A. A. Adegnika, P. B. Matsiegui, R. Binder, B. Lell, J. Wiesner, T. Baranek, H. Jomaa, P. G. Kreamsner, *Lancet* **2002**, *360*, 1941-1942.
- (28) F. Rohdich, A. Bacher, W. Eisenreich, *Bioorg. Chem.* **2004**, *32*, 292-308.
- (29) F. Rohdich, A. Bacher, W. Eisenreich, *Biochem. Soc. Trans.* **2005**, *33*, 785-791.
- (30) A. Disch, M. Rohmer, *FEMS Microbiol. Lett.* **1998**, *168*, 201-208.
- (31) Y. Boucher, W. F. Doolittle, *Mol. Microbiol.* **2000**, *37*, 703-716.
- (32) A. Smit, A. Mushegian, *Genome Res.* **2000**, *10*, 1468-1484.
- (33) E. I. Wilding, J. R. Brown, A. P. Bryant, A. F. Chalker, D. J. Holmes, K. A. Ingraham, S. Iordanescu, Y. S. Chi, M. Rosenberg, M. N. Gwynn, *J. Bacteriol.* **2000**, *182*, 4319-4327.
- (34) H. K. Lichtenthaler, J. Zeidler, J. Schwender, C. Müller, *Z. Naturforsch. C* **2000**, *55*, 305-313.
- (35) A. Bacher, W. Eisenreich, M. Fellermeier, M. Fischer, S. Hecht, S. Herz, K. Kis, H. Lüttgen, F. Rohdich, S. Sagner, C. A. Schuhr, J. Wungsintaweekul, M. H. Zenk, international patent application WO2001011055A1, **2001**.
- (36) R. Hovik, B. Brodal, K. Bartlett, H. Osmundsen, *J. Lipid Res.* **1991**, *32*, 993-999.

- (37) I. Ahumada, A. Cairo, A. Hemmerlin, V. Gonzalez, I. Pateraki, T. J. Bach, M. Rodriguez-Concepcion, N. Campos, A. Boronat, *Funct. Plant Biol.* **2008**, *35*, 1100-1111.
- (38) K. Y. Chun, D. A. Vinarov, H. M. Miziorko, *Biochemistry* **2000**, *39*, 14670-14681.
- (39) G. A. Holdgate, W. H. J. Ward, F. McTaggart, *Biochem. Soc. Trans.* **2003**, *31*, 528-531.
- (40) J. Roitelman, E. H. Olender, S. Barnun, W. A. Dunn, R. D. Simoni, *J. Cell Biol.* **1992**, *117*, 959-973.
- (41) E. E. Slater, J. S. Macdonald, *Drugs* **1988**, *36*, 72-82.
- (42) C. Stancu, A. Sima, *J. Cell. Mol. Med.* **2001**, *5*, 378-387.
- (43) S. Hogenboom, J. J. M. Tuyp, M. Espeel, J. Koster, R. J. A. Wanders, H. R. Waterham, *J. Cell Sci.* **2004**, *117*, 631-639.
- (44) L. M. Olivier, K. L. Chambliss, K. M. Gibson, S. K. Krisans, *J. Lipid Res.* **1999**, *40*, 672-679.
- (45) A. Michihara, K. Akasaki, Y. Yamori, H. Tsuji, *Biol. Pharm. Bull.* **2003**, *26*, 579-584.
- (46) H. M. Miziorko, *Arch. Biochem. Biophys.* **2011**, *505*, 131-143.
- (47) F. M. Hahn, J. W. Xuan, A. F. Chambers, C. D. Poulter, *Arch. Biochem. Biophys.* **1996**, *332*, 30-34.
- (48) J. E. Reardon, R. H. Abeles, *Biochemistry* **1986**, *25*, 5609-5616.
- (49) I. P. Street, D. J. Christensen, C. D. Poulter, *J. Am. Chem. Soc.* **1990**, *112*, 8577-8578.
- (50) J. W. Cornforth, R. H. Cornforth, G. Popjak, L. Yengoyan, *J. Biol. Chem.* **1966**, *241*, 3970-3987.
- (51) G. A. Sprenger, U. Schorken, T. Wiegert, S. Grolle, A. A. deGraaf, S. V. Taylor, T. P. Begley, S. Bringer-Meyer, H. Sahm, *Proc. Natl. Acad. Sci. USA* **1997**, *94*, 12857-12862.
- (52) L. M. Lois, N. Campos, S. R. Putra, K. Danielsen, M. Rohmer, A. Boronat, *Proc. Natl. Acad. Sci. USA* **1998**, *95*, 2105-2110.
- (53) S. Xiang, G. Usunow, G. Lange, M. Busch, L. Tong, *J. Biol. Chem.* **2007**, *282*, 2676-2682.
- (54) L. M. Eubanks, C. D. Poulter, *Biochemistry* **2003**, *42*, 1140-1149.
- (55) R. H. White, *Biochemistry* **1978**, *17*, 3833-3840.
- (56) S. David, B. Estramareix, J. C. Fischer, M. Therisod, *J. Am. Chem. Soc.* **1981**, *103*, 7341-7342.
- (57) R. E. Hill, B. G. Sayer, I. D. Spenser, *J. Am. Chem. Soc.* **1989**, *111*, 1916-1917.
- (58) Y. Matsue, H. Mizuno, T. Tomita, T. Asami, M. Nishiyama, T. Kuzuyama, *J. Antibiot.* **2010**, *63*, 583-588.
- (59) F. Rohdich, J. Wungsintaweeikul, M. Fellermeier, S. Sagner, S. Herz, K. Kis, W. Eisenreich, A. Bacher, M. H. Zenk, *Proc. Natl. Acad. Sci. USA* **1999**, *96*, 11758-11763.

- (60) H. Lüttgen, F. Rohdich, S. Herz, J. Wungsintaweeikul, S. Hecht, C. A. Schuhr, M. Fellermeier, S. Sagner, M. H. Zenk, A. Bacher, W. Eisenreich, *Proc. Natl. Acad. Sci. USA* **2000**, *97*, 1062-1067.
- (61) L. Miallau, M. S. Alphey, L. E. Kemp, G. A. Leonard, S. M. McSweeney, S. Hecht, A. Bacher, W. Eisenreich, F. Rohdich, W. N. Hunter, *Proc. Natl. Acad. Sci. USA* **2003**, *100*, 9173-9178.
- (62) S. Herz, J. Wungsintaweeikul, C. A. Schuhr, S. Hecht, H. Lüttgen, S. Sagner, M. Fellermeier, W. Eisenreich, M. H. Zenk, A. Bacher, F. Rohdich, *Proc. Natl. Acad. Sci. USA* **2000**, *97*, 2486-2490.
- (63) M. Takagi, T. Kuzuyama, K. Kaneda, H. Watanabe, T. Dairi, H. Seto, *Tetrahedron Lett.* **2000**, *41*, 3395-3398.
- (64) S. Steinbacher, J. Kaiser, J. Wungsintaweeikul, S. Hecht, W. Eisenreich, S. Gerhardt, A. Bacher, F. Rohdich, *J. Mol. Biol.* **2002**, *316*, 79-88.
- (65) L. E. Kemp, C. S. Bond, W. N. Hunter, *Proc. Natl. Acad. Sci. USA* **2002**, *99*, 6591-6596.
- (66) S. B. Richard, J. L. Ferrer, M. E. Bowman, A. M. Lillo, C. N. Tetzlaff, D. E. Cane, J. P. Noel, *J. Biol. Chem.* **2002**, *277*, 8667-8672.
- (67) C. Lehmann, K. Lim, J. Toedt, W. Krajewski, A. Howard, E. Eisenstein, O. Herzberg, *Proteins: Struct., Funct., Bioinf.* **2002**, *49*, 135-138.
- (68) H. Kishida, T. Wada, S. Unzai, T. Kuzuyama, M. Takagi, T. Terada, M. Shirouzu, S. Yokoyama, J. R. H. Tame, S. Y. Park, *Acta Crystallogr., Sect. D: Biol. Crystallogr.* **2003**, *59*, 23-31.
- (69) M. Seemann, B. T. S. Bui, M. Wolff, D. Tritsch, N. Campos, A. Boronat, A. Marquet, M. Rohmer, *Angew. Chem., Int. Ed.* **2002**, *41*, 4337-4339; *Angew. Chem.* **2002**, *114*, 4513-4515.
- (70) F. Rohdich, F. Zepeck, P. Adam, S. Hecht, J. Kaiser, R. Laupitz, T. Gräwert, S. Amslinger, W. Eisenreich, A. Bacher, D. Arigoni, *Proc. Natl. Acad. Sci. USA* **2003**, *100*, 1586-1591.
- (71) A. K. Kollas, E. C. Duin, M. Eberl, B. Altincicek, M. Hintz, A. Reichenberg, D. Henschker, A. Henne, I. Steinbrecher, D. N. Ostrovsky, R. Hedderich, E. Beck, H. Jomaa, J. Wiesner, *FEBS Lett.* **2002**, *532*, 432-436.
- (72) M. Lee, T. Gräwert, F. Quitterer, F. Rohdich, J. Eppinger, W. Eisenreich, A. Bacher, M. Groll, *J. Mol. Biol.* **2010**, *404*, 600-610.
- (73) I. Reikittke, T. Nonaka, J. Wiesner, U. Demmer, E. Warkentin, H. Jomaa, U. Ermler, *FEBS Lett.* **2011**, *585*, 447-451.
- (74) I. Reikittke, H. Jomaa, U. Ermler, *FEBS Lett.* **2012**, *586*, 3452-3457.

- (75) F. Rohdich, S. Hecht, K. Gärtner, P. Adam, C. Krieger, S. Amslinger, D. Arigoni, A. Bacher, W. Eisenreich, *Proc. Natl. Acad. Sci. USA* **2002**, *99*, 1158-1163.
- (76) P. Adam, S. Hecht, W. G. Eisenreich, J. Kaiser, T. Gräwert, D. Arigoni, A. Bacher, F. Rohdich, *Proc. Natl. Acad. Sci. USA* **2002**, *99*, 12108-12113.
- (77) M. Wolff, M. Seemann, B. T. S. Bui, Y. Frapart, D. Tritsch, A. G. Estrabot, M. Rodriguez-Concepcion, A. Boronat, A. Marquet, M. Rohmer, *FEBS Lett.* **2003**, *541*, 115-120.
- (78) B. Altincicek, E. C. Duin, A. Reichenberg, R. Hedderich, A. K. Kollas, M. Hintz, S. Wagner, J. Wiesner, E. Beck, H. Jomaa, *FEBS Lett.* **2002**, *532*, 437-440.
- (79) I. Rekkittke, J. Wiesner, R. Roehrich, U. Demmer, E. Warkentin, W. Xu, K. Troschke, M. Hintz, J. H. No, E. C. Duin, E. Oldfield, H. Jomaa, U. Ermler, *J. Am. Chem. Soc.* **2008**, *130*, 17206-17207.
- (80) T. Gräwert, F. Rohdich, I. Span, A. Bacher, W. Eisenreich, J. Eppinger, M. Groll, *Angew. Chem., Int. Ed.* **2009**, *48*, 5756-5759; *Angew. Chem.* **2009**, *121*, 5867-5870.
- (81) T. Gräwert, I. Span, W. Eisenreich, F. Rohdich, J. Eppinger, A. Bacher, M. Groll, *Proc. Natl. Acad. Sci. USA* **2010**, *107*, 1077-1081.
- (82) S.-M. Kim, T. Kuzuyama, Y.-J. Chang, S.-U. Kim, *Plant Cell Rep.* **2006**, *25*, 829-835.
- (83) R. J. M. Wilson, P. W. Denny, P. R. Preiser, K. Rangachari, K. Roberts, A. Roy, A. Whyte, M. Strath, D. J. Moore, P. W. Moore, D. H. Williamson, *J. Mol. Biol.* **1996**, *261*, 155-172.
- (84) S. A. Ralph, G. G. van Dooren, R. F. Waller, M. J. Crawford, M. J. Fraunholz, B. J. Foth, C. J. Tonkin, D. S. Roos, G. I. McFadden, *Nat. Rev. Microbiol.* **2004**, *2*, 203-216.
- (85) T. Kuzuyama, T. Shimizu, S. Takahashi, H. Seto, *Tetrahedron Lett.* **1998**, *39*, 7913-7916.
- (86) S. Takahashi, T. Kuzuyama, H. Watanabe, H. Seto, *Proc. Natl. Acad. Sci. USA* **1998**, *95*, 9879-9884.
- (87) F. J. Sangari, J. Perez-Gil, L. Carretero-Paulet, J. M. Garcia-Lobo, M. Rodriguez-Concepcion, *Proc. Natl. Acad. Sci. USA* **2010**, *107*, 14081-14086.
- (88) J. F. Hoeffler, D. Tritsch, C. Grosdemange-Billiard, M. Rohmer, *Eur. J. Biochem.* **2002**, *269*, 4446-4457.
- (89) A. T. Koppisch, D. T. Fox, B. S. J. Blagg, C. D. Poulter, *Biochemistry* **2002**, *41*, 236-243.
- (90) P. J. Proteau, Y. H. Woo, R. T. Williamson, C. Phaosiri, *Org. Lett.* **1999**, *1*, 921-923.
- (91) T. Radykewicz, F. Rohdich, J. Wungsintaweekul, S. Herz, K. Kis, W. Eisenreich, A. Bacher, M. H. Zenk, D. Arigoni, *FEBS Lett.* **2000**, *465*, 157-160.
- (92) S. Lauw, V. Illarionova, A. Bacher, F. Rohdich, W. Eisenreich, *FEBS J.* **2008**, *275*, 4060-4073.

- (93) S. R. Putra, L. M. Lois, N. Campos, A. Boronat, M. Rohmer, *Tetrahedron Lett.* **1998**, *39*, 23-26.
- (94) T. Gräwert, M. Groll, F. Rohdich, A. Bacher, W. Eisenreich, *Cell. Mol. Life Sci.* **2011**, *68*, 3797-3814.
- (95) U. Wong, R. J. Cox, *Angew. Chem., Int. Ed.* **2007**, *46*, 4926-4929; *Angew. Chem.* **2007**, *119*, 5014-5017.
- (96) J. W. Munos, X. Pu, S. O. Mansoorabadi, H. J. Kim, H.-w. Liu, *J. Am. Chem. Soc.* **2009**, *131*, 2048-2049.
- (97) D. T. Fox, C. D. Poulter, *Biochemistry* **2005**, *44*, 8360-8368.
- (98) D. T. Fox, C. D. Poulter, *J. Org. Chem.* **2005**, *70*, 1978-1985.
- (99) J. Zeidler, J. Schwender, C. Müller, J. Wiesner, C. Weidemeyer, E. Beck, H. Jomaa, H. K. Lichtenthaler, *Z. Naturforsch. C* **1998**, *53*, 980-986.
- (100) S. Yajima, T. Nonaka, T. Kuzuyama, H. Seto, K. Ohsawa, *J. Biochem.* **2002**, *131*, 313-317.
- (101) S. Steinbacher, J. Kaiser, W. Eisenreich, R. Huber, A. Bacher, F. Rohdich, *J. Biol. Chem.* **2003**, *278*, 18401-18407.
- (102) M. Okuhara, Y. Kuroda, T. Goto, M. Okamoto, H. Terano, M. Kohsaka, H. Aoki, H. Imanaka, *J. Antibiot.* **1980**, *33*, 13-17.
- (103) E. Iguchi, M. Okuhara, M. Kohsaka, H. Aoki, H. Imanaka, *J. Antibiot.* **1980**, *33*, 18-23.
- (104) M. Okuhara, Y. Kuroda, T. Goto, M. Okamoto, H. Terano, M. Kohsaka, H. Aoki, H. Imanaka, *J. Antibiot.* **1980**, *33*, 24-28.
- (105) Y. Kuroda, M. Okuhara, T. Goto, M. Okamoto, H. Terano, M. Kohsaka, H. Aoki, H. Imanaka, *J. Antibiot.* **1980**, *33*, 29-35.
- (106) H. P. Kuemmerle, T. Murakawa, F. Desantis, *Chemioterapia* **1987**, *6*, 113-119.
- (107) B. Altincicek, M. Hintz, S. Sanderbrand, J. Wiesner, E. Beck, H. Jomaa, *FEMS Microbiol. Lett.* **2000**, *190*, 329-333.
- (108) J. Wiesner, M. Hintz, B. Altincicek, S. Sanderbrand, C. Weidemeyer, E. Beck, H. Jomaa, *Exp. Parasitol.* **2000**, *96*, 182-186.
- (109) B. Lell, R. Ruangweerayut, J. Wiesner, M. A. Missinou, A. Schindler, T. Baranek, M. Hintz, D. Hutchinson, H. Jomaa, P. G. Kremsner, *Antimicrob. Agents Chemother.* **2003**, *47*, 735-738.
- (110) J. Wiesner, S. Borrmann, H. Jomaa, *Parasitol. Res.* **2003**, *90*, S71-S76.
- (111) H. P. Kuemmerle, T. Murakawa, H. Sakamoto, N. Sato, T. Konishi, F. Desantis, *Int. J. Clin. Pharmacol. Ther.* **1985**, *23*, 521-528.

- (112) T. Tsuchiya, K. Ishibashi, M. Terakawa, M. Nishiyama, N. Itoh, H. Noguchi, *Eur. J. Drug Metab. Pharmacokinet.* **1982**, *7*, 59-64.
- (113) S. Borrmann, A. A. Adegnik, F. Moussavou, S. Oyakhirome, G. Esser, P. B. Matsiegui, M. Ramharter, I. Lundgren, M. Kombila, S. Issifou, D. Hutchinson, J. Wiesner, H. Jomaa, P. G. Kreamsner, *Antimicrob. Agents Chemother.* **2005**, *49*, 3749-3754.
- (114) S. Borrmann, A. A. Adegnik, P. B. Matsiegui, S. Issifou, A. Schindler, D. P. Mawili-Mboumba, T. Baranek, J. Wiesner, H. Jomaa, P. G. Kreamsner, *J. Infect. Dis.* **2004**, *189*, 901-908.
- (115) S. Borrmann, I. Lundgren, S. Oyakhirome, B. Impouma, P.-B. Matsiegui, A. A. Adegnik, S. Issifou, J. F. J. Kun, D. Hutchinson, J. Wiesner, H. Jomaa, P. G. Kreamsner, *Antimicrob. Agents Chemother.* **2006**, *50*, 2713-2718.
- (116) R. K. Dhiman, M. L. Schaeffer, A. M. Bailey, C. A. Testa, H. Scherman, D. C. Crick, *J. Bacteriol.* **2005**, *187*, 8395-8402.
- (117) A. C. Brown, T. Parish, *BMC Microbiol.* **2008**, *8*.
- (118) C. Y. Botte, F. Dubar, G. I. McFadden, E. Marechal, C. Biot, *Chem. Rev.* **2012**, *112*, 1269-1283.
- (119) C. Zingle, L. Kuntz, D. Tritsch, C. Grosdemange-Billiard, M. Rohmer, *J. Org. Chem.* **2010**, *75*, 3203-3207.
- (120) D. Gießmann, P. Heidler, T. Haemers, S. Van Calenbergh, A. Reichenberg, H. Jomaa, C. Weidemeyer, S. Sanderbrand, J. Wiesner, A. Link, *Chem. Biodiversity* **2008**, *5*, 643-656.
- (121) T. Kurz, K. Schlüter, M. Pein, C. T. Behrendt, B. Bergmann, R. D. Walter, *Arch. Pharm.* **2007**, *340*, 339-344.
- (122) V. Devreux, J. Wiesner, H. Jomaa, J. Van der Eycken, S. Van Calenbergh, *Bioorg. Med. Chem. Lett.* **2007**, *17*, 4920-4923.
- (123) T. Haemers, J. Wiesner, R. Busson, H. Jomaa, S. Van Calenbergh, *Eur. J. Org. Chem.* **2006**, 3856-3863.
- (124) V. Devreux, J. Wiesner, J. L. Goeman, J. Van der Eycken, H. Jomaa, S. Van Calenbergh, *J. Med. Chem.* **2006**, *49*, 2656-2660.
- (125) Y. H. Woo, R. P. M. Fernandes, P. J. Proteau, *Bioorg. Med. Chem.* **2006**, *14*, 2375-2385.
- (126) M. Andaloussi, M. Lindh, C. Bjoerkelid, S. Suresh, A. Wieckowska, H. Iyer, A. Karlen, M. Larhed, *Bioorg. Med. Chem. Lett.* **2011**, *21*, 5403-5407.
- (127) J. Xue, J. Diao, G. Cai, L. Deng, B. Zheng, Y. Yao, Y. Song, *ACS Med. Chem. Lett.* **2013**, *4*, 278-282.

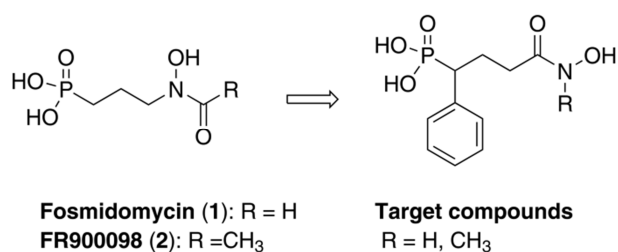
- (128) L. Kuntz, D. Tritsch, C. Grosdemange-Billiard, A. Hemmerlin, A. Willem, T. J. Bacht, M. Rohmer, *Biochem. J.* **2005**, *386*, 127-135.
- (129) R. Ortmann, J. Wiesner, K. Silber, G. Klebe, H. Jomaa, M. Schlitzer, *Arch. Pharm.* **2007**, *340*, 483-490.
- (130) T. Verbrugghen, P. Cos, L. Maes, S. Van Calenbergh, *J. Med. Chem.* **2010**, *53*, 5342-5346.
- (131) L. Merckle, A. de Andres-Gomez, B. Dick, R. J. Cox, C. R. A. Godfrey, *ChemBioChem* **2005**, *6*, 1866-1874.
- (132) T. Kurz, K. Schlüter, U. Kaula, B. Bergmann, R. D. Walter, D. Geffken, *Bioorg. Med. Chem.* **2006**, *14*, 5121-5135.
- (133) K. Schlüter, R. D. Walter, B. Bergmann, T. Kurz, *Eur. J. Med. Chem.* **2006**, *41*, 1385-1397.
- (134) V. Devreux, J. Wiesner, H. Jomaa, J. Rozenski, J. Van der Eycken, S. Van Calenbergh, *J. Org. Chem.* **2007**, *72*, 3783-3789.
- (135) T. Haemers, J. Wiesner, S. Van Poecke, J. Goeman, D. Henschker, E. Beck, H. Jomaa, S. Van Calenbergh, *Bioorg. Med. Chem. Lett.* **2006**, *16*, 1888-1891.
- (136) M. Andaloussi, L. M. Henriksson, A. Wieckowska, M. Lindh, C. Björkelid, A. M. Larsson, S. Suresh, H. Iyer, B. R. Srinivasa, T. Bergfors, T. Unge, S. L. Mowbray, M. Larhed, T. A. Jones, A. Karlen, *J. Med. Chem.* **2011**, *54*, 4964-4976.
- (137) T. Kurz, C. T. Behrendt, M. Pein, U. Kaula, B. Bergmann, R. D. Walter, *Arch. Pharm.* **2007**, *340*, 661-666.
- (138) R. Ortmann, J. Wiesner, A. Reichenberg, D. Henschker, E. Beck, H. Jomaa, M. Schlitzer, *Bioorg. Med. Chem. Lett.* **2003**, *13*, 2163-2166.
- (139) A. Reichenberg, J. Wiesner, C. Weidemeyer, E. Dreiseidler, S. Sanderbrand, B. Altincicek, E. Beck, M. Schlitzer, H. Jomaa, *Bioorg. Med. Chem. Lett.* **2001**, *11*, 833-835.
- (140) J. Wiesner, R. Ortmann, H. Jomaa, M. Schlitzer, *Arch. Pharm.* **2007**, *340*, 667-669.
- (141) L. Deng, S. Sundriyal, V. Rubio, Z.-z. Shi, Y. Song, *J. Med. Chem.* **2009**, *52*, 6539-6542.
- (142) L. Deng, J. Diao, P. Chen, V. Pujari, Y. Yao, G. Cheng, D. C. Crick, B. V. V. Prasad, Y. Song, *J. Med. Chem.* **2011**, *54*, 4721-4734.
- (143) L. Deng, K. Endo, M. Kato, G. Cheng, S. Yajima, Y. Song, *ACS Med. Chem. Lett.* **2011**, *2*, 165-170.
- (144) A. Nordqvist, *PhD thesis*, Uppsala Universitet (Sweden), **2011**.
- (145) K. Reuter, S. Sanderbrand, H. Jomaa, J. Wiesner, I. Steinbrecher, E. Beck, M. Hintz, G. Klebe, M. T. Stubbs, *J. Biol. Chem.* **2002**, *277*, 5378-5384.
- (146) A. Mac Sweeney, R. Lange, R. P. M. Fernandes, H. Schulz, G. E. Dale, A. Douangamath, P. J. Proteau, C. Oefner, *J. Mol. Biol.* **2005**, *345*, 115-127.



- (147) S. Ricagno, S. Grolle, S. Bringer-Meyer, H. Sahm, Y. Lindqvist, G. Schneider, *Biochim. Biophys. Acta, Proteins Proteomics* **2004**, *1698*, 37-44.
- (148) S. Yajima, K. Hara, J. M. Sanders, F. L. Yin, K. Ohsawa, J. Wiesner, H. Jomaa, E. Oldfield, *J. Am. Chem. Soc.* **2004**, *126*, 10824-10825.
- (149) L. M. Henriksson, C. Björkelid, S. L. Mowbray, T. Unge, *Acta Crystallogr., Sect. D: Biol. Crystallogr.* **2006**, *62*, 807-813.
- (150) L. M. Henriksson, T. Unge, J. Carlsson, J. Aqvist, S. L. Mowbray, T. A. Jones, *J. Biol. Chem.* **2007**, *282*, 19905-19916.
- (151) C. Björkelid, T. Bergfors, T. Unge, S. L. Mowbray, T. A. Jones, *Acta Crystallogr., Sect. D: Biol. Crystallogr.* **2012**, *68*, 134-143.
- (152) S. Yajima, K. Hara, D. Iino, Y. Sasaki, T. Kuzuyama, K. Ohsawa, H. Seto, *Acta Crystallogr., Sect. F: Struct. Biol. Cryst. Commun.* **2007**, *63*, 466-470.
- (153) M. Takenoya, A. Ohtaki, K. Noguchi, K. Endo, Y. Sasaki, K. Ohsawa, S. Yajima, M. Yohda, *J. Struct. Biol.* **2010**, *170*, 532-539.
- (154) T. Umeda, N. Tanaka, Y. Kusakabe, M. Nakanishi, Y. Kitade, K. T. Nakamura, *Sci. Rep.* **2011**, *1*, 1-8.
- (155) C. Branden, J. Tooze, *Introduction to Protein Structure*; Garland Publishing, Inc. New York, **1991**.
- (156) S. B. Richard, A. M. Lillo, C. N. Tetzlaff, M. E. Bowman, J. P. Noel, D. E. Cane, *Biochemistry* **2004**, *43*, 12189-12197.
- (157) D. E. Cane, C. Chow, A. Lillo, I. Kang, *Bioorg. Med. Chem.* **2001**, *9*, 1467-1477.
- (158) F. Rohdich, J. Wungsintaweekul, W. Eisenreich, G. Richter, C. A. Schuhr, S. Hecht, M. H. Zenk, A. Bacher, *Proc. Natl. Acad. Sci. USA* **2000**, *97*, 6451-6456.
- (159) T. Kuzuyama, M. Takagi, K. Kaneda, T. Dairi, H. Seto, *Tetrahedron Lett.* **2000**, *41*, 703-706.
- (160) J. Wungsintaweekul, *PhD thesis*, Technische Universität München (Germany), **2001**.
- (161) A. M. Lillo, C. N. Tetzlaff, F. J. Sangari, D. E. Cane, *Bioorg. Med. Chem. Lett.* **2003**, *13*, 737-739.
- (162) S. C. Weller, M. D. K. Owen, W. G. Johnson, *Glyphosate Resistance in Crops and Weeds* Wiley, Hoboken, **2010**.
- (163) K. Okada, H. Kawaide, T. Kuzuyama, H. Seto, I. S. Curtis, Y. Kamiya, *Planta* **2002**, *215*, 339-344.
- (164) M. Fellermeier, M. Raschke, S. Sagner, J. Wungsintaweekul, C. A. Schuhr, S. Hecht, K. Kis, T. Radykewicz, P. Adam, F. Rohdich, W. Eisenreich, A. Bacher, D. Arigoni, M. H. Zenk, *Eur. J. Biochem.* **2001**, *268*, 6302-6310.

- (165) V. Illarionova, J. Kaiser, E. Ostrozhenkova, A. Bacher, M. Fischer, W. Eisenreich, F. Rohdich, *J. Org. Chem.* **2006**, *71*, 8824-8834.
- (166) M. C. Witschel, H. W. Höffken, M. Seet, L. Parra, T. Mietzner, F. Thater, R. Niggeweg, F. Roehl, B. Illarionov, F. Rohdich, J. Kaiser, M. Fischer, A. Bacher, F. Diederich, *Angew. Chem., Int. Ed.* **2011**, *50*, 7931-7935; *Angew. Chem.* **2011**, *123*, 8077-8081.
- (167) M. Gabrielsen, J. Kaiser, F. Rohdich, W. Eisenreich, R. Laupitz, A. Bacher, C. S. Bond, W. N. Hunter, *FEBS J.* **2006**, *273*, 1065-1073.
- (168) S. B. Richard, M. E. Bowman, W. Kwiatkowski, I. Kang, C. Chow, A. M. Lillo, D. E. Cane, J. P. Noel, *Nat. Struct. Biol.* **2001**, *8*, 641-648.
- (169) J. Badger, J. M. Sauder, J. M. Adams, S. Antonysamy, K. Bain, M. G. Bergseid, S. G. Buchanan, M. D. Buchanan, Y. Batiyenko, J. A. Christopher, S. Emtage, A. Eroshkina, I. Feil, E. B. Furlong, K. S. Gajiwala, X. Gao, D. He, J. Hendle, A. Huber, K. Hoda, P. Kearins, C. Kissinger, B. Laubert, H. A. Lewis, J. Lin, K. Loomis, D. Lorimer, G. Louie, M. Maletic, C. D. Marsh, I. Miller, J. Molinari, H. J. Müller-Dieckmann, J. M. Newman, B. W. Noland, B. Pagarigan, F. Park, T. S. Peat, K. W. Post, S. Radojicic, A. Ramos, R. Romero, M. E. Rutter, W. E. Sanderson, K. D. Schwinn, J. Tresser, J. Winhoven, T. A. Wright, L. Wu, J. Xu, T. J. R. Harris, *Proteins: Struct., Funct., Bioinf.* **2005**, *60*, 787-796.
- (170) L. E. Kemp, C. S. Bond, W. N. Hunter, *Acta Crystallogr., Sect. D: Biol. Crystallogr.* **2003**, *59*, 607-610.
- (171) J. Behnen, H. Koester, G. Neudert, T. Craan, A. Heine, G. Klebe, *ChemMedChem* **2012**, *7*, 248-261.

## 2 SYNTHESIS AND ANTIPLASMODIAL ACTIVITY OF HIGHLY ACTIVE REVERSE ANALOGS OF FOSMIDOMYCIN



This chapter is adapted with permission from the following publication:

“Synthesis and antiplasmodial activity of highly active reverse analogs of the antimalarial drug candidate fosmidomycin”

Christoph T. Behrendt, **Andrea Kunfermann**, Victoriya Illarionova, An Matheussen, Tobias Gräwert, Michael Groll, Felix Rohdich, Adelbert Bacher, Wolfgang Eisenreich, Markus Fischer, Louis Maes, and Thomas Kurz.

*ChemMedChem* **2010**, 5 (10), 1673-1676.

Copyright (2010) John Wiley & Sons, Inc.



## 2.2 Zusammenfassung

Für eine lange Zeit war nur der Mevalonat-abhängige Weg für die Biosynthese der Vorläufer von Isoprenoiden, IPP und DMAPP, bekannt. In den frühen 90er Jahren wurde ein alternativer Weg entdeckt: der Desoxyxylulosephosphat-Weg, auch Mevalonat-unabhängiger Weg genannt. Dieser alternative Stoffwechselweg kommt in diversen pathogenen Bakterien (z. B. *M. tuberculosis*), in Pflanzen und in apicomplexen Protozoen (z. B. *P. falciparum*) vor, jedoch nicht in Säugetieren. Aus diesem Grund sind die Enzyme des Mevalonat-unabhängigen Weges im zentralen Fokus für potentielle Antiinfektiva und Anti-Malariamittel. Besonders IspC hat sich über die Jahre zu einem validierten Angriffsziel für Inhibitoren entwickelt. In klinischen Studien mit dem natürlich vorkommenden Hemmstoff Fosmidomycin (**1**) konnten bereits Erfolge mit hoher Effizienz bei der Behandlung von Malaria tropica erzielt werden, jedoch ist die orale Bioverfügbarkeit von **1** gering. Deshalb ist es wichtig, neue IspC Inhibitoren zu entwickeln, die dieses Problem angehen. Eine Serie von verbesserten Analoga von **1** wurde synthetisiert und ihre inhibitorische Aktivität gegen rekombinantes *EclspC* und *PflspC* sowie deren *in vitro* antiplasmodiale Aktivität und Zytotoxizität untersucht. Diese neuen Verbindungen weisen eine Substitution an der  $\alpha$ -Arylposition sowie eine reverse Orientierung der Hydroxamsäuregruppe auf. Die neu synthetisierten Liganden (**12**, **14**, **19** und **20**) sowie die Referenzverbindungen (**1** und FR900098 (**2**)) wurden in photometrischen Aktivitätsassays gegen *PflspC* und *EclspC* analysiert. Es konnte gezeigt werden, dass die Verbindungen **12** und **14** starke und selektive Hemmstoffe gegen *PflspC* sind. Verbindung **14** mit der *N*-Methyl-substituierten Hydroxamsäure ist mit einem  $IC_{50}$  Wert von 3.1 nM der stärkste bisher bekannte Inhibitor gegen *PflspC*. Die Aktivität von **14** gegen *EclspC* ist vergleichbar mit **1** und etwas schwächer als **2**, die Hemmwirkung befindet sich jedoch immer noch im nanomolaren Bereich. Bemerkenswerterweise sind erst einige wenige *N*-Methyl-substituierte Hydroxamsäureverbindungen als Hemmstoffe von Metalloenzymen identifiziert worden. Folglich repräsentiert **14** eine neue, vielversprechende Leitstruktur für die Entwicklung von anti-Malaria und antibakteriellen Wirkstoffen.

Mein Beitrag zu dieser Veröffentlichung war die Durchführung der photometrischen Aktivitätsassays mit *EclspC* zur Bestimmung der  $IC_{50}$  Werte der oben genannten Verbindungen. Zusätzlich war ich zusammen mit Dr. Christoph T. Behrendt an der Herstellung des Manuskripts beteiligt. Bei dieser Publikation bin ich Zweitautorin.

## 2.3 Background

Although potent antimalarial drugs are available, the spread of drug resistance has led to an increase in morbidity and mortality rates in malaria-endemic regions. To overcome these problems, new antimalarial drugs with novel modes of action have to be developed. The recently discovered non-mevalonate pathway of isoprenoid biosynthesis is an important target for the design of novel antimalarial drugs.<sup>[1-4]</sup> Various pathogenic bacteria (e.g. *M. tuberculosis*) and apicomplexan protozoa (e.g. *P. falciparum*) use the non-mevalonate pathway for the production of IPP and DMAPP.<sup>[5-7]</sup> These products are important precursors for the biosynthesis of various essential isoprenoids. In contrast to the mentioned microorganisms, humans produce IPP and DMAPP exclusively via the mevalonate pathway. The second enzyme of the non-mevalonate pathway, 1-deoxy-D-xylulose-5-phosphate reductoisomerase (IspC, DXR) represents a validated target enzyme for the development of new antimalarial drugs.<sup>[7]</sup> In 1998, the natural product **1** was identified as a potent inhibitor of *PfIspC*.<sup>[8-10]</sup> IspC catalyzes the rearrangement and reduction of DXP into MEP. While the first step of the reaction requires a divalent cation (e.g.  $Mn^{2+}$  or  $Mg^{2+}$ ), the reduction step is NADPH-dependent.<sup>[11]</sup> Clinical trials performed with **1** have already shown high efficiency in the treatment of acute, uncomplicated malaria tropica.<sup>[12-14]</sup> However, the oral bioavailability of **1** is only moderate, with a resorption rate of about 10-30%.<sup>[8-10,15]</sup>

Various research groups are involved in the design of novel IspC inhibitors.<sup>[6]</sup> Molecular field analyses, as well as crystallographic studies, could already contribute in defining structural requirements for the development of potent IspC inhibitors.<sup>[16-19]</sup> Consequently, different types of IspC inhibitors have been synthesized and biologically evaluated.<sup>[6,7,20,21]</sup> Important structural elements for potent antimalarial activity are the hydroxamic acid functionality and the phosphonic acid group.<sup>[7,20,21]</sup> The **1**:IspC complex crystal structure clearly revealed that the hydroxamic acid functionality chelates the divalent cation, while the phosphonic acid group occupies the phosphate binding site.<sup>[17-19]</sup> Moreover, a defined distance between both functional groups is essential for potent antimalarial activity. Schlitzer and Klebe have shown that the two negative charges of the phosphonic acid group are necessary for high inhibitory activity.<sup>[22]</sup> Furthermore, phosphonate prodrugs have been designed to improve the bioavailability of **1** and FR900098 (**2**) (Figure 2.1).<sup>[23-30]</sup> A combinatorial approach for the synthesis of non-hydrolysable phosphate mimics was reported by Link and coworkers,<sup>[31]</sup> while Song recently described a coordination chemistry-based approach for the development of lipophilic IspC inhibitors that exhibit good to moderate activity against various pathogenic bacteria.<sup>[32]</sup> To the best of our

knowledge,  $\alpha$ -aryl-substituted derivatives (**4**, Figure 2.1) of **1** are among the most active analogs known so far.<sup>[33-37]</sup> Recently, Van Calenbergh reported that  $\beta$ -oxa isosters of **1** (**3a** and **3b**, Figure 2.1) exhibit strong *in vitro* antimalarial activity.<sup>[38]</sup> Interestingly, some of the new compounds contain an *N*-methyl-substituted hydroxamic acid group with a reverse orientation of the hydroxamate group (**3b**) compared to the lead compounds (**1** and **2**).

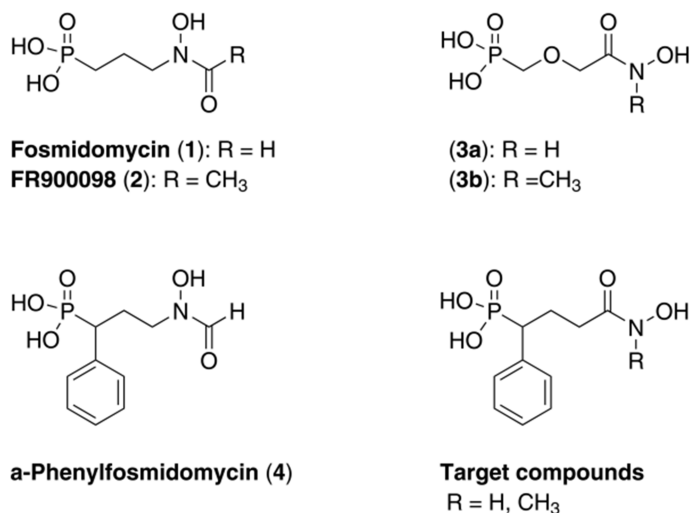


**Figure 2.1** Schematic representation of compounds.

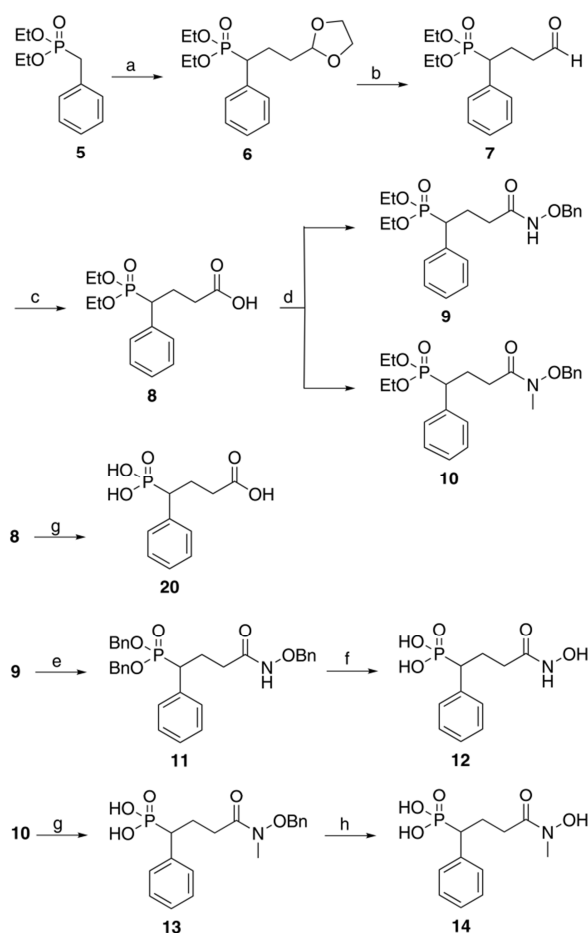
Due to difficulties associated with the handling of *PflspC*, no data concerning the inhibitory activity of these analogs toward *PflspC* have been reported.<sup>[7,38]</sup> Furthermore, Rohmer and coworkers presented several reverse analogs of **1**, which in part inhibit recombinant *EclspC*.<sup>[39,40]</sup> In order to improve the antiplasmodial activity and lipophilicity of lead compounds **1** and **2**, we investigated the synthesis and antiplasmodial activity of reverse  $\alpha$ -phenyl-substituted analogs of the natural products **1** and **2**. Our novel analogs contain the promising  $\alpha$ -phenyl substitution, as well as the reverse orientation of the hydroxamic acid group.

## 2.4 Results and discussion

### 2.4.1 Synthesis of the compounds

Both lead compounds, **1** and **2**, were synthesized as mono-sodium salts according to established literature procedures.<sup>[41]</sup> Diethyl benzylphosphonate **5** was chosen as the starting material for the preparation of target compounds **12** and **14**.<sup>[42]</sup> C-Alkylation of substrate **5** with [2-(1,3-

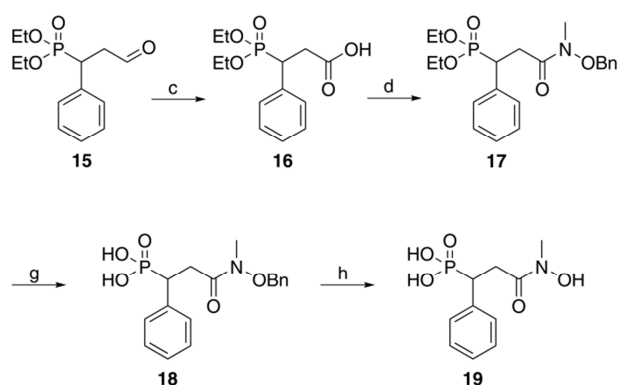
dioxolan-2-yl)ethyl]bromide in the presence of *n*-butyllithium (*n*-BuLi) provided 1,3-dioxolane **6** in 92% yield. Acidic hydrolysis of the 1,3-dioxolane moiety of compound **6** furnished the expected aldehyde **7**, which was smoothly oxidized to the corresponding carboxylic acid **8** by treatment with SeO<sub>2</sub> and H<sub>2</sub>O<sub>2</sub> (Scheme 2.1).<sup>[43]</sup> Conversion of **8** into phosphonic acid **20** was achieved by reacting **8** subsequently with bromotrimethylsilane and water. The synthesis of *O*-benzylprotected hydroxamic acids **9** and **10** was accomplished by 1,1'-carbonyldiimidazole (CDI)-mediated coupling reactions of compound **8** with *O*-benzyl-hydroxylamine and *N*-methyl-*O*-benzyl-hydroxylamine, respectively.<sup>[44]</sup> Cleavage of the phosphonic acid ester group of intermediate **9** using trimethylsilyl bromide (TMSBr) led to the corresponding oily and hygroscopic phosphonic acid, which was directly converted into dibenzylphosphonate **11**.<sup>[45]</sup>



**Scheme 2.1** Synthesis of reverse analogs **12** and **14**. Reagents and conditions: a) *n*-BuLi, [2-(1,3-dioxolan-2-yl)ethyl]bromide, toluene, -78 °C, 12 h, 92%; b) 2 M HCl, acetone, 50 °C, 3 h, 85%; c) SeO<sub>2</sub>, H<sub>2</sub>O<sub>2</sub>, THF, 65 °C, 4 h, 92%; d) CDI, BnONHR (R=H, CH<sub>3</sub>), CH<sub>2</sub>Cl<sub>2</sub>, rt, 12 h, 80–95%; e) 1. TMSBr, CH<sub>2</sub>Cl<sub>2</sub>, rt, 24 h; 2. THF/H<sub>2</sub>O (100:1), rt, 1 h; 3. *N,N'*-dicyclohexylcarbodiimide (DCC), BnOH, benzene, 80 °C, 4 h, 12% (three steps); f) H<sub>2</sub>, Pd-C, MeOH, rt, 3 h, 67%; g) 1. TMSBr, CH<sub>2</sub>Cl<sub>2</sub>, rt, 24 h; 2. THF/H<sub>2</sub>O (100:1), rt, 1 h, 74% (two steps); h) H<sub>2</sub>, Pd-C, MeOH, rt, 1 h, 92%.



In contrast to the behavior of **9**, dealkylation of diethyl phosphonate **10** provided phosphonic acid **13** as white and crystalline solid. Finally, catalytic hydrogenation of precursors **11** and **13** afforded target compounds **12** and **14** in good yields and high purity (Scheme 2.1). Starting from aldehyde **15**,<sup>[46]</sup> the chain-shortened derivative **19** was accessible using the same synthetic concept as described for compound **14** (Scheme 2.2). Structure elucidation was accomplished by IR, <sup>1</sup>H and <sup>13</sup>C NMR spectroscopy, as well as by mass spectrometry, elemental analysis and HPLC analysis.



**Scheme 2.2** Synthesis of chain-shortened derivative **19**. Reagents and conditions: a)  $\text{SeO}_2$ ,  $\text{H}_2\text{O}_2$ , THF, 65 °C, 4 h, 94%; b) CDI,  $\text{BnONHCH}_3$ ,  $\text{CH}_2\text{Cl}_2$ , rt, 12 h, 99%; c) 1. Trimethylsilylbromide,  $\text{CH}_2\text{Cl}_2$ , rt, 24 h; 2. THF/ $\text{H}_2\text{O}$  (100:1), rt, 1 h, 89% (two steps); d)  $\text{H}_2$ , Pd-C, MeOH, rt, 1 h, 92%.

#### 2.4.2 Photometric activity assays

To prove the mode of action and to evaluate the biological activity, the new analogs (**12**, **14**, **19**, and **20**) and both reference compounds (**1** and **2**) were first tested for the inhibition of recombinant IspC from *P. falciparum* and *E. coli*. For that purpose, recombinant *E. coli* strain harboring a synthetic gene that was optimized for expression under the control of a T5 promoter and a *lac* operator direct the synthesis of the protozoan enzyme in substantial amounts. The recombinant protein can be isolated rapidly by affinity chromatography and fulfills the stability requirements for the biological evaluation of new IspC inhibitors. Both enzyme assays are based on the photometric determination of NADPH turnover, which is associated with the IspC-catalyzed reaction (Table 2.1).

**Table 2.1** *In vitro* activity<sup>[a]</sup> and cytotoxicity<sup>[a]</sup>.

Compound	IC <sub>50</sub> [nM]		IC <sub>50</sub> [μM]	
	<i>Pf</i> spC	<i>Ecl</i> spC	<i>Pf</i> -K1 <sup>[b]</sup>	MRC-5
<b>1</b>	143.7 ± 15.5	221.3 ± 14.4	3.71 ± 2.47	> 62
<b>2</b>	15.3 ± 1.2	131.3 ± 2.9	1.48 ± 0.84	> 59
<b>12</b>	11.6 ± 3.1	592 ± 25.0	3.87 ± 1.81	> 59
<b>14</b>	3.1 ± 0.3	243 ± 29.6	0.59 ± 0.2	> 60
<b>19</b>	inactive	inactive	inactive	> 64
<b>20</b>	inactive	inactive	inactive	> 64

<sup>[a]</sup>Values are the mean ± SD of three or more independent experiments.

<sup>[b]</sup>Multi-drug resistant strain of *P. falciparum*.

Hydroxamic acids **12** and **14** were found to be strong and selective inhibitors of *Pf*spC. Compounds **12** and **14** exhibited stronger inhibitory activity against the plasmodial enzyme than the reference compounds **1** and **2**. With an IC<sub>50</sub> value of 3.1 nM, the *N*-methyl-substituted hydroxamic acid **14** represents the most powerful *Pf*spC inhibitor described so far. However, compound **14** is less active than **2** towards *Ecl*spC and approximately as active as **1**. Compared to compounds **1**, **2**, and **14** the inhibitory potency of compound **12** against the *E. coli* enzyme is significantly weaker.

The *K<sub>i</sub>* values of compounds **1**, **2**, **12**, and **14**, determined experimentally in case of *Pf*spC and calculated in case of *Ecl*spC, further support our findings (Table 2.2). In contrast, carboxylic acid **20**, as well as the chain-shortened derivative **19**, did not show any inhibitory activity against either recombinant IspC enzymes. Next, compounds **1**, **2**, **12**, and **14** were evaluated for their *in vitro* antiplasmodial activity against the multidrug-resistant K1 strain of *P. falciparum* and for their cytotoxicity on human MRC-5 cells. Again, the *N*-methyl-substituted hydroxamic acid **14** demonstrated the highest inhibitory activity (IC<sub>50</sub>=0.59 μM), while the free hydroxamic acid **12** was approximately as active as **1**. We assume that the high activity of compound **14** is most likely due to the *N*-methyl group, which might mimic the methyl group present in **2**. None of the evaluated compounds showed cytotoxic effects on human MRC-5 cells (Table 2.1).

**Table 2.2**  $K_i$  values of compounds **1**, **2**, **12**, and **14**, determined experimentally for *PflspC* and calculated for *EclspC*.

Compound	<i>PflspC</i>	<i>EclspC</i> <sup>[b]</sup>
	$K_i$ [nM] <sup>[a]</sup>	$K_i$ [nM] <sup>[a]</sup>
<b>1</b>	8.4 ± 0.6	21.2
<b>2</b>	2.6 ± 0.2	12.6
<b>12</b>	2.1 ± 0.1	56.7
<b>14</b>	0.42 ± 0.03	23.3

<sup>[a]</sup>Values are the mean ± SD of three or more independent experiments.

<sup>[b]</sup>Values were calculated using Cheng-Prusoff equation:  $K_i = IC_{50} / (1 + [S] / K_m)$ .<sup>[47]</sup>

### 2.4.3 Conclusion

In conclusion, we have developed a highly active and selective *PflspC* inhibitor with a unique chemical structure. To the best of our knowledge, compound **14** is the most active inhibitor of *PflspC* described so far. In contrast to both lead compounds, compound **14** contains a lipophilic aromatic region in the  $\alpha$ -position relative to the phosphonic acid moiety, as well as an *N*-methyl-substituted hydroxamic acid functionality. Up to now, only very few *N*-substituted hydroxamic acids have been identified as metalloenzyme inhibitors.<sup>[48]</sup> Therefore, compound **14** represents a promising new lead compound for the development of novel antimalarial drugs.

## 2.5 Experimental section

### 2.5.1 Enzyme assays

#### Materials

[3,4,5-<sup>13</sup>C<sub>3</sub>]-DXP was prepared as reported earlier.<sup>[49]</sup> Recombinant IspC protein from *E. coli* was prepared as reported earlier.<sup>[50]</sup> The amino acid sequence of the *ispC* gene from *P. falciparum* (GenBank: HQ018930), with omission of amino acid residues 1–73, was back-translated in line with the codon usage of *E. coli* (<http://www.kazusa.or.jp/codon/>). The artificial open reading frame was cloned into the vector pQE30 (Qiagen; Hilden, Germany). The vector-derived amino acid sequence resulted in the extension MRGSHHHHHGS preceding residue 74 of the N-terminus of the synthetic construct (pQEispCplart). The supernatant of *E. coli* XL1-

pQEispCplasart cells was applied to a column of Ni<sup>2+</sup>-chelating Sepharose Fast Flow<sup>®</sup> (Amersham Pharmacia Biotech; Freiburg, Germany; column volume: 20 mL) and the column was washed with 100 mM Tris-HCl (pH 7.5), containing 500 mM NaCl, 20 mM imidazole and 10% glycerol (v/v), and was then developed with a gradient of 20-500 mM imidazole in 100 mM Tris-HCl (pH 7.5), containing 500 mM NaCl and 10% glycerol (total volume: 200 mL). Fractions were combined, concentrated by ultrafiltration (10 kDa) and desalted with a HIPREP 26/10 column (Amersham Pharmacia Biotech; Freiburg, Germany) in 50 mM Tris-HCl (pH 7.5), containing 10% glycerol. After addition of dithiothreitol (DTT) to give a final concentration of 5 mM, the protein was stored at -80 °C. NADPH was purchased from BioMol (Hamburg, Germany). Fosmidomycin sodium salt was purchased from Molekula Deutschland Ltd. (Taufkirchen, Germany).

### **IC<sub>50</sub> determination using the photometric assay**

Assays were conducted in 96-well Nunc plates (Sigma-Aldrich; St. Louis, USA) with a transparent flat bottom. Assay mixtures (total volume: 200 mL) contained 100 mM Tris-HCl (pH 7.6), 4 mM MnCl<sub>2</sub>, 0.5 mM DTT, 0.5 mM NADPH, and 10-30 nM of recombinant IspC protein (*P. falciparum*) or 100 mM Tris-HCl (pH 8.0), 10 mM MgCl<sub>2</sub>, 1 mM NADPH, and 27 nM of recombinant IspC protein (*E. coli*). Dilution series (1:2) of inhibitors covered the concentration range of 200 μM to 1 nM. The reaction was started by addition of DXP to a final concentration of 1 mM. The reaction was monitored photometrically (room temperature for *P. falciparum* or 37 °C for *E. coli*) at 340 nm in a microplate reader (*P. falciparum*: Multiskan Spectrum (Thermo Scientific; Waltham, USA); *E. coli*: SpectraMax M2 (Molecular Devices; Sunnyvale, USA)). Initial rate values were evaluated with a nonlinear regression method using the program Dynafit.<sup>[51]</sup>

### **2.5.2 Biological evaluation of antiplasmodial activity and cytotoxicity**

#### **Test plate production**

The experiments were performed in 96-well Greiner plates (Greiner Bio-One; Kremsmünster, Austria) at four-fold dilutions in a dose titration range of 64 μg mL<sup>-1</sup> to 0.25 μg mL<sup>-1</sup>. Dilutions were carried out by a programmable precision robotic station (Biomek 2000; Beckman Coulter, Brea, USA). Each plate also contained medium controls (blanks: 0% growth), infected untreated controls (negative control: 100% growth) and reference controls (positive control: chloroquine). Tests were run in triplicate.

### **Biological screening tests**

The integrated panel of microbial screens used in this study and the standard screening methodologies were adopted from those described by Cos and coworkers.<sup>[52]</sup>

#### ***In vitro P. falciparum* culture and drug assay**

The chloroquine-resistant K1 strain was used. Parasites were cultured in human erythrocytes A+ at 37 °C under a low oxygen atmosphere (3% O<sub>2</sub>, 4% CO<sub>2</sub>, and 93% N<sub>2</sub>) in a modular incubation chamber. The culture medium was RPMI-1640, supplemented with 10% human serum. A suspension of infected human red blood cells (1% parasitaemia, 2% haematocrit; 200 mL) was added to each well of the plates with test compounds and incubated for 72 h. After incubation, test plates were frozen at -20 °C. Parasite multiplication was measured by the Malstat method.<sup>[53]</sup> Malstat reagent (100 mL) was transferred in a new plate and mixed with hemolysed parasite suspension (20 mL) for 15 min at rt. After addition of NBT/PES solution (20 mL) and 2 h incubation in the dark, the absorbance was spectrophotometrically read at 655 nm (Biorad 3550-UV microplate reader). Percentage growth inhibition was calculated by comparison to the negative blanks.

#### **Cytotoxic test upon MRC-5 cells**

MRC-5 SV2 cells, human fetal lung fibroblast, were cultivated in minimum essential medium supplemented with 20 mM L-glutamine, 16.5 mM NaHCO<sub>3</sub> and 5% fetal calf serum at 37 °C and 5% CO<sub>2</sub>. For the assay, MRC-5 cells (10<sup>4</sup> per well) were seeded onto the test plates containing the prediluted compounds and incubated at 37 °C and 5% CO<sub>2</sub> for 72 h. After incubation, parasite growth was assessed fluorimetrically by adding resazurin for 24 h at 37 °C. Fluorescence was measured using a GENios Tecan fluorimeter (excitation 530 nm, emission 590 nm).

### **2.5.3 Supporting Information**

The Supporting Information and the full article are available under DOI: 10.1002/cmdc.201000276.

## 2.6 References

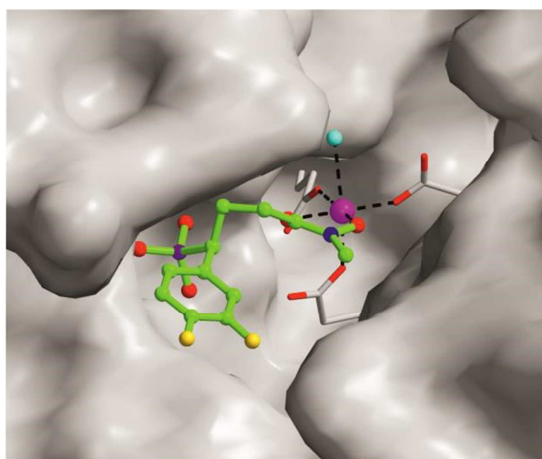
- (1) M. Rohmer, M. Knani, P. Simonin, B. Sutter, H. Sahn, *Biochem. J.* **1993**, *295*, 517-524.
- (2) H. K. Lichtenthaler, J. Schwender, A. Disch, M. Rohmer, *FEBS Lett.* **1997**, *400*, 271-274.
- (3) M. Rohmer, *Nat. Prod. Rep.* **1999**, *16*, 565-573.
- (4) W. Eisenreich, A. Bacher, D. Arigoni, F. Rohdich, *Cell. Mol. Life Sci.* **2004**, *61*, 1401-1426.
- (5) M. Rohmer, C. Grosdemange-Billiard, M. Seemann, D. Tritsch, *Curr. Opin. Invest. Drugs* **2004**, *5*, 154-162.
- (6) N. Singh, G. Chev e, M. A. Avery, C. R. McCurdy, *Curr. Pharm. Des.* **2007**, *13*, 1161-1177.
- (7) J. Wiesner, H. Jomaa, *Curr. Drug Targets* **2007**, *8*, 3-13.
- (8) H. Jomaa, J. Wiesner, S. Sanderbrand, B. Altincicek, C. Weidemeyer, M. Hintz, I. Turbachova, M. Eberl, J. Zeidler, H. K. Lichtenthaler, D. Soldati, E. Beck, *Science* **1999**, *285*, 1573-1576.
- (9) M. Okuhara, Y. Kuroda, T. Goto, M. Okamoto, H. Terano, M. Kohsaka, H. Aoki, H. Imanaka, *J. Antibiot.* **1980**, *33*, 13-17.
- (10) M. Okuhara, Y. Kuroda, T. Goto, M. Okamoto, H. Terano, M. Kohsaka, H. Aoki, H. Imanaka, *J. Antibiot.* **1980**, *33*, 24-28.
- (11) P. J. Proteau, *Bioorg. Chem.* **2004**, *32*, 483-493.
- (12) B. Lell, R. Ruangweerayut, J. Wiesner, M. A. Missinou, A. Schindler, T. Baranek, M. Hintz, D. Hutchinson, H. Jomaa, P. G. Kremsner, *Antimicrob. Agents Chemother.* **2003**, *47*, 735-738.
- (13) S. Borrmann, I. Lundgren, S. Oyakhirome, B. Impouma, P. B. Matsiegui, A. A. Adegnika, S. Issifou, J. F. J. Kun, D. Hutchinson, J. Wiesner, H. Jomaa, P. G. Kremsner, *Antimicrob. Agents Chemother.* **2006**, *50*, 2713-2718.
- (14) K. Na-Bangchang, R. Ruengweerayut, J. Karbwang, A. Chauemung, D. Hutchinson, *Malar. J.* **2007**, *6*, 70.
- (15) T. Murakawa, H. Sakamoto, S. Fukada, T. Konishi, M. Nishida, *Antimicrob. Agents Chemother.* **1982**, *21*, 224-230.
- (16) K. Silber, P. Heidler, T. Kurz, G. Klebe, *J. Med. Chem.* **2005**, *48*, 3547-3563.
- (17) S. Steinbacher, J. Kaiser, W. Eisenreich, R. Huber, A. Bacher, F. Rohdich, *J. Biol. Chem.* **2003**, *278*, 18401-18407.
- (18) A. Mac Sweeney, R. Lange, R. P. M. Fernandes, H. Schulz, G. E. Dale, A. Douangamath, P. J. Proteau, C. Oefner, *J. Mol. Biol.* **2005**, *345*, 115-127.
- (19) S. Yajima, K. Hara, D. Iino, Y. Sasaki, T. Kuzuyama, K. Ohsawa, H. Seto, *Acta Crystallogr., Sect. F: Struct. Biol. Cryst. Commun.* **2007**, *63*, 466-470.

- (20) T. Kurz, D. Geffken, C. Wackendorff, *Z. Naturforsch., B: J. Chem. Sci.* **2003**, *58*, 106-110.
- (21) T. Kurz, D. Geffken, C. Wackendorff, *Z. Naturforsch., B: J. Chem. Sci.* **2003**, *58*, 457-461.
- (22) J. Perruchon, R. Ortmann, M. Altenkaemper, K. Silber, J. Wiesner, H. Jomaa, G. Klebe, M. Schlitzer, *ChemMedChem* **2008**, *3*, 1232-1241.
- (23) A. Reichenberg, J. Wiesner, C. Weidemeyer, E. Dreiseidler, S. Sanderbrand, B. Altincicek, E. Beck, M. Schlitzer, H. Jomaa, *Bioorg. Med. Chem. Lett.* **2001**, *11*, 833-835.
- (24) K. Schlüter, R. D. Walter, B. Bergmann, T. Kurz, *Eur. J. Med. Chem.* **2006**, *41*, 1385-1397.
- (25) V. Devreux, J. Wiesner, J. L. Goeman, J. Van der Eycken, H. Jomaa, S. Van Calenbergh, *J. Med. Chem.* **2006**, *49*, 2656-2660.
- (26) R. Ortmann, J. Wiesner, A. Reichenberg, D. Henschker, E. Beck, H. Jomaa, M. Schlitzer, *Bioorg. Med. Chem. Lett.* **2003**, *13*, 2163-2166.
- (27) T. Kurz, K. Schlüter, U. Kaula, B. Bergmann, R. D. Walter, D. Geffken, *Bioorg. Med. Chem.* **2006**, *14*, 5121-5135.
- (28) T. Kurz, C. T. Behrendt, U. Kaula, B. Bergmann, R. D. Walter, *R. D. Aust. J. Chem.* **2007**, *60*, 154-158.
- (29) T. Kurz, C. T. Behrendt, M. Pein, U. Kaula, B. Bergmann, R. D. Walter, *Arch. Pharm.* **2007**, *340*, 661-666.
- (30) R. Ortmann, J. Wiesner, A. Reichenberg, D. Henschker, E. Beck, H. Jomaa, M. Schlitzer, *Arch. Pharm.* **2005**, *338*, 305-314.
- (31) D. Gießmann, P. Heidler, T. Haemers, S. Van Calenbergh, A. Reichenberg, H. Jomaa, C. Weidemeyer, S. Sanderbrand, J. Wiesner, A. Link, *Chem. Biodiversity* **2008**, *5*, 643-656.
- (32) L. Deng, S. Sundriyal, V. Rubio, Z. Shi, Y. Song, *J. Med. Chem.* **2009**, *52*, 6539-6542.
- (33) T. Haemers, J. Wiesner, S. Van Poecke, J. Goeman, D. Henschker, E. Beck, H. Jomaa, S. Van Calenbergh, *Bioorg. Med. Chem. Lett.* **2006**, *16*, 1888-1891.
- (34) V. Devreux, J. Wiesner, H. Jomaa, J. Van der Eycken, S. Van Calenbergh, *Bioorg. Med. Chem. Lett.* **2007**, *17*, 4920-4923.
- (35) V. Devreux, J. Wiesner, H. Jomaa, J. Rozenski, J. Van der Eycken, S. Van Calenbergh, *J. Org. Chem.* **2007**, *72*, 3783-3789.
- (36) S. Van der Jeught, C. V. Stevens, N. Dieltiens, *Synlett* **2007**, 3183-3187.
- (37) T. Kurz, D. Geffken, U. Kaula, (Bioagency AG; Hamburg, Germany), WO 2005/048715A2, **2005**.
- (38) T. Haemers, J. Wiesner, R. Busson, H. Jomaa, S. Van Calenbergh, *Eur. J. Org. Chem.* **2006**, 3856-3863.
- (39) L. Kuntz, D. Tritsch, C. Grosdemange-Billiard, A. Hemmerlin, A. Willem, T. J. Bacht, M.

- Rohmer, *Biochem. J.* **2005**, *386*, 127-135.
- (40) C. Zingle, L. Kuntz, D. Tritsch, C. Grosdemange-Billiard, M. Rohmer, *J. Org. Chem.* **2010**, *75*, 3203-3207.
- (41) T. Kamiya, K. Hemmi, H. Takeno, M. Hashimoto, *Tetrahedron Lett.* **1980**, *21*, 95-98.
- (42) E. V. Matveeva, I. L. Odinets, V. A. Kozlov, A. S. Shaplov, T. A. Mastryukova, *Tetrahedron Lett.* **2006**, *47*, 7645-7648.
- (43) M. Brzascz, K. Kloc, M. Maposah, J. Mlochowski, *Synth. Commun.* **2000**, *30*, 4425-4434.
- (44) K. Ramasamy, R. K. Olsen, T. Emery, *J. Org. Chem.* **1981**, *46*, 5438-5441.
- (45) L. J. Mathias, *Synthesis* **1979**, 561-576.
- (46) R. G. Harvey, *Tetrahedron* **1966**, *22*, 2561-2573.
- (47) Y. Cheng, W. H. Prusoff, *Biochem. Pharmacol.* **1973**, *22*, 3099-3108.
- (48) H. K. Smith, R. P. Beckett, J. M. Clements, S. Doel, S. P. East, S. B. Launchbury, L. M. Pratt, Z. M. Spavold, W. Thomas, R. S. Todd, M. Whittaker, *Bioorg. Med. Chem. Lett.* **2002**, *12*, 3595-3599.
- (49) V. Illarionova, J. Kaiser, E. Ostrozhenkova, A. Bacher, M. Fischer, W. Eisenreich, F. Rohdich, *J. Org. Chem.* **2006**, *71*, 8824-8834.
- (50) S. Hecht, J. Wungsintaweekul, F. Rohdich, K. Kis, T. Radykewicz, C. A. Schuhr, W. Eisenreich, G. Richter, A. Bacher, *J. Org. Chem.* **2001**, *66*, 7770-7775.
- (51) P. Kuzmic, *Anal. Biochem.* **1996**, *237*, 260-273.
- (52) P. Cos, A. J. Vlietinck, D. Vanden Berghe, L. Maes, *J. Ethnopharmacol.* **2006**, *106*, 290-302.
- (53) M. T. Makler, J. M. Ries, J. A. Williams, J. E. Bancroft, R. C. Piper, B. L. Gibbins, D. J. Hinrichs, *Am. J. Trop. Med. Hyg.* **1993**, *48*, 739-741.



### 3 REVERSE FOSMIDOMYCIN DERIVATIVES AGAINST THE ANTIMALARIAL DRUG TARGET ISPC



This chapter is adapted with permission from the following publication:

“Reverse fosmidomycin derivatives against the antimalarial drug target IspC (Dxr)”

Christoph T. Behrendt, \* **Andrea Kunfermann**,\* Victoriya Illarionova, An Matheussen, Miriam K. Pein, Tobias Gräwert, Johannes Kaiser, Adelbert Bacher, Wolfgang Eisenreich, Boris Illarionov, Markus Fischer, Louis Maes, Michael Groll, and Thomas Kurz.

*J. Med. Chem.* **2011**, *54* (19), 6796-6802.

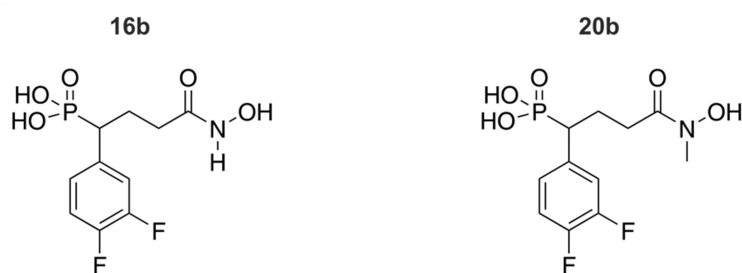
\*These authors contributed equally.

Copyright (2011) American Chemical Society.

### 3.1 Summary

Nowadays, novel therapeutic agents are urgently needed in order to deal with the ongoing problems of malarial as well as bacterial infections. A well-known target is the non-mevalonate pathway enzyme IspC that is present in *P. falciparum* as well as *M. tuberculosis* and *E. coli*, but absent in mammals. The natural product fosmidomycin (**1**) exhibited strong inhibition of IspC *in vitro* and has been successfully used in clinical malaria trials. Unfortunately, the pharmacokinetic properties are not satisfying yet, therefore improvement of **1** is still required. In this chapter, novel reverse analogs of **1** are presented whose mode of action was determined by a combination of *in vivo* experiments using a mouse model, *in vitro* kinetic characterization and crystallographic studies. It was shown in the acute mouse model that compound **16b** has some potential against *Plasmodium berghei* as its *in vivo* efficacy was comparable to a known antimalarial positive control (chloroquine), suggesting that **16b** is a promising candidate for future pharmacological studies. The kinetic *in vitro* experiments revealed that compound **16b** as well as **20b** are stronger inhibitors against *Pf*IspC than **1**, with IC<sub>50</sub> values of 3 nM. In comparison with *Ecl*IspC, the values are still in the nanomolar range, but exceed those of *Pf*IspC by one to three orders of magnitude. Crystallographic studies determined that the coordination of a divalent metal ion by the new, reverse hydroxamic acid compounds is the same as for **1**. Furthermore, binding of compound **20b** lead to an open conformation as the loop that covers the active site is distorted. The residues in the binding site are strictly conserved between *E. coli* and *P. falciparum*, although the overall sequence homology is very low (29%). As a consequence, the problem of strong cross-reactions of inhibitors against *Ecl*IspC and *Pf*IspC in e.g., the human body, can be diminished.

My major contribution to this publication was the accomplishment of initial kinetic studies on *Ecl*IspC and the crystallographic work. In addition, I was directly involved in writing the manuscript together with Dr. Christoph T. Behrendt. On this publication, I am first author with equal contribution of Dr. Christoph T. Behrendt.



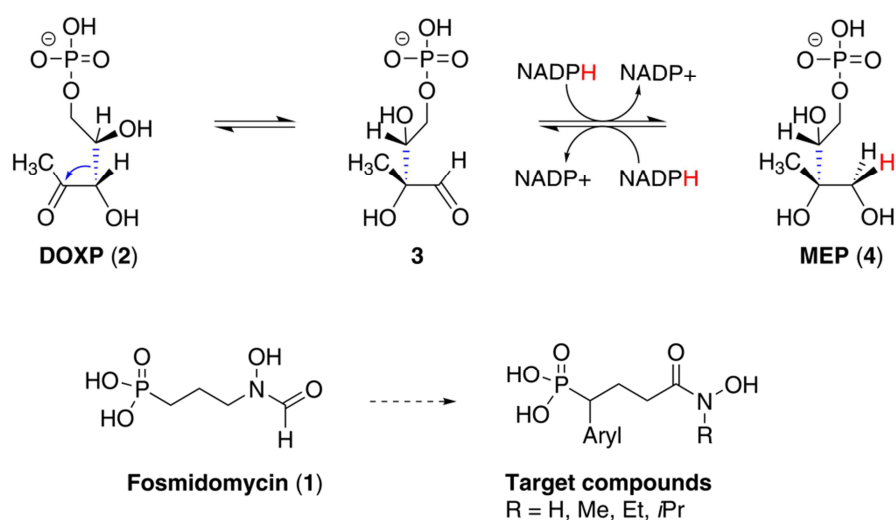
### 3.2 Zusammenfassung

Heutzutage sind neue therapeutische Medikamente gegen Malaria und bakterielle Infektionen von immenser Bedeutung, um den gegenwärtigen Problemen hinsichtlich Bioverfügbarkeit und Resistenzentwicklung entgegenzuwirken. Ein bekanntes Zielenzym ist IspC aus dem Mevalonat-unabhängigen Weg, welcher in *P. falciparum* sowie in *M. tuberculosis* und *E. coli* vorkommt, nicht jedoch in Säugetieren. Es wurde gezeigt, dass der Naturstoff Fosmidomycin (**1**) *in vitro* starke Hemmwirkung gegen IspC aufweist, so dass diese Verbindung bereits erfolgreich in klinischen Malariastudien getestet wurde. Bedauerlicherweise sind die pharmakokinetischen Eigenschaften für die Anwendung am Menschen nicht zufriedenstellend, weshalb weitere Optimierungen von **1** notwendig sind. In diesem Kapitel werden neue, reverse Analoga von **1** vorgestellt, deren Wirkungsweise durch eine Kombination von *in vivo* Mausexperimenten, kinetischer *in vitro* Charakterisierung sowie kristallographischer Untersuchungen analysiert wurden. In Studien mit einem Mausmodell konnte gezeigt werden, dass Verbindung **16b** inhibitorisches Potenzial gegen *Plasmodium berghei* hat und dass die *in vivo* Effektivität vergleichbar mit einer bekannten Anti-Malaria-Positivkontrolle (Chloroquin) ist. Dies lässt vermuten, dass **16b** ein vielversprechender Kandidat für zukünftige pharmakologische Studien ist. In den kinetischen *in vitro* Experimenten wurde gezeigt, dass die Verbindungen **16b** und **20b** mit IC<sub>50</sub> Werten von 3 nM stärkere Inhibitoren gegen *PfIspC* sind als **1**. Die Hemmwirkung der neuen Liganden gegen *EclspC* befindet sich ebenfalls im nanomolaren Bereich und übersteigt diejenigen von *PfIspC* um bis zu drei Größenordnungen. Die Röntgenstruktur von IspC im Komplex mit **20b** zeigte, dass das an der katalytischen Reaktion beteiligte Metallion trotz der Umkehrung der Hydroxamsäure analog zu **1** an den Liganden koordiniert. Weiter führt die Bindung von **20b** durch das Enzym zu einer offenen Konformation, da die Schlaufe, welche das aktive Zentrum überspannt, in der Kristallstruktur nicht definiert ist. Obwohl die Seitenketten des aktiven Zentrums zwischen *E. coli* und *P. falciparum* identisch sind, ist die Homologie der gesamten Enzymsequenzen sehr niedrig (29%). Dadurch können starke Kreuzreaktionen der Hemmstoffe gegen *EclspC* und *PfIspC*, zum Beispiel im menschlichen Körper, gezielt eingegrenzt werden.

Mein Beitrag zu dieser Veröffentlichung war die Durchführung der kinetischen Studien mit *EclspC* sowie der kristallographischen Experimente. Zusätzlich habe ich zusammen mit Dr. Christoph T. Behrendt das Manuskript verfasst. Bei dieser Publikation bin ich Erstautorin mit gleichwertigem Beitrag von Dr. Christoph T. Behrendt.

### 3.3 Background

Each year, malaria causes several hundred million infections resulting in approximately one million fatalities.<sup>[1]</sup> All currently used antimalarial drugs are subject to rapidly progressing attrition by resistance development.<sup>[2-4]</sup> The urgent need for novel therapeutic agents is universally acknowledged, but the resources for their development are still sadly limited. *Pf*ispC is a clinically validated antimalarial target.<sup>[5,6]</sup> The antibiotic **1**, which acts as a slow-binding IspC inhibitor,<sup>[7]</sup> has been used successfully in clinical malaria trials.<sup>[8]</sup> However, its therapeutic use is hampered by the requirement for large and frequent doses, due to its unsatisfactory pharmacokinetic properties.<sup>[9]</sup> IspC catalyzes the first committed step of the non-mevalonate pathway,<sup>[10]</sup> supplying essential isoprenoids in apicomplexan protozoa including *Plasmodium* but not in mammals that use the mevalonate pathway for that purpose.<sup>[11]</sup> Specifically, IspC converts a carbohydrate (DXP, **2**) into a branched polyol (MEP, **4**) by a skeletal rearrangement via **3** followed by a hydride transfer.<sup>[12]</sup> The enzyme requires NADPH and a divalent cation as cosubstrates (Scheme 3.1). Initially isolated from *S. lavendulae*, **1** resembles the structure of the IspC substrate but is endowed with a metabolically stable phosphonate group and a hydroxamic acid motif that is perfectly suited for formation of a chelate complex with the essential divalent metal ion of the enzyme.<sup>[13,14]</sup> Derivatives of **1** have been synthesized with the intention to provide drug candidates with improved pharmacokinetic and pharmacodynamic properties.<sup>[15-28]</sup> We now report on the synthesis and antiplasmodial activity of novel reverse fosmidomycin analogs. In addition, we provide kinetic and crystallographic evidence for their mode of action.

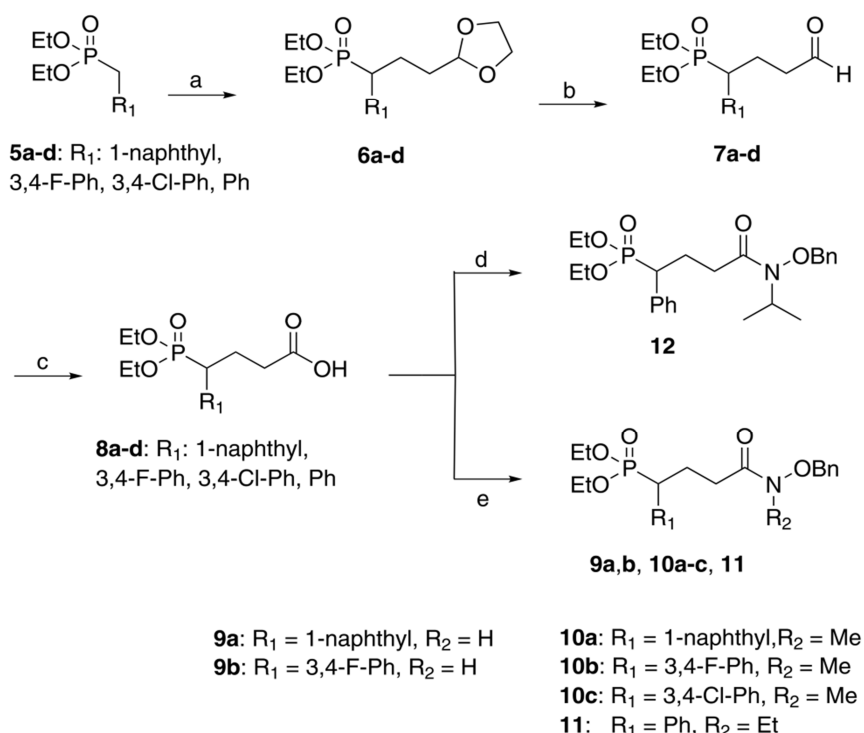


**Scheme 3.1** Target compounds and IspC-catalyzed reaction.

### 3.4 Results and discussion

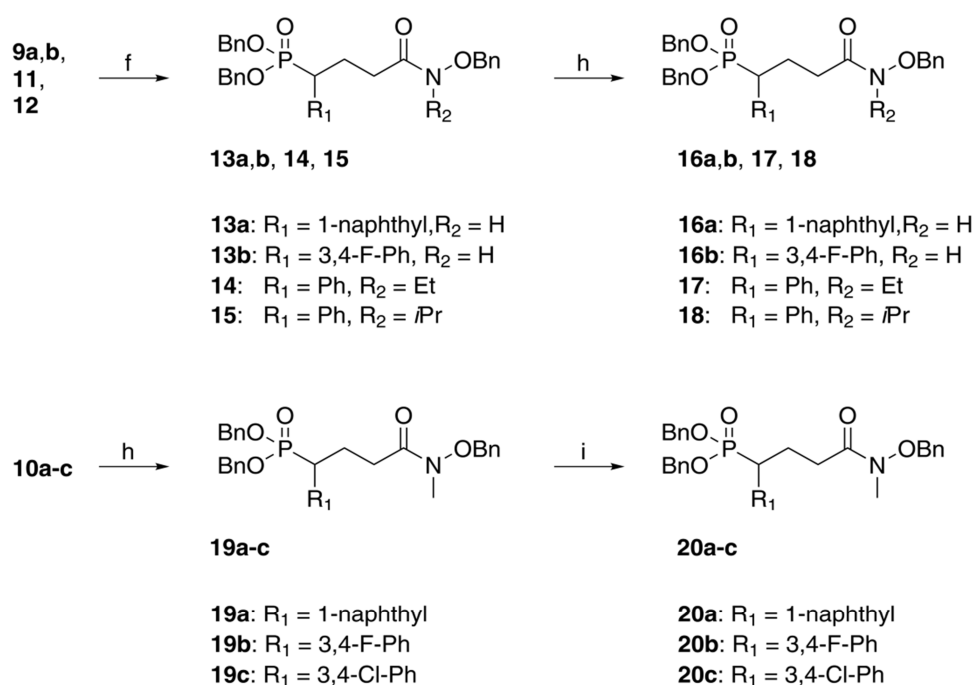
#### 3.4.1 Synthesis of the compounds

C-Alkylation of starting materials **5a–d** with 2-(2-bromoethyl)-1,3-dioxolane in the presence of *n*-BuLi provided 1,3-dioxolanes **6a–d** in good yields of 60–92%. Acidic hydrolysis of **6a–d** afforded the corresponding aldehydes **7a–d**, which were converted into carboxylic acids **8a–d** by oxidation with SeO<sub>2</sub> and H<sub>2</sub>O<sub>2</sub>.<sup>[29]</sup> The synthesis of *O*-benzyl-protected hydroxamic acids **9a, 9b, 10a–c**, and **11** was accomplished by CDI-mediated coupling reactions of carboxylic acids **8a–d** with *O*-benzylhydroxylamine, *N*-methyl-*O*-benzylhydroxylamine, and *N*-ethyl-*O*-benzylhydroxylamine, respectively.<sup>[30,31]</sup> However, the acylation of *N*-isopropyl-*O*-benzylhydroxylamine under similar reaction conditions failed. Finally, the *N*-isopropyl-substituted hydroxamic acid **12** was accessible in 81% yield by subsequent treatment of **8d** with oxalyl chloride, dimethyl fumarate (DMF), and *N*-isopropyl-*O*-benzylhydroxylamine (Scheme 3.2).



**Scheme 3.2** Synthesis of intermediates **9–12**. Reagents and conditions: a) *n*-BuLi, 2-(2-bromoethyl)-1,3-dioxolane, toluene,  $-78\text{ }^{\circ}\text{C}$ ; b) HCl, acetone,  $50\text{ }^{\circ}\text{C}$ , 3 h; c) SeO<sub>2</sub>, H<sub>2</sub>O<sub>2</sub>, THF,  $65\text{ }^{\circ}\text{C}$ , 4 h; d) CDI, BnONHR<sub>2</sub> (R<sub>2</sub> = H, Me, Et), CH<sub>2</sub>Cl<sub>2</sub>, rt; e) C<sub>2</sub>O<sub>2</sub>Cl<sub>2</sub>/DMF, BnONH-*i*-Pr, rt. Ph, phenyl; Me, methyl.

Next, we studied the two-step deprotection of *N*-methyl-substituted benzyloxyamides **10a–c**. Their reactions with TMSBr afforded crystalline phosphonic acids **19a–c** in good yields and high purity.<sup>[32]</sup> Catalytic hydrogenation<sup>[32]</sup> of **19a–c** finally yielded the required *N*-methyl-substituted hydroxamic acids **20a–c** in 87–98% yield. In contrast to the smooth dealkylation of substrates **10a–c**, the cleavage of ethyl phosphonates **9a**, **9b**, **11**, and **12** in the presence of TMSBr was incomplete, and only crude product mixtures were obtained. However, transesterification of diethyl esters **9a**, **9b**, **11**, and **12** provided *O*-benzyl protected compounds **13a**, **13b**, **14**, and **15**, which were deprotected by catalytic hydrogenation to afford target compounds **16a**, **16b**, **17**, and **18** (Scheme 3.3).<sup>[33]</sup>



**Scheme 3.3** Synthesis of target compounds **16–20**. Reagents and conditions: f) 1. TMSBr, CH<sub>2</sub>Cl<sub>2</sub>, rt, 24 h; 2. THF/H<sub>2</sub>O, rt, 1 h; 3. DCC, BnOH, benzene, 80 °C, 4 h; g) H<sub>2</sub>, Pd–C, MeOH, 3 h; h) 1. TMSBr, CH<sub>2</sub>Cl<sub>2</sub>, rt, 24 h; 2. THF/H<sub>2</sub>O, rt, 1 h; i) H<sub>2</sub>, Pd–C, MeOH, 1 h.

### 3.4.2 Photometric *in vitro* activity assay

As shown in Table 3.1, several compounds under study inhibit *Pf*lspC with IC<sub>50</sub> values in the single-digit nanomolar range, whereas the IC<sub>50</sub> values for *Ecl*spC exceed those for the *P. falciparum* enzyme by one to three orders of magnitude. Some of the compounds studied are strong inhibitors of *P. falciparum* replication in erythrocytes *in vitro*, with IC<sub>50</sub> values in the low micromolar range (Table 3.1, column 4). Notably, compounds **16b**, **20b**, and **20c** have about ten-

fold higher potency than **1** against the chloroquine-resistant K1 strain of *P. falciparum*. Moreover, their toxicity in cell culture experiments is low, with IC<sub>50</sub> values above 60 μM (Table 3.1, column 5).

**Table 3.1** *In vitro* inhibition potency<sup>[a]</sup> and cytotoxicity<sup>[c]</sup> of target compounds.

Compound	IC <sub>50</sub> [μM]			
	<i>Pf</i> ispC <sup>[a]</sup>	<i>Ecl</i> spC <sup>[a]</sup>	<i>Pf</i> -K1 <sup>[a],[b]</sup>	MRC-5 <sup>[c]</sup>
<b>1</b> <sup>[d]</sup>	0.14 ± 0.02	0.22 ± 0.01	3.7 ± 2.5	>62
<b>16a</b>	0.037 ± 0.003	7.4 ± 0.2	2.4 ± 1.1	>64
<b>16b</b>	0.003 ± 0.001	0.21 ± 0.02	0.38 ± 0.17	>64
<b>17</b>	0.015 ± 0.002	15 ± 0.4	1.3 ± 1.5	>64
<b>18</b>	inactive	inactive	inactive	>64
<b>20a</b>	0.009 ± 0.001	3.8 ± 0.2	0.97 ± 0.79	>62
<b>20b</b>	0.003 ± 0.001	0.12 ± 0.07	0.29 ± 0.20	>64
<b>20c</b>	0.004 ± 0.001	0.18 ± 0.02	0.41 ± 0.25	>64

<sup>[a]</sup>Enzyme assay. Values are the mean ± SD of three or more independent experiments.

<sup>[b]</sup>Replication of *P. falciparum* in human erythrocytes.

<sup>[c]</sup>Cytotoxicity test with MRC-5 cells.

<sup>[d]</sup>IC<sub>50</sub> values according to reference 15.

In summary, the *in vitro* evaluation has demonstrated that not only free but also *N*-methyl-substituted hydroxamic acids are promising candidates for further investigation. In contrast, the bulky *N*-isopropyl substituent of compound **17** caused a complete loss of *in vitro* activity. Referring to the selection of aryl substituents in the α-position of the connecting spacer, it is an interesting outcome that the α-naphthyl derivative **20a** inhibits *Pf*ispC in the low nanomolar range with an IC<sub>50</sub> value of 9.4 nM.

### 3.4.3 Structure elucidation

Structure elucidation of *Ecl*spC in complex with **20b** at 2.1 Å showed that the space group of the protein can vary according to the crystallization conditions (Figures 3.1 and 3.2).<sup>[34,35]</sup> The overall structure is virtually identical with other published *Ecl*spC structures except for a flexible loop region (amino acids Arg208–Ser213), which is distorted most likely because of the lack of

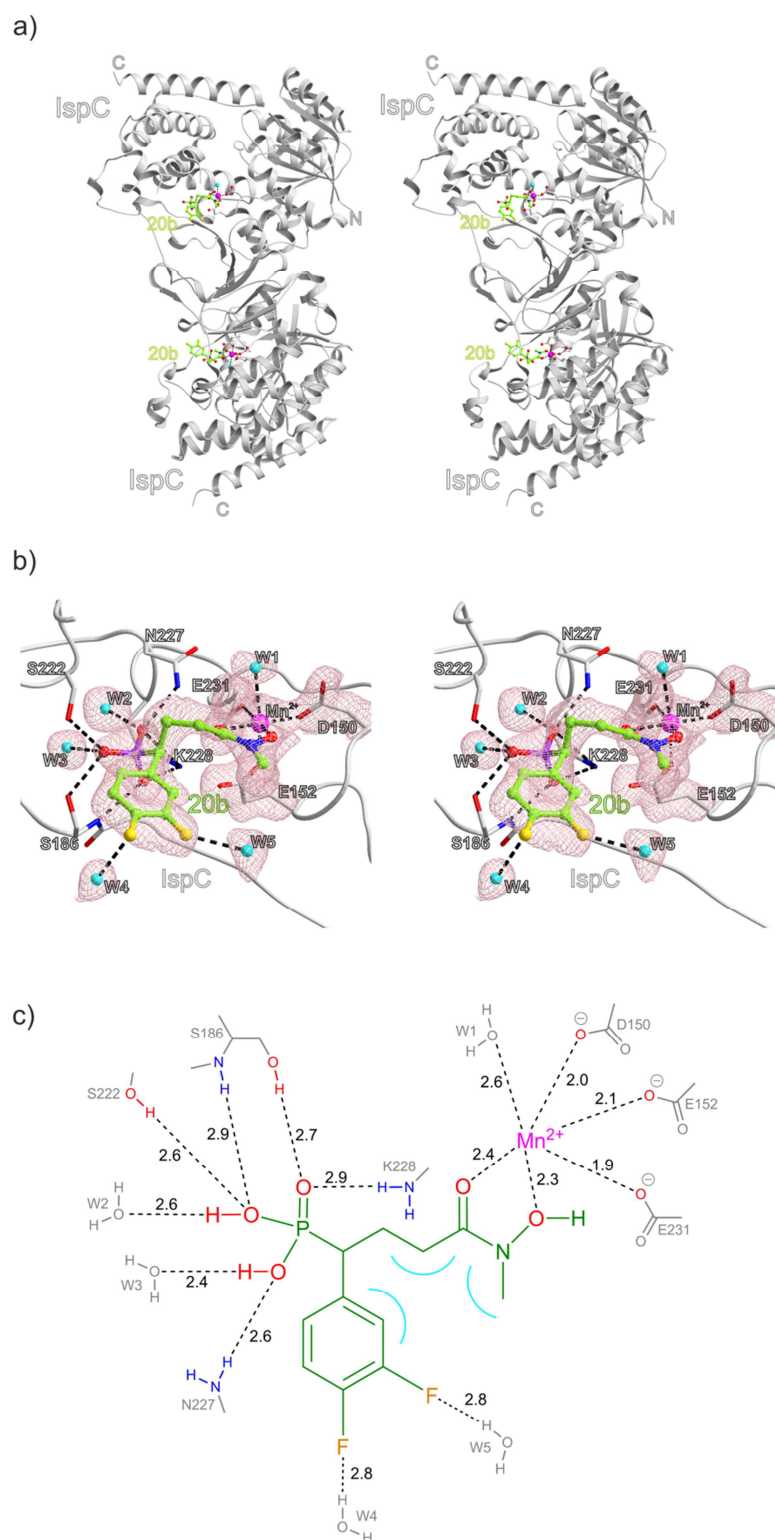
NADPH. In its closed conformation, this loop stabilizes the substrate or **1** by hydrophobic interactions.

A structural overlay of the **1**:EclspC complex with **20b**:EclspC complex (Figure 3.2a) documents the consistency of the ligand binding mode.<sup>[34]</sup> It reveals that, irrespective of the hydroxamic acid in **1** or the reverse hydroxamic acid in **20b**, the coordination of the divalent metal ion is octahedral in both cases. This is reminiscent of the catalytic mechanism of the isomerization of **2**, in which an alcohol and a hydroxyketone are converted into a hydroxyaldehyde (a “reverse” hydroxycarbonyl analog).

Structural superpositioning of the **20b**:EclspC complex with the **1**:EclspC:NADPH (closed conformation) complex<sup>[35]</sup> clearly shows that some amino acid side chains (Figure 3.2b; only Asn211, Trp212, and Met214 are shown) of the loop region would clash with the difluorophenyl ring of **20b**. This explains why the loop cannot adopt the closed conformation in the **20b** complex, where binding of the inhibitor necessitates a major reorientation of the amino acid side chains of the protein. In contrast, binding of **1** occurs in the closed conformation because it perfectly fits into the closed active site. Interestingly, binding of **20b** in the open conformation might not have suggested that **20b** is, in fact, a stronger inhibitor of the enzyme than **1**, which can bind to the closed conformation.

The **20b**:EclspC complex structure reveals intramolecular van der Waals interactions of the *N*-methyl group of **20b** with the difluorophenyl ring (3.9 Å) as well as with the main chain atoms of the ligand. The *N*-methyl group though has no contact to the enzyme. Thus, **20b** is enthalpically and entropically stabilized despite the missing stabilization through the loop, and ligand binding may thereby be favored. This observation is in good agreement with the obtained *in vitro* data for compounds **16b** and **20b**. Although the residues in the active site of IspC are conserved between *E. coli* and *P. falciparum*, the overall sequence homology is very low. The considerable degree of species specificity that is revealed by our kinetic data emphasizes the necessity to actually use IspC from *P. falciparum* in screening programs for antimalarials directed at IspC.





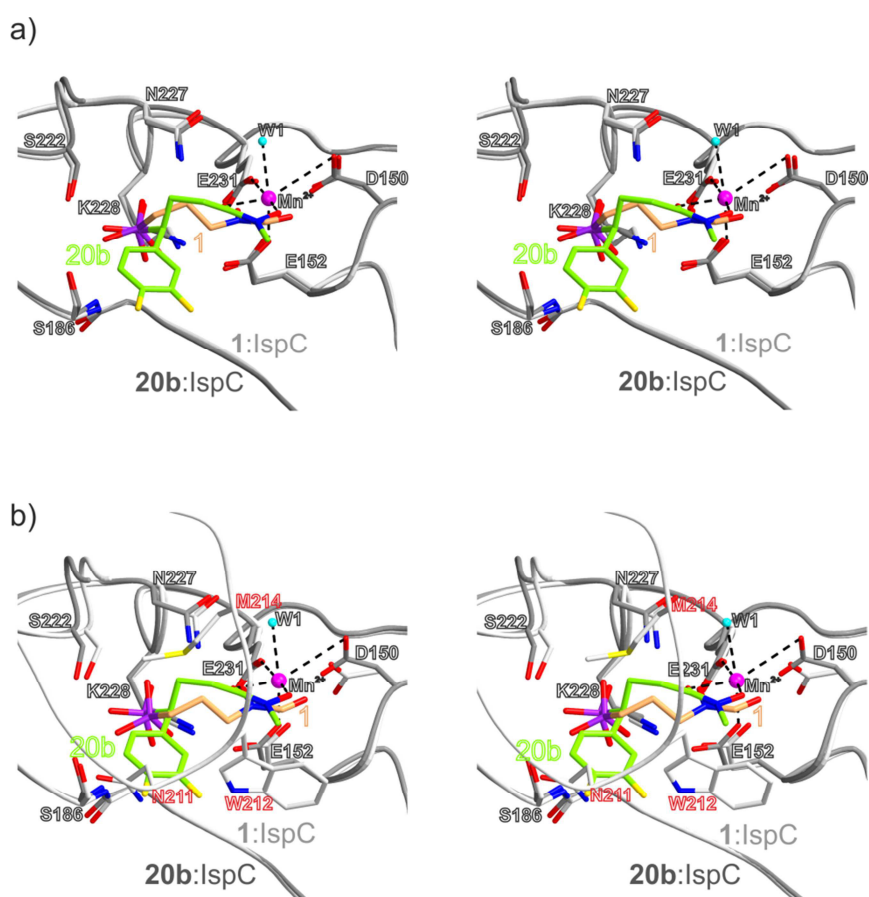


**Figure 3.2** a) Structural superposition (stereo view) of **20b** and **1** at the active site of *EclspC* in the open conformation (PDB codes 3ROI (**20b**) and 1ONP<sup>[34]</sup> (**1**)). b) Superposition (stereo view) of **20b** and **1**:NADPH:*EclspC* (closed conformation) complex (PDB codes 3ROI (**20b**) and 1QOL<sup>[35]</sup> (**1**)).

### 3.4.4 *In vivo* activity assay

Compounds **16b** and **20b** were tested in the *Plasmodium berghei* mouse model.<sup>[36]</sup> Drug treatment of animals was initiated 2 h after artificial infection by intraperitoneal injection of infected erythrocytes and was continued for 5 days. The *in vivo* efficacy of **16b** was similar to that of **1** and chloroquine (Figure 3.3). On the other hand, **20b** had less effect on survival, although the percentage of infected erythrocytes was significantly reduced (Figure 3.3, Table 3.2).

Thus, whereas the novel compounds show high potency in the nanomolar range when assayed against *P. falciparum* in human erythrocytes and against IspC protein from that pathogen, the small-scale animal study using a different *Plasmodium* species gave less impressive results. It should be noted, however, that *in vitro* studies on IspC protein of *P. berghei* are not available, and species differences may well be relevant for the different outcomes of the *in vitro* assays and the animal experiments.

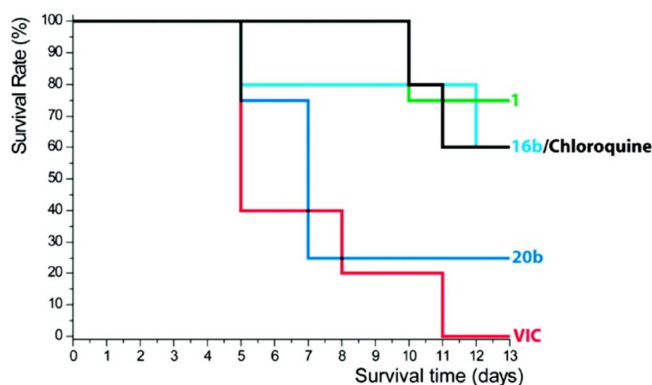


**Figure 3.3** Kaplan–Meier analysis of experiments with mice that had been artificially infected with *P. berghei*: red, control; black, chloroquine ( $10 \text{ mg kg}^{-1}$ ); green, **1** ( $80 \text{ mg kg}^{-1}$ ); light blue, **16b** ( $80 \text{ mg kg}^{-1}$ ); dark blue, **20b** ( $80 \text{ mg kg}^{-1}$ ).

**Table 3.2** *In vivo* activity in the *P. berghei* acute mouse model<sup>[a]</sup>.

Treatment <sup>[b]</sup>	Mean % suppression of infected red blood cells (day 4)
Vehicle	0
Chloroquine ( $10 \text{ mg kg}^{-1}$ ) <sup>[c]</sup>	98
<b>1</b> ( $80 \text{ mg kg}^{-1}$ ) <sup>[c]</sup>	92
<b>16b</b> ( $80 \text{ mg kg}^{-1}$ ) <sup>[c]</sup>	89
<b>20b</b> ( $80 \text{ mg kg}^{-1}$ ) <sup>[c]</sup>	78

<sup>[a]</sup>GFP ANKA strain.

<sup>[b]</sup>ip for 5 consecutive days.

<sup>[c]</sup>Dose was divided into two administrations of  $40 \text{ mg kg}^{-1} \text{ day}^{-1}$ . Ritonavir was coadministered orally at  $10 \text{ mg kg}^{-1}$  (CYP3A4 inhibitor to minimize possible metabolic degradation).

### 3.4.5 Conclusion

In summary, we provide kinetic and crystallographic evidence for the mode of action of a series of novel hydroxamate-based IspC inhibitors. Several new analogs inhibit IspC protein of *P. falciparum* with  $\text{IC}_{50}$  values in the low nanomolar range. In contrast, the new compounds are significantly weaker inhibitors of the *E. coli* enzyme. Finally, pilot *in vivo* experiments have shown that compound **16b** has some potential and is believed to be a promising candidate for further pharmacological studies, structural modifications, and the design of prodrugs.

### 3.5 Experimental section

#### 3.5.1 General procedures in synthesis

All solvents and chemicals were used as purchased without further purification. The progress of all reactions was monitored on Merck precoated silica gel plates (with fluorescence indicator UV<sub>254</sub>) using EtOAc/*n*-hexane as solvent system. Column chromatography was performed with Fluka silica gel 60 (230–400 mesh ASTM) with the solvent mixtures specified in the corresponding experiment. Spots were visualized by irradiation with ultraviolet light (254 nm). Melting points (mp) were taken in open capillaries on a Mettler FP 5 melting-point apparatus and are uncorrected. Proton (<sup>1</sup>H) and carbon (<sup>13</sup>C) NMR spectra were recorded on a Bruker Avance 500 (500.13 MHz for <sup>1</sup>H; 125.76 MHz for <sup>13</sup>C) using DMSO-*d*<sub>6</sub> and CDCl<sub>3</sub> as solvents. Chemical shifts are given in parts per million (ppm) (δ relative to residual solvent peak for <sup>1</sup>H and <sup>13</sup>C and to external tetramethylsilane). Elemental analysis was performed on a Perkin-Elmer PE 2400 CHN elemental analyzer. IR spectra were recorded on a Varian 800 FT-IR Scimitar series. Analytical high performance liquid chromatography (HPLC) was performed in analogy to a previously reported procedure.<sup>[25]</sup> The instrument was an Elite LaChrom system [Hitachi L-2130 (pump) and L-2400 (UV-detector)]. The column was a Phenomenex Luna C-18(2), 1.8 μm particle (250 mm × 4.6 mm), supported by Phenomenex Security Guard Cartridge Kit C18 (4.0 mm × 3.0 mm). The purity of all final compounds was 95% or higher.

#### 3.5.2 Experimental data for the compounds

Experimental data are listed below for selected compounds **10b**, **19b**, and **20b**.

#### General procedure for the synthesis of *O*-Bn-protected hydroxamic acids (**9a**, **9b**, **10a–c**, **11**, and **12**)

To a solution of the respective carboxylic acid **8a–d** (1 equiv., 5 mmol) in dry CH<sub>2</sub>Cl<sub>2</sub> (50 mL) was added CDI (1.1 equiv., 0.9 g, 5.5 mmol) in small portions. After the mixture was stirred at rt for 45 min, the appropriate hydroxylamine was added in one portion. The solution was stirred overnight, and the solvent was removed under reduced pressure. The remaining residue was dissolved in EtOAc (30 mL), and the organic layer was washed three times with an aqueous solution of citric acid (10%, 10 mL) and once more with a saturated aqueous solution of NaHCO<sub>3</sub>.

(10 mL). The organic layer was dried over  $\text{MgSO}_4$ , filtered, and concentrated under reduced pressure. Hydroxamic acids (**9a**, **10b**, and **10c**) were obtained by crystallization from diethyl ether at 7 °C. Hydroxamic acids **9b**, **10a**, and **11** were purified by column chromatography on silica gel using EtOAc/*n*-hexane (1:1) as the eluent.

Diethyl [4-[(Benzyloxy)(methyl)amino]-1-(3,4-difluorophenyl)-4-oxobutyl]phosphonate (**10b**)

White solid (2.10 g, 92%). Mp: 60.2 °C.  $^1\text{H}$  NMR (500.13 MHz,  $\text{DMSO}-d_6$ ):  $\delta$  = 7.61–7.28 (m, 5H), 7.28–7.01 (m, 3H), 4.71 (PhCH<sub>2</sub>, s, 2H), 4.25–3.92 (CH<sub>3</sub>CH<sub>2</sub>, m, 2H), 3.92–3.70 (CH<sub>3</sub>CH<sub>2</sub>, m, 2H), 3.34–3.22 (PCH, dd,  $J_1$  = 11.0 Hz,  $J_2$  = 24.0 Hz, 1H), 3.10 (NCH<sub>3</sub>, s, 3H), 2.42–2.07 (CH<sub>2</sub>, m, 3H), 2.08–1.76 (CHCH<sub>2</sub>, m, 1H), 1.20 (CH<sub>3</sub>, t,  $J$  = 6.9 Hz, 3H), 1.06 (CH<sub>3</sub>, t,  $J$  = 7.0 Hz, 3H) ppm.  $^{13}\text{C}$  NMR (125.76 MHz,  $\text{CDCl}_3$ ):  $\delta$  = 172.65 (C=O), 149.07 (dd,  $^2J_{\text{C-F}}$  = 14.1 Hz,  $^1J_{\text{C-F}}$  = 246.9 Hz), 148.43 (dd,  $^2J_{\text{C-F}}$  = 12.0 Hz,  $^1J_{\text{C-F}}$  = 242.7 Hz), 134.38, 133.97, 129.27, 128.58, 128.24, 125.92, 117.87 (dd,  $^3J_{\text{C-F}}$  = 6.5 Hz,  $^2J_{\text{C-F}}$  = 17.4 Hz), 117.26 (dd,  $^3J_{\text{C-F}}$  = 1.4 Hz,  $^2J_{\text{C-F}}$  = 16.7 Hz), 75.08 (PhCH<sub>2</sub>), 61.73 (POCH<sub>2</sub>, d,  $^2J_{\text{C-P}}$  = 6.8 Hz), 61.45 (POCH<sub>2</sub>, d,  $^2J_{\text{C-P}}$  = 7.1 Hz), 41.28 (CHP, d,  $^1J_{\text{C-P}}$  = 136.9 Hz), 32.63 (NCH<sub>3</sub>), 29.17 (CH<sub>2</sub>, d,  $^2J_{\text{C-P}}$  = 15.5 Hz), 24.31 (CH<sub>2</sub>), 16.14 (CH<sub>3</sub>, d,  $^3J_{\text{C-P}}$  = 5.5 Hz), 15.99 (CH<sub>3</sub>, d,  $^3J_{\text{C-P}}$  = 5.4 Hz) ppm. IR (KBr):  $\tilde{\nu}$  = 3037 (C–H<sub>arom.</sub>), 2985 (C–H<sub>aliph.</sub>), 1673 (C=O), 1233 (P=O), 1053 (P–O)  $\text{cm}^{-1}$ . Anal. Calcd. for C<sub>22</sub>H<sub>28</sub>F<sub>2</sub>NO<sub>5</sub>P: C 58.02, H 6.20, N 3.08. Found: C 58.29, H 6.29, N 2.78.

**General procedure for the synthesis of phosphonic acids (19a–c)**

To a solution of the respective phosphonic acid diethyl ester **10a–c** (1 equiv., 3 mmol) in dry dichloromethane (10 mL) was added TMSBr (5 equiv., 1.99 mL, 15 mmol) at 0 °C. After 1 h, the solution was allowed to warm to rt and stirred for an additional 23 h. The solvent was removed under reduced pressure. The remaining residue was dissolved in THF (10 mL), and water (0.1 mL) was added. After 30 min the solvent was evaporated and the resulting residue dried *in vacuo* overnight. Pure phosphonic acids (**19a–c**) were obtained as white solids at –20 °C after digestion with EtOAc.

[4-[(Benzyloxy)(methyl)amino]-1-(3,4-difluorophenyl)-4-oxobutyl]phosphonic acid (**19b**)

White solid (0.480 g, 40%). Mp: 143.5 °C.  $^1\text{H}$  NMR (500.13 MHz,  $\text{DMSO}-d_6$ ):  $\delta$  = 7.62–7.15 (m, 7H), 7.08 (s, 1H), 4.70 (PhCH<sub>2</sub>, s, 2H), 3.09 (NCH<sub>3</sub>, s, 3H), 2.94 (PCH, dd,  $J_1$  = 11.0 Hz,  $J_2$  = 20.2 Hz, 1H), 2.22 (CH<sub>2</sub>, s, 3H), 1.94 (CH<sub>2</sub>, m, 1H) ppm.  $^{13}\text{C}$  NMR (125.76 MHz,  $\text{DMSO}-d_6$ ):  $\delta$  = 172.66 (C=O), 149.02 (dd,  $^2J_{\text{C-F}}$  = 12.7 Hz,  $^1J_{\text{C-F}}$  = 233.9 Hz), 148.12 ( $^2J_{\text{C-F}}$  = 13.3 Hz,  $^1J_{\text{C-F}}$  = 228.1 Hz), 136.11 (d,  $^2J_{\text{C-P}}$  = 8.8 Hz), 134.39, 129.29, 128.58, 128.23, 125.80, 117.57 (dd,  $^3J_{\text{C-F}}$  = 5.7 Hz,  $^2J_{\text{C-F}}$  =

16.5 Hz), 116.84 (dd,  $^2J_{C-F} = 16.4$  Hz), 75.06 (PhCH<sub>2</sub>), 43.53 (CHP, d,  $^1J_{C-P} = 133.4$  Hz), 32.68 (NCH<sub>3</sub>), 29.57 (CH<sub>2</sub>, d,  $^2J_{C-P} = 16.8$  Hz), 24.90 (CH<sub>2</sub>, d,  $^3J_{C-P} = 2.1$  Hz) ppm. IR (KBr):  $\tilde{\nu} = 3437$  (N–H), 3037 (C–H<sub>arom.</sub>), 2944 (C–H<sub>aliph.</sub>), 1607 (C=O), 1277 (P=O), 999 (P–O) cm<sup>-1</sup>. Anal. Calcd. for C<sub>18</sub>H<sub>20</sub>F<sub>2</sub>NO<sub>5</sub>P: C 54.14, H 5.05, N 3.51. Found: C 54.02, H 5.06, N 3.23.

### General procedure for the synthesis of target compounds (16a, 16b, 17, 18, and 20a–c)

To a solution of the appropriate *O*-Bn-protected acid (1 mmol) in freshly distilled MeOH (20 mL) was added Pd–C catalyst (10%, 40 mg). The mixture was hydrogenated at a pressure of 2 bar for 1.5 h (in the case of compounds **13a**, **13b**, **14**, and **15**) or 3 h (in the case of compounds **19a–c**). The suspension was filtered through a SPE tube RP-18, and the solvent was removed under reduced pressure. Whereas compounds **17**, **18**, and **20c** were obtained as hygroscopic oils, compounds **16a**, **16b**, **20a**, and **20b** were crystallized from appropriate solvents as described below.

#### [1-(3,4-Difluorophenyl)-4-[hydroxy(methyl)amino]-4-oxobutyl]phosphonic acid (**20b**)

White solid (0.258 g, 84% after recrystallization in EtOAc). Mp: 116.8 °C. <sup>1</sup>H NMR (500.13 MHz, DMSO-*d*<sub>6</sub>):  $\delta = 9.67$  (NOH, s, 1H), 7.35 (dd,  $J_1 = 8.9$  Hz,  $J_2 = 19.0$  Hz, 1H), 7.30–7.22 (m, 1H), 7.18–6.86 (m, 1H), 3.02 (NCH<sub>3</sub>, s, 3H), 2.97 (PCH, dd,  $J_1 = 9.6$  Hz,  $J_2 = 21.7$  Hz, 1H), 2.20 (CH<sub>2</sub>, s, 3H), 1.98–1.82 (CHCH<sub>2</sub>, m, 1H) ppm. <sup>13</sup>C NMR (125.76 MHz, DMSO-*d*<sub>6</sub>):  $\delta = 172.20$  (C=O), 149.76 (dd,  $^2J_{C-F} = 10.8$  Hz,  $^1J_{C-F} = 242.9$  Hz), 148.96 (dd,  $^2J_{C-F} = 13.9$  Hz,  $^1J_{C-F} = 250.6$  Hz), 136.13, 125.82, 117.54 (dd,  $^3J_{C-F} = 5.8$  Hz,  $^2J_{C-F} = 16.9$  Hz), 116.77 (dd,  $^3J_{C-F} = 1.5$  Hz,  $^2J_{C-F} = 16.6$  Hz), 43.61 (CHP, d,  $^1J_{C-P} = 133.4$  Hz), 35.54 (NCH<sub>3</sub>), 29.69 (CH<sub>2</sub>, d,  $^2J_{C-P} = 15.1$  Hz), 25.00 (CH<sub>2</sub>) ppm. IR (KBr):  $\tilde{\nu} = 3405$  (N–H), 1615 (C=O), 1282 (P=O), 1019 (P–O) cm<sup>-1</sup>. Anal. Calcd. for C<sub>11</sub>H<sub>14</sub>F<sub>2</sub>NO<sub>5</sub>P: C 42.73, H 4.56, N 4.53. Found: C 43.00, H 4.77, N 4.50.

More details on experimental data for the compounds can be found under DOI: 10.1021/jm200694q.

### 3.5.3 Crystallization and structure determination

Crystals were grown using the hanging drop vapor diffusion method at 20 °C. *EclspC* protein concentration used for crystallization was 17 mg mL<sup>-1</sup> in 100 mM Tris-HCl (pH 8.0), containing 2 mM DTT and 0.02% NaN<sub>3</sub>. Crystals were obtained in drops containing 5 µL of protein solution and 5 µL of reservoir solution as described earlier (8% PEG4000, 80-140 mM Na-Ac, 110 mM HEPES (pH 5.6-6.2), 100 mM glycine, 100 mM guanidinium chloride, 10 mM EDTA and 12 mM DTT).<sup>[34]</sup> Crystals grew to a final size of 1000 x 150 x 150 µm<sup>3</sup> within 3-10 days. *EclspC* crystals in complex with **20b** (1 mM) and Mn<sup>2+</sup> (0.5 mM) were soaked for 24 h in the mother liquor including 8% PEG400 in absence of EDTA, and were flash-frozen after incubation for 5 min with 25% glycerol in a stream of nitrogen gas at 100 K (Oxford Cryosystems Ltd; Oxfordshire, UK). Datasets to 2.1 Å resolution were collected using our in-house X-ray facility (CuK<sub>α</sub>-rotating anode). Data were processed using the program package XDS.<sup>[37]</sup> For more details and parameters see Table 3.3. Crystal structure analysis was performed by molecular replacement using coordinates of *EclspC* deposited at the PDB with the code 1ONN.<sup>[34]</sup> The anisotropy of diffraction was corrected by TLS-refinement using the program REFMAC5.<sup>[38]</sup> Electron density was improved by averaging and back transforming the reflections ten times over the two-fold non-crystallographic symmetry axis using the program package MAIN.<sup>[39]</sup> Conventional crystallographic rigid body, positional and temperature factor refinements were carried out with REFMAC5. The model was completed using the interactive three-dimensional graphic program MAIN. The atomic coordinates for *EclspC* in complex with **20b** and Mn<sup>2+</sup> have been deposited at the PDB, Research Collaboratory for Structural Bioinformatics at Rutgers University under accession code 3R0I.

**Table 3.3** Data collection and refinement statistics.

<b>20b:EclspC</b>	
<b>Crystal parameter</b>	
Space group	P2 <sub>1</sub>
Cell dimensions	a=91.3 Å, b=54.6 Å, c=107.8 Å; β=93.2 °
Molecules per AU <sup>[a]</sup>	2
<b>Data collection</b>	
Beam line	CuK <sub>α</sub>
Wavelength (Å)	1.5418
Resolution range (Å) <sup>[b]</sup>	20-2.1 (2.2-2.1)
Observed / unique reflections <sup>[c]</sup>	62373 / 62350
Completeness (%) <sup>[b]</sup>	99.9 (99.9)
R <sub>merge</sub> (%) <sup>[b],[d]</sup>	7.2 (40.3)
I/σ (I) <sup>[b]</sup>	12.5 (2.6)
<b>Refinement</b>	
Resolution (Å)	10-2.1
R <sub>work</sub> / R <sub>free</sub> <sup>[e]</sup>	16.3 / 21.7
No. atoms	6771
Protein	5956
Ligand	40
Mn <sup>2+</sup>	2
Water	773
B-factors	14.1
R.m.s. deviations <sup>[f]</sup>	
Bond lengths (Å)	0.025
Bond angles (°)	2.06
Ramachandran (%) <sup>[g]</sup>	97.9 / 2.1 / 0.0
PDB accession code	3R0I

<sup>[a]</sup>Asymmetric unit.

<sup>[b]</sup>Values in parenthesis of resolution range, completeness, R<sub>merge</sub> and I/σ (I) correspond to the last resolution shell.

<sup>[c]</sup>Friedel pairs were treated as identical reflections.

<sup>[d]</sup> $R_{\text{merge}}(I) = \frac{\sum_{hkl} \sum_j |I(hkl)_j - \langle I(hkl) \rangle|}{\sum_{hkl} I(hkl)}$ , where  $I(hkl)_j$  is the measurement of the intensity of reflection  $hkl$  and  $\langle I(hkl) \rangle$  is the average intensity.

<sup>[e]</sup> $R = \frac{\sum_{hkl} | |F_{\text{obs}}| - |F_{\text{calc}}| |}{\sum_{hkl} |F_{\text{obs}}|}$ , where R<sub>free</sub> is calculated without a sigma cut off for a randomly chosen 5% of reflections, which were not used for structure refinement, and R<sub>work</sub> is calculated for the remaining reflections.

<sup>[f]</sup>Root-mean-square deviations (r.m.s.d.) from ideal bond lengths / angles.

<sup>[g]</sup>Number of residues in favored region / allowed region / outlier region.

### 3.5.4 Supporting Information

The Supporting Information and the full article are available under DOI: 10.1021/jm200694q.



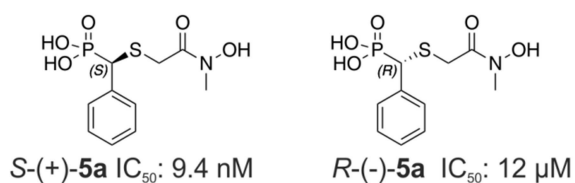
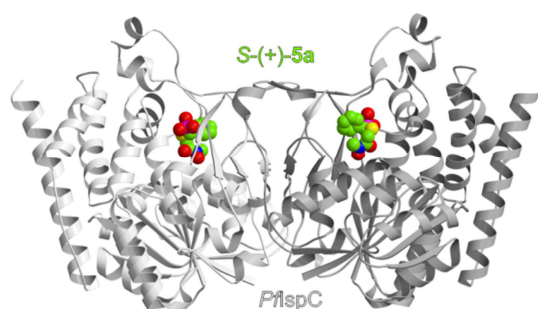
### 3.6 References

- (1) World malaria report, **2009**.  
[http://www.who.int/malaria/world\\_malaria\\_report\\_2009/en/index.html](http://www.who.int/malaria/world_malaria_report_2009/en/index.html); 01.12.2013.
- (2) T. N. Wells, E. M. Poll, *Discovery Med.* **2010**, *9*, 389-398.
- (3) A. M. Dondorp, F. Nosten, P. Yi, D. Das, A. P. Phyto, J. Tarning, K. M. Lwin, F. Ariey, W. Hanpithakpong, S. J. Lee, P. Ringwald, K. Silamut, M. Imwong, K. Chotivanich, P. Lim, T. Herdman, S. S. An, S. Yeung, P. Singhasivanon, N. P. J. Day, N. Lindegardh, D. Socheat, N. J. White, *N. Engl. J. Med.* **2009**, *361*, 455-467.
- (4) N. J. White, *J. Clin. Invest.* **2004**, *113*, 1084-1092.
- (5) H. Jomaa, J. Wiesner, S. Sanderbrand, B. Altincicek, C. Weidemeyer, M. Hintz, I. Turbachova, M. Eberl, J. Zeidler, H. K. Lichtenthaler, D. Soldati, E. Beck, *Science* **1999**, *285*, 1573-1576.
- (6) T. Kuzuyama, T. Shimizu, S. Takahashi, H. Seto, *Tetrahedron Lett.* **1998**, *39*, 7913-7916.
- (7) L. Kuntz, D. Tritsch, C. Grosdemange-Billiard, A. Hemmerlin, A. Willem, T. J. Bacht, M. Rohmer, *Biochem. J.* **2005**, *386*, 127-135.
- (8) S. Oyakhrome, S. Issifou, P. Pongratz, F. Barondi, M. Rarnharter, J. F. Kun, M. A. Missinou, B. Lell, P. G. Kremsner, *Antimicrob. Agents Chemother.* **2007**, *51*, 1869-1871.
- (9) T. Murakawa, H. Sakamoto, S. Fukada, T. Konishi, M. Nishida, *Antimicrob. Agents Chemother.* **1982**, *21*, 224-230.
- (10) S. Takahashi, T. Kuzuyama, H. Watanabe, H. Seto, *Proc. Natl. Acad. Sci. USA* **1998**, *95*, 9879-9884.
- (11) W. Eisenreich, A. Bacher, D. Arigoni, F. Rohdich, *Cell. Mol. Life Sci.* **2004**, *61*, 1401-1426.
- (12) S. Lauw, V. Illarionova, A. Bacher, F. Rohdich, W. Eisenreich, *FEBS J.* **2008**, *275*, 4060-4073.
- (13) T. Radykewicz, F. Rohdich, J. Wungsintaweekul, S. Herz, K. Kis, W. Eisenreich, A. Bacher, M. H. Zenk, D. Arigoni, *FEBS Lett.* **2000**, *465*, 157-160.
- (14) K. Silber, P. Heidler, T. Kurz, G. Klebe, *J. Med. Chem.* **2005**, *48*, 3547-3563.
- (15) C. T. Behrendt, A. Kunfermann, V. Illarionova, A. Matheussen, T. Gräwert, M. Groll, F. Rohdich, A. Bacher, W. Eisenreich, M. Fischer, L. Maes, T. Kurz, *ChemMedChem* **2010**, *5*, 1673-1676.
- (16) K. Schlüter, R. D. Walter, B. Bergmann, T. Kurz, *Eur. J. Med. Chem.* **2006**, *41*, 1385-1397.
- (17) J. Perruchon, R. Ortman, M. Altenkaemper, K. Silber, J. Wiesner, H. Jomaa, G. Klebe, M. Schlitzer, *ChemMedChem* **2008**, *3*, 1232-1241.

- (18) D. Gießmann, P. Heidler, T. Haemers, S. Van Calenbergh, A. Reichenberg, H. Jomaa, C. Weidemeyer, S. Sanderbrand, J. Wiesner, A. Link, *Chem. Biodiversity* **2008**, *5*, 643-656.
- (19) L. Deng, S. Sundriyal, V. Rubio, Z. Shi, Y. Song, *J. Med. Chem.* **2009**, *52*, 6539-6542.
- (20) C. Zingle, L. Kuntz, D. Tritsch, C. Grosdemange-Billiard, M. Rohmer, *J. Org. Chem.* **2010**, *75*, 3203-3207.
- (21) Y. H. Woo, R. P. M. Fernandes, P. J. Proteau, *Bioorg. Med. Chem.* **2006**, *14*, 2375-2385.
- (22) D. T. Fox, C. D. Poulter, *J. Org. Chem.* **2005**, *70*, 1978-1985.
- (23) T. Haemers, J. Wiesner, D. Gießmann, T. Verbrugghen, U. Hillaert, R. Ortmann, H. Jomaa, A. Link, M. Schlitzer, S. Van Calenbergh, *Bioorg. Med. Chem.* **2008**, *16*, 3361-3371.
- (24) T. Kurz, K. Schlüter, U. Kaula, B. Bergmann, R. D. Walter, D. Geffken, *Bioorg. Med. Chem.* **2006**, *14*, 5121-5135.
- (25) R. Ortmann, J. Wiesner, A. Reichenberg, D. Henschker, E. Beck, H. Jomaa, M. Schlitzer, *Bioorg. Med. Chem. Lett.* **2003**, *13*, 2163-2166.
- (26) T. Kurz, C. T. Behrendt, U. Kaula, B. Bergmann, R. D. Walter, *Aust. J. Chem.* **2007**, *60*, 154-158.
- (27) T. Haemers, J. Wiesner, S. Van Poecke, J. Goeman, D. Henschker, E. Beck, H. Jomaa, S. Van Calenbergh, *Bioorg. Med. Chem. Lett.* **2006**, *16*, 1888-1891.
- (28) T. Kurz, D. Geffken, U. Kaula; (Bioagency AG; Hamburg, Germany), WO2005048715A2, **2005**.
- (29) M. Brzasczcz, K. Kloc, M. Maposah, J. Mlochowski, *Synth. Commun.* **2000**, *30*, 4425-4434.
- (30) K. Ramasamy, R. K. Olsen, T. Emery, *J. Org. Chem.* **1981**, *46*, 5438-5441.
- (31) H. A. Staab, *Angew. Chem., Int. Ed.* **1962**, *1*, 351-367; *Angew. Chem.* **1962**, *74*, 407-423
- (32) C. E. McKenna, M. T. Higa, N. H. Cheung, M. C. McKenna, *Tetrahedron Lett.* **1977**, 155-158.
- (33) L. J. Mathias, *Synthesis* **1979**, 561-576.
- (34) S. Steinbacher, J. Kaiser, W. Eisenreich, R. Huber, A. Bacher, F. Rohdich, *J. Biol. Chem.* **2003**, *278*, 18401-18407.
- (35) A. Mac Sweeney, R. Lange, R. P. M. Fernandes, H. Schulz, G. E. Dale, A. Douangamath, P. J. Proteau, C. Oefner, *J. Mol. Biol.* **2005**, *345*, 115-127.
- (36) All animal experiments were approved by the ethical committee of the University of Antwerp: reference 2010-17. Our lab has the approval of the Ministry of the public health to perform work with human and animal pathogens: reference LA-1100158.
- (37) W. Kabsch, *J. Appl. Crystallogr.* **1993**, *26*, 795-800.

- (38) G. N. Murshudov, A. A. Vagin, E. J. Dodson, *Acta Crystallogr., Sect. D: Biol. Crystallogr.* **1997**, *53*, 240-255.
- (39) D. Turk, *PhD thesis*, Technische Universität München (Germany), **1992**.

## 4 ISPC AS TARGET FOR ANTIINFECTIVE DRUG DISCOVERY



This chapter is adapted with permission from the following publication:

“IspC as target for antiinfective drug discovery: synthesis, enantiomeric separation and structural biology of fosmidomycin thia isosters”

**Andrea Kunfermann**,\* Claudia Lienau,\* Boris Illarionov, Jana Held, Tobias Gräwert, Christoph T. Behrendt, Philipp Werner, Saskia Hähn, Wolfgang Eisenreich, Ulrich Riederer, Benjamin Mordmüller, Adelbert Bacher, Markus Fischer, Michael Groll, and Thomas Kurz.

*J. Med. Chem.* **2013**, *56* (20), 8151-8162.

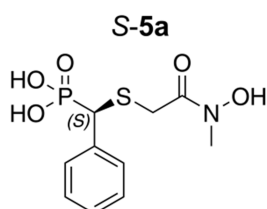
\*These authors contributed equally.

Copyright (2013) American Chemical Society.

## 4.1 Summary

The emergence and spread of multidrug-resistant pathogens are widely believed to endanger human health. New drug targets and lead compounds exempt from cross-resistance with existing drugs are of urgent demand. This chapter reports on the synthesis and properties of “reverse” thia-analogs of fosmidomycin (**1**), which inhibit IspC, the first committed enzyme of the non-mevalonate pathway that is essential for the causative agents of tuberculosis and malaria but is absent in the human host. Notably, IspC displays a high level of enantioselectivity for an  $\alpha$ -substituted derivative of **1**. Based on the work described in chapters 2 and 3 and in the publication Brücher *et. al.*, *J. Med. Chem.* (2012), new reverse analogs of **1** with a sulfur atom at the  $\beta$ -methylene position were synthesized and tested *in vitro* in photometric inhibition assays against IspC for their antibacterial, antituberculosis and antimalarial activity. Compared to the inhibitors described in the chapters before, the thia-analogs led to an improvement of  $IC_{50}$  values in case of *EclspC* and *MtlspC*. Cocrystallization experiments with *PflspC* and the racemic mixture of compound **5a** revealed the interesting finding that the enzyme exclusively binds the *S*-enantiomer into the active site cavity. Additional effort was put in the enantiomeric separation of the racemic mixture of **5a** by HPLC using a chiral column. Kinetic experiments showed that the apparent  $IC_{50}$  values of the (+)- and (-)-enantiomer differ by a factor of 1000. Based on the crystallographic and the kinetic data, the more active enantiomer could be irrevocably assigned for the first time as the *S*-enantiomer.

My contribution to this publication was the accomplishment of the crystallographic studies. Together with Prof. Dr. Adelbert Bacher and Claudia Lienau, I was directly involved in writing the manuscript. On this publication, I am first author with equal contribution of Claudia Lienau.



## 4.2 Zusammenfassung

Die Präsenz und Verbreitung von multiplen Resistenzen von Pathogenen gegenüber Medikamenten ist eine Bedrohung für die Gesundheit des Menschen. Deshalb bedarf es der Entwicklung neuer Zielmoleküle und Leitstrukturen, die unter anderem auch keine Kreuzreaktionen mit bereits bekannten Medikamenten verursachen. In diesem Kapitel wird die Synthese von Schwefelanaloga von Fosmidomycin (**1**) behandelt, welche das erste Enzym (IspC) des Mevalonat-unabhängigen Weges inhibieren, welcher essentiell für die Erreger von Tuberkulose und Malaria ist, aber im Menschen nicht vorkommt. Bemerkenswerterweise zeigt IspC eine hohe Enantioselektivität für ein  $\alpha$ -Aryl substituiertes Derivat von **1**. Basierend auf der Arbeit, die in den Kapiteln 2 und 3 sowie in der Publikation Brücher *et al.*, *J. Med. Chem.* (2012), beschrieben wurde, sind neue Analoga von **1** synthetisiert worden, die ein Schwefelatom an der  $\beta$ -Methylenposition besitzen. Die antibakterielle, anti-Tuberkulose und anti-Malaria Wirkung der Verbindungen wurde *in vitro* in einem photometrischen Aktivitätsassay gegen IspC getestet. Im Vergleich zu den bereits in den vorangehenden Kapiteln beschriebenen Liganden wiesen diese Schwefelderivate bessere  $IC_{50}$  Werte gegen *EcIspC* sowie *MtIspC* auf. Kokkristallisationsexperimente mit *PfIspC* und der racemischen Mischung von Verbindung **5a** deckten auf, dass das Enzym ausschließlich das *S*-Enantiomer in der aktiven Tasche gebunden hatte. Deshalb wurden die Enantiomere von **5a** zum ersten Mal mittels HPLC unter Verwendung einer chiralen Säule getrennt. Kinetische Experimente zeigten, dass sich die apparenten  $IC_{50}$  Werte von dem (+)- und dem (-)-Enantiomer um den Faktor 1000 unterscheiden. Basierend auf den kristallographischen und kinetischen Ergebnissen kann das potentere Enantiomer zum ersten Mal als *S*-Enantiomer festgelegt werden.

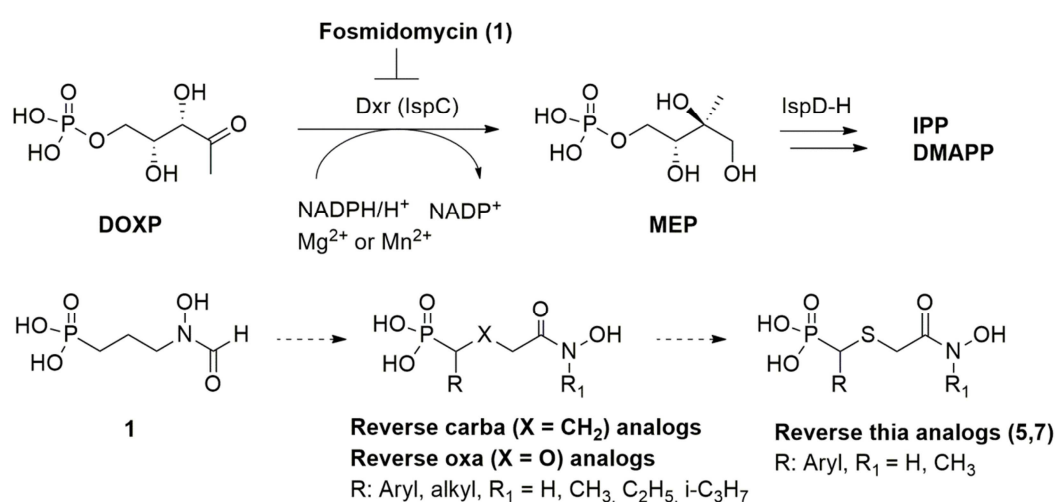
Mein Beitrag zu dieser Arbeit war die Durchführung der kristallographischen Arbeit. Zusätzlich habe ich zusammen mit Prof. Dr. Adelbert Bacher und Claudia Lienau das Manuskript verfasst. Bei dieser Publikation bin ich Erstautorin mit gleichwertigem Beitrag von Claudia Lienau.

### 4.3 Background

The discussion on the current and future management of malaria, a dominant cause of morbidity and mortality, is characterized by apparently antipodal points of view. Optimistic speculations about the feasibility of eradication coexist with the actual problem of progressing resistance against most or all available drugs and the paucity of recent pharmacological innovation.<sup>[1-4]</sup>

A phosphonate antibiotic with a hydroxamate pharmacophore (**1**) that was originally isolated from *S. lavendulae*,<sup>[5,6]</sup> is known to have antibacterial and herbicidal activity and was more recently shown to be active against the *Plasmodium* species causing malaria.<sup>[7,8]</sup> Its molecular target, IspC, catalyzes the first committed step in the non-mevalonate isoprenoid biosynthesis pathway that is essential in *Plasmodium* spp. but absent in mammals (Scheme 4.1).<sup>[9,10]</sup> **1** can cure human malaria and has a favorable toxicity profile, but has shortcomings with regard to pharmacokinetic aspects, which prompted structural modifications in several laboratories.<sup>[11-27]</sup>

Also of note, **1** and its analogs are expected to be exempt from target-related toxicity and from cross-resistance with established antimalarials and may even be able to target the malaria liver stages, which are insufficiently addressed by current antimalarials.<sup>[28,29]</sup> We report the synthesis of thia isosters of reversed hydroxamic acid analogs of **1** and their enzymatic, antiparasite and structural biology features. Furthermore, we show that IspC has a high degree enantioselectivity for a reverse  $\alpha$ -aryl derivative of **1**.

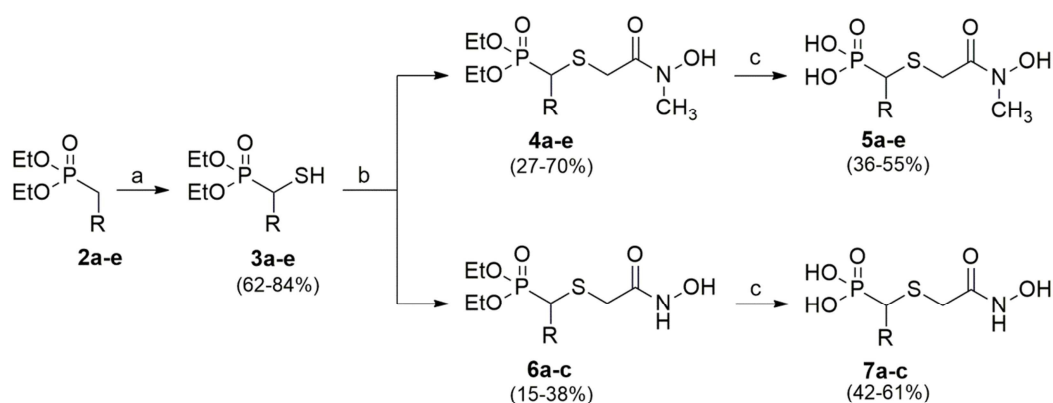


**Scheme 4.1** Fosmidomycin and reverse IspC inhibitors.

## 4.4 Results and discussion

### 4.4.1 Synthesis of the compounds

The retrosynthetic analysis of the target structures **5a-e** and **7a-c** suggested  $\alpha$ -mercaptophosphonates (**3a-e**), 2-chloro-*N*-hydroxyacetamide and 2-chloro-*N*-hydroxy-*N*-methylacetamide as suitable building blocks. The alkylating reagents 2-chloro-*N*-hydroxyacetamide and 2-chloro-*N*-hydroxy-*N*-methylacetamide were obtained by published procedures.<sup>[30,31]</sup> Previously unreported  $\alpha$ -mercaptophosphonates **3b-d** were accessible according to a known procedure developed for the preparation of building block **3a**.<sup>[32]</sup> S-Alkylation of  $\alpha$ -mercaptophosphonates (**3a-e**) with 2-chloro-*N*-hydroxyacetamides afforded partially protected intermediates **4a-e** and **6a-c** (Scheme 4.2). Deprotection of their respective phosphonate moieties by treatment with TMSBr afforded the racemic thia-analogs **5a-e** and **7a-c** as solids or oils.<sup>[33]</sup>



a: R = Ph; b: R = 3,4-F-Ph; c: R = 3,4-Cl-Ph; d: R = naphthalene-1-yl; e: R = 4-CH<sub>3</sub>-Ph

**Scheme 4.2** Reagents and conditions: a) 1. *n*-BuLi, S, THF, -78 °C, 1 h; 2. -20 °C, THF, 1 h; 3. rt, THF, 1 h; b) **4a-e**: 2-chloro-*N*-hydroxy-*N*-methylacetamide, DMF, Na<sub>2</sub>CO<sub>3</sub>, 0 °C → rt; **6a-c**: 2-chloro-*N*-hydroxyacetamide, DMF, Na<sub>2</sub>CO<sub>3</sub>, 0 °C → rt; c) 1. TMSBr, CH<sub>2</sub>Cl<sub>2</sub>, 0 °C, 1 h; 2. CH<sub>2</sub>Cl<sub>2</sub>, rt, 47 h; 3. THF/H<sub>2</sub>O, rt, 45 min.

### 4.4.2 Photometric activity assay

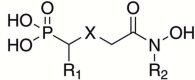
Inhibition of *Pfl*spC by thia-analogs **5** and **7** was monitored using a photometric assay. IC<sub>50</sub> values for inhibition of *Pfl*spC and drug sensitivity assay for two different *P. falciparum* strains were in the low nanomolar to micromolar range (Tables 4.1 and 4.2 and Figure S1 in the Supporting Information). Typical dose-response curves are shown in Figure 4.1. Detailed information on the methods can be found in the Supporting Information. In parallel with earlier findings, the *N*-



methyl substituted hydroxamates **5** showed lower IC<sub>50</sub> values than the respective unsubstituted hydroxamic acids **7**.<sup>[21,34]</sup> Recently we reported reverse carba- and oxa-analogs of **1** that act as potent inhibitors of IspC and of *P. falciparum* growth.<sup>[20,21,35]</sup>

In order to unequivocally establish the generic impact of sulfur, oxygen or methylene in the  $\beta$ -position of  $\alpha$ -phenylated reverse derivatives of **1**, the inhibitory activity of small compound libraries comprising isosteric sets of thia-, oxa- and carba-analogs were determined using IspC orthologs from *E. coli*, *M. tuberculosis* and *P. falciparum* (see Tables 4.1 and 5.2 for an overview of all IC<sub>50</sub> values). By comparison with the carba compounds, the thia isosters show increased inhibition (by more than a factor of ten) for IspC proteins of bacterial origin (black ellipse, Figure 4.2a), but decreased inhibition for PfIspC (red ellipse, Figure 4.2a). The oxa isosters were less potent inhibitors than the cognate carba compounds for all enzymes under study (red and dashed ellipses, Figure 4.2a). The correlation between inhibition of IspC protein and of *P. falciparum* blood stages is illustrated in Figures 4.2b and 4.2c. One cannot observe a perfect match between activity against the enzyme and against the parasite *in vitro*. Consistently, the IC<sub>50</sub> values of the isolated enzyme are lower than the IC<sub>50</sub> values for parasite growth. This is derived from the fact that the compounds must penetrate several membranes in order to reach the site of IspC in the apicoplast (the membranes of the erythrocyte and the parasitophorous vacuole, the outer membrane of the parasite cell and four membranes of the apicoplast).<sup>[36]</sup> In agreement with the enzyme assays, the *N*-methyl substituted derivatives **5** also showed higher inhibitory activity towards strains 3D7 and Dd2 than the free hydroxamic acids **7**. The most active thia-analog **5a** showed an IC<sub>50</sub> value of 30 nM against the *Plasmodium* 3D7 strain. Differences in membrane permeability of the compounds might also be the reason for deviating results between activities against the PfIspC and the whole parasite *in vitro*, explaining the correlation discrepancy of the assays.

**Table 4.1** IC<sub>50</sub> values of thia-analogs **5** and **7** versus IspC of *E. coli*, *M. tuberculosis*, and *P. falciparum*.

	<i>E</i> clspC <sup>[a]</sup> IC <sub>50</sub> [nM]			<i>Mt</i> lspC <sup>[a]</sup> IC <sub>50</sub> [nM]			<i>Pf</i> lspC <sup>[a]</sup> IC <sub>50</sub> [nM]				
	X =	S	O	C	S	O	C	S	O	C	
R <sub>1</sub> = Ph R <sub>2</sub> = CH <sub>3</sub>	<b>5a</b> 8.2 ± 0.8	<b>5aO</b> 940 ± 50	<b>5aC</b> 243 ± 30	<b>5a</b> 280 ± 30	<b>5aO</b> 16000 ± 1000	<b>5aC</b> 2000 ± 100	<b>5a</b> 24 ± 2	<b>5aO</b> 37 ± 2	<b>5aC</b> 3.1 ± 0.3		
R <sub>1</sub> = 3,4-F-Ph R <sub>2</sub> = CH <sub>3</sub>	<b>5b*</b> 8.5 ± 1	<b>5bO</b> 240 ± 10	<b>5bC</b> 117 ± 7	<b>5b</b> 42 ± 2	<b>5bO</b> 4600 ± 200	<b>5bC</b> 770 ± 60	<b>5b</b> 14 ± 1	<b>5bO</b> 12 ± 1	<b>5bC</b> 3.4 ± 0.4		
R <sub>1</sub> = 3,4-Cl-Ph R <sub>2</sub> = CH <sub>3</sub>	<b>5c</b> 5.9 ± 0.6	<b>5cO</b> 200 ± 20	<b>5cC</b> 208 ± 16	<b>5c*</b> 9.2 ± 0.6	<b>5cO</b> 1600 ± 100	<b>5cC</b> 280 ± 30	<b>5c</b> 4.5 ± 0.4	<b>5cO</b> 14 ± 1	<b>5cC</b> 2.8 ± 0.4		
R <sub>1</sub> = naphthalene-1-yl R <sub>2</sub> = CH <sub>3</sub>	<b>5d</b> 140 ± 10	<b>5dO</b> 4600 ± 300	<b>5dC</b> 3830 ± 170	<b>5d*</b> 550 ± 10	<b>5dO</b> 15000 ± 1000	<b>5dC</b> 13000 ± 1000	<b>5d*</b> 9.8 ± 0.9	<b>5dO</b> 39 ± 4	<b>5dC</b> 9.4 ± 1.3		
R <sub>1</sub> = 4-CH <sub>3</sub> -Ph R <sub>2</sub> = CH <sub>3</sub>	<b>5e</b> 33 ± 9	<b>5eO</b> 320 ± 20	<b>5eC</b> 286 ± 19	<b>5e</b> 110 ± 10	<b>5eO</b> 4000 ± 200	<b>5eC</b> 1800 ± 100	<b>5e</b> 18 ± 4	<b>5eO</b> 25 ± 3	<b>5eC</b> 14 ± 2		
R <sub>1</sub> = Ph R <sub>2</sub> = H	<b>7a*</b> 600 ± 90	<b>7aO</b> 20000 ± 2000	<b>7aC</b> 592 ± 25	<b>7a*</b> 15000 ± 1000	<b>7aO</b> 466000 ± 60000	<b>7aC</b> 14000 ± 1000	<b>7a</b> 110 ± 20	<b>7aO</b> 1500 ± 100	<b>7aC</b> 12 ± 3		
R <sub>1</sub> = 3,4-F-Ph R <sub>2</sub> = H	<b>7b*</b> 77 ± 6	<b>7bO</b> 49000 ± 2000	<b>7bC</b> 178 ± 20	<b>7b*</b> 1700 ± 100	<b>7bO</b> > 500000	<b>7bC</b> 3400 ± 300	<b>7b</b> 15 ± 2	<b>7bO</b> 3900 ± 200	<b>7bC</b> 3.9 ± 0.4		
R <sub>1</sub> = 3,4-Cl-Ph R <sub>2</sub> = H	<b>7c</b> 44 ± 2	<b>7cO</b> n.s.	<b>7cC</b> n.s.	<b>7c*</b> 720 ± 50	<b>7cO</b> n.s.	<b>7cC</b> n.s.	<b>7c</b> 200 ± 10	<b>7cO</b> n.s.	<b>7cC</b> n.s.		
Fosmidomycin		221 ± 14.4 <sup>[b]</sup>				230 ± 20			160 ± 20 <sup>[c]</sup>		

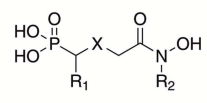
<sup>[a]</sup>Enzyme assay. Values were calculated from at least eight data points. In general two to three independent determinations have been performed.<sup>[37,38]</sup> The asterik (\*) indicates single determination.

<sup>[b]</sup>IC<sub>50</sub> value according to reference 20.

<sup>[c]</sup>IC<sub>50</sub> value according to reference 35.

n.s., not synthesized.

**Table 4.2** IC<sub>50</sub> values of thia-analogs **5** and **7** versus *Plasmodium* strains 3D7 and Dd2.

	<i>Pf</i> 3D7 <sup>[a]</sup> IC <sub>50</sub> [nM]			<i>Pf</i> Dd2 <sup>[a]</sup> IC <sub>50</sub> [nM]		
	X = S	O	C	S	O	C
R <sub>1</sub> = Ph R <sub>2</sub> = CH <sub>3</sub>	<b>5a</b> 30	<b>5aO</b> 1200	<b>5aC</b> 90	<b>5a</b> 75	<b>5aO</b> 700	<b>5aC</b> 74
R <sub>1</sub> = 3,4-F-Ph R <sub>2</sub> = CH <sub>3</sub>	<b>5b</b> 111	<b>5bO</b> 540	<b>5bC</b> 122	<b>5b</b> 88	<b>5bO</b> 130	<b>5bC</b> 40
R <sub>1</sub> = 3,4-Cl-Ph R <sub>2</sub> = CH <sub>3</sub>	<b>5c</b> 91	<b>5cO</b> 240	n.d.	<b>5c</b> 85	<b>5cO</b> 140	n.d.
R <sub>1</sub> = naphthalene-1-yl R <sub>2</sub> = CH <sub>3</sub>	<b>5d</b> 380	<b>5dO</b> 520	n.d.	<b>5d</b> 510	<b>5dO</b> 350	n.d.
R <sub>1</sub> = 4-CH <sub>3</sub> -Ph R <sub>2</sub> = CH <sub>3</sub>	<b>5e</b> 111	<b>5eO</b> 180	n.d.	<b>5e</b> 95	<b>5eO</b> 190	n.d.
R <sub>1</sub> = Ph R <sub>2</sub> = H	<b>7a</b> 2900	> 50000	400	<b>7a</b> 3770	n.d.	570
R <sub>1</sub> = 3,4-F-Ph R <sub>2</sub> = H	<b>7b</b> 160	> 50000	75	<b>7b</b> 330	n.d.	65
R <sub>1</sub> = 3,4-Cl-Ph R <sub>2</sub> = H	<b>7c</b> 540	n.s.	n.s.	<b>7c</b> 870	n.s.	n.s.
Fosmidomycin			880 <sup>[b]</sup>			810 <sup>[b]</sup>

<sup>[a]</sup>*In vitro* assay. Values are the mean of two independent double determinations.

<sup>[b]</sup>IC<sub>50</sub> value according to reference 35.

n.d., not determined; n.s., not synthesized.

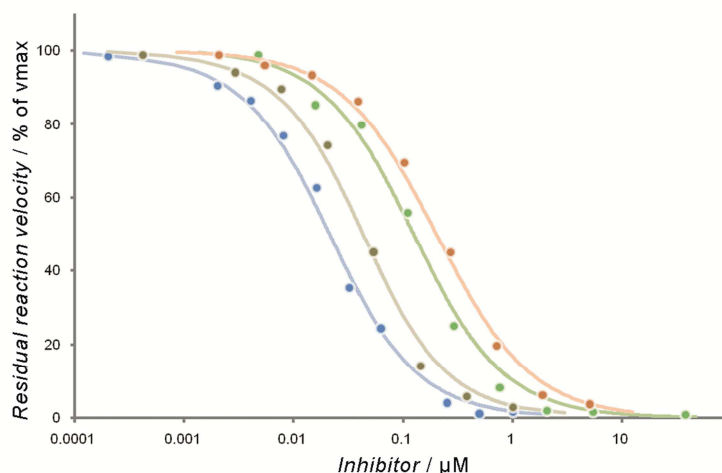


**Figure 4.1** Inhibition of PflSpC by compounds **5a** (blue), **7c** (brown), **7a** (green), **7b** (orange). Residual reaction velocity vs. inhibitor concentration.

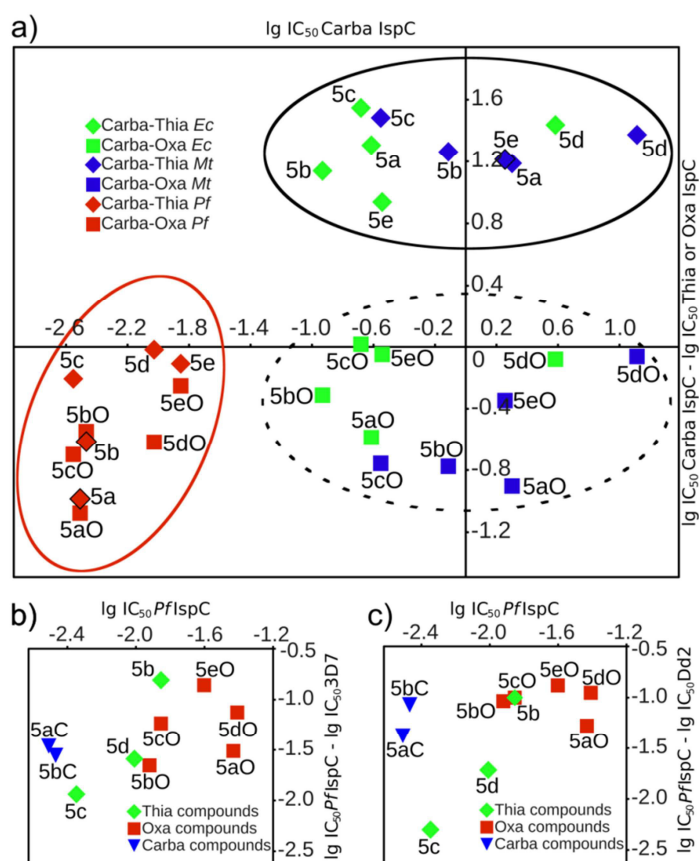


**Figure 4.2** a) Inhibition of IspC orthologs by minilibraries of carba-, oxa- and thia-analogs. Abscissa is the  $\log IC_{50}$  of carba compound. Ordinate is the activity gain with respect to loss caused by sulfur with respect to oxygen in the  $\beta$ -position. The sulfur isosters show increased inhibition for EclspC and MtlspC (black ellipse), but decreased inhibition for PflSpC (red ellipse). The oxa isosters exhibit decreased inhibition throughout (red and dashed ellipses). b, c) Enzyme inhibition compared to inhibition of two different *P. falciparum* strains: b) strain 3D7; c) strain Dd2. Abscissa is the  $IC_{50}$  for PflSpC. Ordinate is the difference of  $\log IC_{50}$  (enzyme) and  $\log IC_{50}$  (parasite proliferation). "C" and "O" after compound numbers designates carba and oxa isosters, respectively. See Tables 4.1 and 4.2 for details on the  $IC_{50}$  values.

#### 4.4.3 Crystal structure elucidation of *PflspC* in complex with **5a**

Next, we determined the three-dimensional structure of *PflspC* in complex with  $Mn^{2+}$ , NADPH and **5a** at a resolution of 2.0 Å (PDB code 4KP7,  $R_{free}=24.9\%$ ) applying Patterson search calculations with the coordinates of *PflspC* (PDB code 3AU8)<sup>[39]</sup> as starting model. Details on data collection and refinement statistics can be found in Table 4.4 in the experimental section. The overall structure is similar to previously reported *PflspC* structures (r.m.s.d. of  $C_{\alpha}<0.6$  Å for PDB code 3AU8). The reversed hydroxamate moiety of the bound **5a** chelates the metal ion ( $Mn^{2+}$ ), which is also coordinated by Asp231, Glu233 and Glu315 of the enzyme (Figures 4.3a and 4.3b). In contrast to *EclspC*, where the coordination of  $Mn^{2+}$  is octahedral due to an additional water molecule, the metal ion is five-fold coordinated in case of *PflspC* and *MtlspC* complex structures (see also the Supporting Information Figures S2–S4). The phosphonate group forms hydrogen bonds with Ser269, Ser270, Ser306, Asn311, Lys312 and two water molecules. Apart from Ser269, the amino acids involved in direct contact with the ligand are strictly conserved (Supporting Information Figure S5).

The loop that covers the ligand is well-defined, whereas it is typically disordered in previously reported *IspC* structures.<sup>[40]</sup> The Trp296 and Met298 residues in this region further stabilize the bound ligand by hydrophobic interactions. As shown by the Connolly surface representation (Figure 4.3c), **5a**,  $Mn^{2+}$  and two water molecules are enclosed in the active site cavity. The loop region over the active site is highly mobile and can thereby accept more bulky residues like the phenyl group in **5a** or the naphthyl group in **5d**.

As seen in the crystal structure, the sulfur atom of the ligand is involved in hydrophobic interactions with the strictly conserved Met298. In contrast, the oxygen atom at the  $\beta$ -methylene position would have a repulsive effect with the sulfur atom of Met298. This is in good agreement with the corresponding  $IC_{50}$  values. The carbon atom at this position is not in contact with the protein. Since the  $IC_{50}$  values for the thia-analogs are significantly lower than for the carba derivatives, it can be assumed that the increased flexibility caused by the sulfur introduction facilitates the binding process of the ligand into the active site cavity. This effect can be clearly seen for *EclspC* as well as *MtlspC*. However, this correlation is less distinctive regarding *PflspC*.

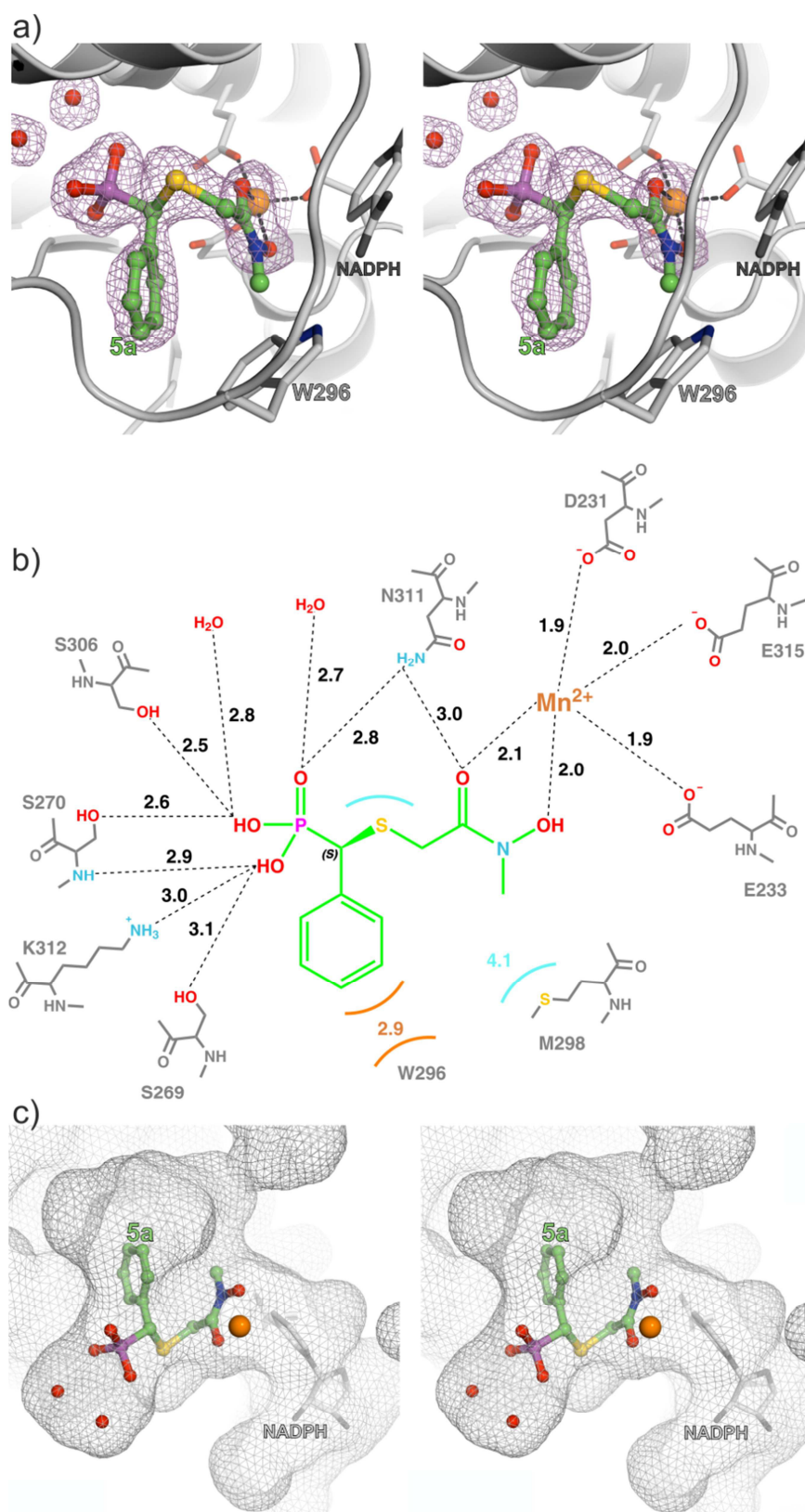


**Figure 4.3** a) Stereo view of **5a** (green) bound to the active site of PflspC (gray) at 2.0 Å resolution; NADPH is shown in gray,  $Mn^{2+}$  in orange, and the electron density (purple mesh) is displayed at  $1.0 \sigma$  contour level. Ligands have been excluded prior to phase calculating. b) Interactions of amino acid residues in contact with **5a** and  $Mn^{2+}$ . Distances are given in Å; van der Waals interactions are indicated by colored curves. c) Stereo view of the Connolly surface representation of the active site cavity.

Whereas cocrystallization had been performed with the racemic inhibitor, the omit map clearly illustrates that the enzyme selectively binds the *S*-enantiomer. Notably, the high contrast provided by the electron-rich sulfur strongly supports the chirality assignment. To illustrate the strength of the crystallographic information, different contour levels for the electron density of the sulfur atom are provided in Figure 4.4. In previous crystallographic studies using several IspC orthologs in complex with  $\alpha$ -phenylated derivatives of **1**, *S*-configuration of the enzyme-bound ligands had been the preferred interpretation,<sup>[21,22,41]</sup> but a definitive chirality assignment had not been possible up to now.

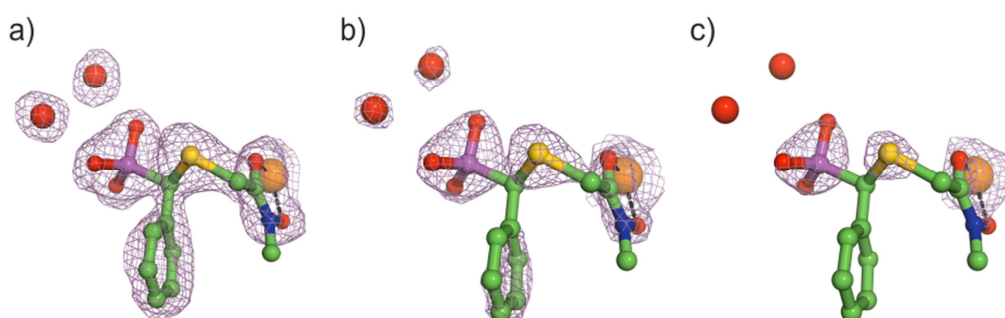


**Figure 4.4** Different contour levels for the electron density map (purple mesh) of *S*-**5a**: NADPH:PfIspC calculated at 2.0 Å resolution. Density is displayed at a) 1.0  $\sigma$ , b) 2.0  $\sigma$ , and c) 3.0  $\sigma$  contour level.

#### 4.4.4 Enantiomeric separation of the racemic mixture of **5a**

In order to quantitatively assess the enantioselectivity toward IspC, the enantiomers of **5a** were separated by chiral HPLC (with ee >99.9%). The apparent IC<sub>50</sub> values of the (+)- and (-)-enantiomers measured against PfIspC are 9.4 nM (+) and >10  $\mu$ M (-), respectively (Table 4.3, Figure 4.5), a similar range that has also been recorded for the bacterial enzymes. On the basis of the kinetic data and the crystallographic complex structure, the more active enantiomer can now be unequivocally assigned as *S*-(+)-**5a**. Thus, because of the strong enantioselectivity, the inhibitory activity of  $\alpha$ -substituted derivatives of **1** can be virtually doubled by racemate separation, while undesirable effects can be diminished by the removal of the less active enantiomer.

**Table 4.3** Inhibition of *IspC* enzymes of *E. coli*, *M. tuberculosis* and *P. falciparum* by **5a**.

Compound <b>5a</b>	IC <sub>50</sub> [nM] <sup>[a]</sup>		
	<i>EclspC</i>	<i>MtlspC</i>	<i>PflspC</i>
<i>R</i> -(-)	4,000 ± 700	83,000 ± 13,000	12,000 ± 1,000
<i>S</i> -(+)	5.1 ± 1.6	120 ± 20	9.4 ± 0.6
Racemate	8.2 ± 0.8	280 ± 30	24 ± 2.0

<sup>[a]</sup>Enzyme assay. Values were calculated from at least eight data points. In general two to three independent determinations have been performed. See the Supporting Information Figure S3 for details on the multiple reaction monitoring.

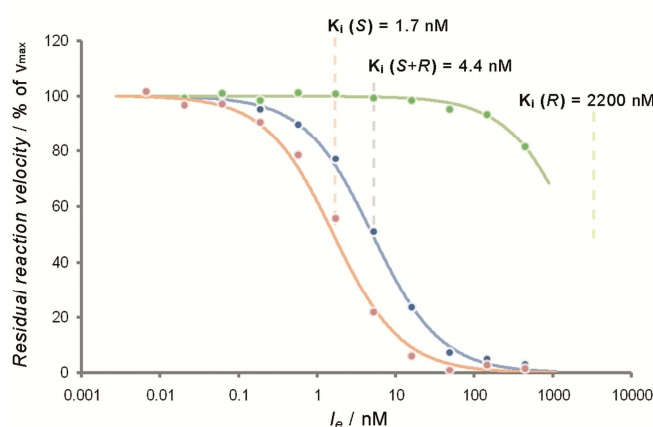


**Figure 4.5** Inhibition of *PflspC* by inhibitor **5a**: *S*-(+)-enantiomer, orange; *R*-(-)-enantiomer, green; racemate, blue.  $I_e$  is the effective inhibitor concentration, which is calculated according to  $I_e = I / (1 + [S]/K_m)$ , where  $I$  is the inhibitor concentration,  $[S]$  is the substrate concentration, and  $K_m$  is the Michaelis-Menten constant. At a residual reaction velocity of 50%,  $I_e$  is equal to the  $K_i$  (inhibition constant) of the inhibitor.

#### 4.4.5 Conclusion

In summary, we provided kinetic and crystallographic evidence for the mode of action of a novel type of reverse hydroxamate-based *IspC* inhibitors. We could show that certain reverse analogs of **1** inhibit *IspC* with IC<sub>50</sub> values in the single-digit nanomolar range while inhibiting the parasite growing in human erythrocytes with IC<sub>50</sub> values in the low nanomolar range. The introduction of a sulfur atom at the  $\beta$ -methylene group of the main chain of the ligands led to an improvement of the IC<sub>50</sub> values in case of *EclspC* and *MtlspC*, compared to the respective carba and oxa ligands. The presented results highlight the more potent inhibitory activity of the *S*-(+)-enantiomer; thus, the long pending question of the stereochemistry of chiral *IspC* ligands is now



clarified. The achievements in the mode of action to block IspC activity might be a helpful guide for the development for more potent chiral inhibitors.

## 4.5 Experimental section

### 4.5.1 General procedures in synthesis

All solvents and chemicals were used as purchased without further purification. The progress of all reactions was monitored on Merck precoated silica gel plates (with fluorescence indicator UV<sub>254</sub>) using EtOAc/*n*-hexane as solvent system. Column chromatography was performed with Fluka silica gel 60 (230-400 mesh ASTM) with the solvent mixtures specified in the corresponding experiment. Spots were visualized by irradiation with ultraviolet light (254 nm). Melting points were taken in open capillaries on a Stuart melting point apparatus SMP11 and are uncorrected. Proton (<sup>1</sup>H) and carbon (<sup>13</sup>C) NMR spectra were recorded on a Bruker Avance 500 (500.13 MHz for <sup>1</sup>H; 125.76 MHz for <sup>13</sup>C) using DMSO-d<sub>6</sub> as solvent. Chemical shifts are given in ppm, (δ relative to residual solvent peak for <sup>1</sup>H and <sup>13</sup>C). Elemental analysis was performed on a Perkin Elmer PE 2400 CHN elemental analyzer and a vario MICRO cube elemental analyzer (Elementar Analysensysteme GmbH; Hanau, Germany). IR spectra were recorded on a Varian 800 FT-IR Scimitar series. Optical rotation was determined by a Krüss P8000 polarimeter; values are given in deg cm<sup>3</sup>g<sup>-1</sup> dm<sup>-1</sup>. Specific rotations  $[\alpha]_D^{20}$  values are given in g cm<sup>-3</sup>. High resolution mass spectrometry (HRMS) analysis was performed using a UHR-TOF maXis 4G instrument (Bruker Daltonics; Bremen, Germany). If necessary, the purity was determined by HPLC. Purity of all final compounds was 95% or higher. Instrument: Elite LaChrom system [Hitachi L-2130 (pump) and L-2400 (UV-detector)]; column: Phenomenex Luna C-18(2) 5 μm particle size (250 mm × 4.6 mm), supported by Phenomenex Security Guard Cartridge Kit C18 (4.0 mm × 3.0 mm). Chiral HPLC separation of compound **5a** was performed on HP Series 1100 (Agilent); column: Chiralcel OZ-H (Chiral Technologies Europe), 5 μm particle size (250 mm × 4.6 mm); eluent A: *n*-heptane, eluent B: propan-2-ol with 0.1% trifluoroacetic acid, isocratic (70:30) with a flow rate of 1 mL min<sup>-1</sup> and detection at 240 nm; column temperature: 25 °C; injection: 50 μL 34.3 mM **5a** in *n*-heptane/propan-2-ol (70:30).

## Materials

Diethylphosphonates **2a-e**,  $\alpha$ -mercaptophosphonates **3a** and **3e**, 2-chloro-*N*-hydroxy-*N*-methylacetamide and 2-chloro-*N*-hydroxyacetamide have been prepared according to known procedures.<sup>[30,31]</sup>  $\alpha$ -Mercaptophosphonates **3a-e** were synthesized according to the procedure of Mikolajczyk.<sup>[32]</sup> Compound **3a** has been previously described by Mikolajczyk<sup>[32]</sup> and compound **3e** by Creary.<sup>[42]</sup>

### 4.5.2 Gene expression and protein purification

The recombinant *E. coli* strain M15[pREP4]pQEIspCplasart<sup>[20]</sup> was grown to an optical density of 0.6 at 37 °C in LB medium supplemented with ampicillin (180 mg L<sup>-1</sup>) and kanamycin (50 mg L<sup>-1</sup>). Isopropylthiogalactoside (IPTG) was added to a final concentration of 1 mM and the cell suspension was cultivated overnight at 30 °C under shaking (120 rpm). Cells were harvested by centrifugation, washed with 0.9% NaCl solution and resuspended in loading buffer (100 mM Tris-HCl (pH 7.4), containing 500 mM NaCl and 20 mM imidazole). The suspension was passed through a cell disruption device (Basic Z Model; Constant Systems Limited, Northamptonshire, UK) and was then centrifuged. The supernatant was subjected to a Ni<sup>2+</sup>-chelating Sepharose Fast Flow<sup>®</sup> column (volume: 40 mL) that had been pre-equilibrated with loading buffer. The column was flushed with 100 mM Tris-HCl (pH 7.4), containing 500 mM NaCl and 100 mM imidazole to remove unbound protein and was then developed with 100 mM Tris-HCl (pH 7.4), containing 500 mM NaCl and 250 mM imidazole. Fractions were combined and dialysed at 4 °C overnight against 50 mM Tris-HCl (pH 7.4), containing 2 mM DTT and 0.02% NaN<sub>3</sub>. PflspC was obtained with approximately 95% purity, as estimated by SDS-PAGE analysis.

### 4.5.3 Crystallization and structure determination

PflspC protein (11 mg mL<sup>-1</sup> in 50 mM Tris-HCl (pH 7.4), containing 2 mM DTT and 0.02% NaN<sub>3</sub>) was incubated with 1.5 mM **5a** (racemate), 640  $\mu$ M MnCl<sub>2</sub> and 800  $\mu$ M NADPH prior to crystallization. Crystals were prepared using the sitting drop vapor diffusion method at 20 °C. The droplets comprised 0.1  $\mu$ L protein solution and 0.1  $\mu$ L reservoir solution (2% PEG4000, 100 mM NaOAc and 15% MPD (pH 5.0)). Crystals grew to a final size of 500  $\times$  100  $\times$  50  $\mu$ m<sup>3</sup> within six weeks. PflspC cocrystals were flash-frozen without further cryoprotectant in a stream of nitrogen gas at 100 K (Oxford Cryosystems Ltd; Oxfordshire, UK). A native dataset at 2.0 Å

resolution was collected using synchrotron radiation at the X06SA beamline, Swiss Light Source, Villigen, Switzerland. Data were processed using the program package XDS<sup>[43]</sup> and data reduction was performed with XSCALE with a final  $R_{\text{free}}$  value of 24.9% and r.m.s.d bond length and angle values of 0.09 Å and 1.2 °, respectively (Table 4.4). Crystal structure analysis was carried out by molecular replacement using coordinates of *PflspC* deposited at the PDB with the code 3AU8.<sup>[39]</sup> The anisotropy of diffraction was corrected by TLS-refinement using the program REFMAC5.<sup>[44]</sup> Electron density was improved by averaging and back transforming the reflections ten times over the two-fold non-crystallographic symmetry axis using the program package MAIN.<sup>[45]</sup> Conventional crystallographic rigid body, positional and temperature factor refinements were calculated with REFMAC5. The model was completed using the interactive three-dimensional graphic program MAIN. The atomic coordinates for *PflspC* in complex with *S-5a*,  $\text{Mn}^{2+}$  and NADPH have been deposited in the PDB, Research Collaboratory for Structural Bioinformatics at Rutgers University under the accession code 4KP7.

**Table 4.4** Data collection and refinement statistics.

S-5a:NADPH:PflspC	
<b>Crystal parameter</b>	
Space group	P2 <sub>1</sub>
Cell dimensions	a=51.5 Å, b=78.1 Å, c=100.0 Å; β=91.5 °
Molecules per AU <sup>a</sup>	2
<b>Data collection</b>	
Beam line	SLS, X06SA
Wavelength (Å)	1.0
Resolution range (Å) <sup>b</sup>	40-2.0 (2.1-2.0)
Observed / unique <sup>c</sup> reflections	196791 / 52039
Completeness (%) <sup>b</sup>	97.1 (96.7)
R <sub>merge</sub> (%) <sup>b,d</sup>	8.2 (53.3)
I/σ (I) <sup>b</sup>	12.7 (3.0)
<b>Refinement</b>	
Resolution (Å)	15-2.0
R <sub>work</sub> / R <sub>free</sub> <sup>e</sup>	18.5 / 24.9
No. atoms	6790
Protein	6468
Ligand	84
Mn <sup>2+</sup>	2
Water	236
B-factors	37.0
R.m.s. deviations <sup>f</sup>	
Bond lengths (Å)	0.009
Bond angles (°)	1.20
Ramachandran (%) <sup>g</sup>	97.3 / 2.7 / 0.0
PDB accession code	4KP7

<sup>[a]</sup>Asymmetric unit.

<sup>[b]</sup>Values in parenthesis of resolution range, completeness, R<sub>merge</sub> and I/σ (I) correspond to the last resolution shell.

<sup>[c]</sup>Friedel pairs were treated as identical reflections.

<sup>[d]</sup> $R_{\text{merge}}(I) = \frac{\sum_{hkl} \sum_j |I(hkl)_j - \langle I(hkl) \rangle|}{\sum_{hkl} I_{hkl}}$ , where I(hkl)<sub>j</sub> is the measurement of the intensity of reflection hkl and <I(hkl)> is the average intensity.

<sup>[e]</sup> $R = \frac{\sum_{hkl} | |F_{\text{obs}}| - |F_{\text{calc}}| |}{\sum_{hkl} |F_{\text{obs}}|}$ , where R<sub>free</sub> is calculated without a sigma cut off for a randomly chosen 5% of reflections, which were not used for structure refinement, and R<sub>work</sub> is calculated for the remaining reflections.

<sup>[f]</sup>Deviations from ideal bond lengths / angles.

<sup>[g]</sup>Number of residues in favored region / allowed region / outlier region.

#### 4.5.4 Supporting Information

Additional information on material and methods, the Supporting Information, and the full article are available under DOI: 10.1021/jm4012559.

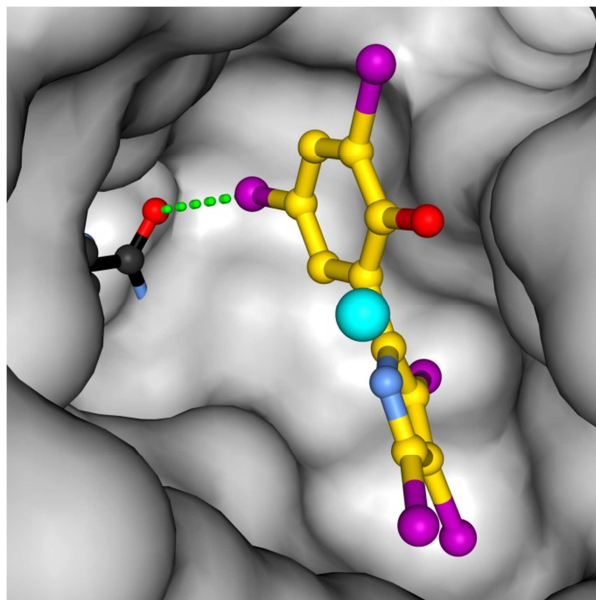
## 4.6 References

- (1) Y. V. Ershov, *Appl. Biochem. Microbiol.* **2007**, *43*, 115-138.
- (2) C. J. L. Murray, L. C. Rosenfeld, S. S. Lim, K. G. Andrews, K. J. Foreman, D. Haring, N. Fullman, M. Naghavi, R. Lozano, A. D. Lopez, *Lancet* **2012**, *379*, 413-431.
- (3) B. Mordmüller, P. G. Kremsner, *Curr. Mol. Med.* **2006**, *6*, 247-251.
- (4) T. N. Wells, E. M. Poll, *Discovery Med.* **2010**, *9*, 389-398.
- (5) M. Okuhara, Y. Kuroda, T. Goto, M. Okamoto, H. Terano, M. Kohsaka, H. Aoki, H. Imanaka, *J. Antibiot.* **1980**, *33*, 24-28.
- (6) Y. Kuroda, M. Okuhara, T. Goto, M. Okamoto, H. Terano, M. Kohsaka, H. Aoki, H. Imanaka, *J. Antibiot.* **1980**, *33*, 29-35.
- (7) H. Jomaa, J. Wiesner, S. Sanderbrand, B. Altincicek, C. Weidemeyer, M. Hintz, I. Turbachova, M. Eberl, J. Zeidler, H. K. Lichtenthaler, D. Soldati, E. Beck, *Science* **1999**, *285*, 1573-1576.
- (8) N. Singh, G. Chevé, M. A. Avery, C. R. McCurdy, *Curr. Pharm. Des.* **2007**, *13*, 1161-1177.
- (9) M. Rohmer, C. Grosdemange-Billiard, M. Seemann, D. Tritsch, *Curr. Opin. Invest. Drugs* **2004**, *5*, 154-162.
- (10) F. Rohdich, A. Bacher, W. Eisenreich, *Biochem. Soc. Trans.* **2005**, *33*, 785-791.
- (11) A. Reichenberg, J. Wiesner, C. Weidemeyer, E. Dreiseidler, S. Sanderbrand, B. Altincicek, E. Beck, M. Schlitzer, H. Jomaa, *Bioorg. Med. Chem. Lett.* **2001**, *11*, 833-835.
- (12) R. Ortman, J. Wiesner, A. Reichenberg, D. Henschker, E. Beck, H. Jomaa, M. Schlitzer, *Arch. Pharm.* **2005**, *338*, 305-314.
- (13) T. Kurz, D. Geffken, U. Kaula, (Bioagency AG; Hamburg, Germany), international patent application DE10356410A1, WO2005048715A2, and WO2005048715A3, **2005**.
- (14) L. Kuntz, D. Tritsch, C. Grosdemange-Billiard, A. Hemmerlin, A. Willem, T. J. Bacht, M. Rohmer, *Biochem. J.* **2005**, *386*, 127-135.
- (15) T. Kurz, K. Schlüter, U. Kaula, B. Bergmann, R. D. Walter, D. Geffken, *Bioorg. Med. Chem.* **2006**, *14*, 5121-5135.
- (16) T. Haemers, J. Wiesner, S. Van Poecke, J. Goeman, D. Henschker, E. Beck, H. Jomaa, S. Van Calenbergh, *Bioorg. Med. Chem. Lett.* **2006**, *16*, 1888-1891.
- (17) K. Schlüter, R. D. Walter, B. Bergmann, T. Kurz, *Eur. J. Med. Chem.* **2006**, *41*, 1385-1397.
- (18) T. Haemers, J. Wiesner, D. Gießmann, T. Verbrugghen, U. Hillaert, R. Ortman, H. Jomaa, A. Link, M. Schlitzer, S. Van Calenbergh, *Bioorg. Med. Chem.* **2008**, *16*, 3361-3371.
- (19) T. Verbrugghen, P. Cos, L. Maes, S. Van Calenbergh, *J. Med. Chem.* **2010**, *53*, 5342-5346.

- (20) C. T. Behrendt, A. Kunfermann, V. Illarionova, A. Matheeussen, T. Gräwert, M. Groll, F. Rohdich, A. Bacher, W. Eisenreich, M. Fischer, L. Maes, T. Kurz, *ChemMedChem* **2010**, *5*, 1673-1676.
- (21) C. T. Behrendt, A. Kunfermann, V. Illarionova, A. Matheeussen, M. K. Pein, T. Gräwert, J. Kaiser, A. Bacher, W. Eisenreich, B. Illarionov, M. Fischer, L. Maes, M. Groll, T. Kurz, *J. Med. Chem.* **2011**, *54*, 6796-6802.
- (22) M. Andaloussi, L. M. Henriksson, A. Wieckowska, M. Lindh, C. Björkelid, A. M. Larsson, S. Suresh, H. Iyer, B. R. Srinivasa, T. Bergfors, T. Unge, S. L. Mowbray, M. Larhed, T. A. Jones, A. Karlen, *J. Med. Chem.* **2011**, *54*, 4964-4976.
- (23) T. Kurz, C. T. Behrendt, U. Kaula, B. Bergmann, R. D. Walter, *Aust. J. Chem.* **2007**, *60*, 154-158.
- (24) C. T. Behrendt, *PhD thesis*, Heinrich Heine Universität Düsseldorf (Germany), **2011**.
- (25) K. Brücher, *PhD thesis*, Heinrich Heine Universität Düsseldorf (Germany), **2012**.
- (26) T. Murakawa, H. Sakamoto, S. Fukada, T. Konishi, M. Nishida, *Antimicrob. Agents Chemother.* **1982**, *21*, 224-230.
- (27) H. P. Kuemmerle, T. Murakawa, F. Desantis, *Chemioterapia* **1987**, *6*, 113-119.
- (28) S. Borrmann, S. Issifou, G. Esser, A. A. Adegnika, M. Ramharter, P. B. Matsiegui, S. Oyakhirome, D. P. Mawili-Mboumba, M. A. Missinou, J. F. J. Kun, H. Jomaa, P. G. Kremsner, *J. Infect. Dis.* **2004**, *190*, 1534-1540.
- (29) S. H. I. Kappe, A. M. Vaughan, J. A. Boddey, A. F. Cowman, *Science* **2010**, *328*, 862-866.
- (30) R. V. Hoffman, N. K. Nayyar, *J. Org. Chem.* **1994**, *59*, 3530-3539.
- (31) M. A. Casadei, B. Dirienzo, A. Inesi, F. M. Moracci, *J. Chem. Soc., Perkin Trans.* **1992**, 375-378.
- (32) M. Mikolajczyk, S. Grzejszczak, A. Chefczynska, A. Zatorski, *J. Org. Chem.* **1979**, *44*, 2967-2972.
- (33) C. E. McKenna, M. T. Higa, N. H. Cheung, M. C. McKenna, *Tetrahedron Lett.* **1977**, 155-158.
- (34) C. S. Leung, S. S. F. Leung, J. Tirado-Rives, W. L. Jorgensen, *J. Med. Chem.* **2012**, *55*, 4489-4500.
- (35) K. Brücher, B. Illarionov, J. Held, S. Tschan, A. Kunfermann, M. K. Pein, A. Bacher, T. Gräwert, L. Maes, B. Mordmüller, M. Fischer, T. Kurz, *J. Med. Chem.* **2012**, *55*, 6566-6575.
- (36) C. Y. Botte, F. Dubar, G. I. McFadden, E. Marechal, C. Biot, *Chem. Rev.* **2012**, *112*, 1269-1283.
- (37) P. Kuzmic, *Anal. Biochem.* **1996**, *237*, 260-273.

- (38) W. H. Press, S. A. Teukolsky, W. T. Vetterling, B. P. Flannery, *Numerical Recipes: The Art of Scientific Computing*; Cambridge University Press: New York, **2007**; 3<sup>rd</sup> edition.
- (39) T. Umeda, N. Tanaka, Y. Kusakabe, M. Nakanishi, Y. Kitade, K. T. Nakamura, *Sci. Rep.* **2011**, *1*, 1-8.
- (40) S. Steinbacher, J. Kaiser, W. Eisenreich, R. Huber, A. Bacher, F. Rohdich, *J. Biol. Chem.* **2003**, *278*, 18401-18407.
- (41) L. Deng, J. Diao, P. Chen, V. Pujari, Y. Yao, G. Cheng, D. C. Crick, B. V. V. Prasad, Y. Song, *J. Med. Chem.* **2011**, *54*, 4721-4734.
- (42) X. Creary, M. E. Mehrsheikhmohammadi, *J. Org. Chem.* **1986**, *51*, 7-15.
- (43) W. Kabsch, *J. Appl. Crystallogr.* **1993**, *26*, 795-800.
- (44) G. N. Murshudov, A. A. Vagin, E. J. Dodson, *Acta Crystallogr., Sect. D: Biol. Crystallogr.* **1997**, *53*, 240-255.
- (45) D. Turk, *PhD thesis*, Technische Universität München (Germany), **1992**.

## 5 PSEUDILINS: HALOGENATED, ALLOSTERIC INHIBITORS OF THE NON-MEVALONATE PATHWAY ENZYME ISPD



This chapter is adapted with permission from the following publication:

“Pseudilins: halogenated, allosteric inhibitors of the non-mevalonate pathway enzyme IspD”

**Andrea Kunfermann**,\* Matthias Witschel,\* Boris Illarionov, René Martin, Matthias Rottmann, Wolfgang Höffken, Michael Seet, Wolfgang Eisenreich, Hans-Joachim Knölker, Markus Fischer, Adelbert Bacher, Michael Groll, and François Diederich.

*Angew. Chem., Int. Ed.* **2014**, *53* (8), 2235-2239.

*Angew. Chem.* **2014**, *126* (8), 2267-2272.

\*These authors contributed equally.

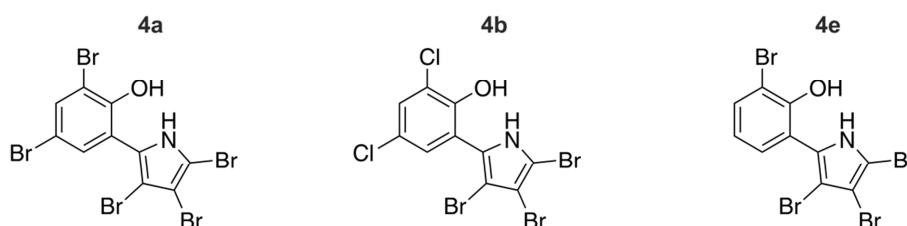
Copyright (2014) John Wiley & Sons, Inc.



## 5.1 Summary

Nowadays, one of the most challenging problems for the treatment of infectious diseases is the rapid formation of resistances against known anti-infectives or herbicides. Therefore, new chemical entities as well as new targets are in the focus of current drug research. Pseudilins, highly halogenated marine natural products, inhibit the second enzyme of the non-mevalonate pathway, IspD, by an allosteric mode of action using halogen bonding and metal ion coordination. Notably, they exhibit herbicidal and antiplasmodial activity *in vitro* and *in vivo*. A high throughput screening of a compound library against *AthIspD* led to pseudilin derivatives with potential herbicidal activity, **4a** and **4b**. Further photometric and NMR based assays confirmed the IC<sub>50</sub> values in the single-digit micromolar range. Additional experiments with blood stages of *P. falciparum* exhibited promising EC<sub>50</sub> values in the double-digit micromolar range. However, photometric activity assays with *P. vivax* IspD (*PvIspD*) showed only moderate IC<sub>50</sub> values in the micromolar range. Crystallization of *AthIspD* in complex with different pseudilin derivatives exhibited interesting insights into the binding mode of the ligands. The pseudilins are located in an allosteric pocket in close proximity to the active site. Formation of this pocket induces structural rearrangements to the surrounding residues, which inhibits binding of the cosubstrate CTP. Furthermore, the pseudilins adopt the *syn*-conformation and thereby chelate a Cd<sup>2+</sup> that is present in the crystallization buffer by its phenolic hydroxyl group and by the pyrrole nitrogen. In addition, the halogen atom in *para*-position to the phenolic hydroxyl group interacts with the oxygen atom of the enzyme-backbone. Compound **4e** seems not to be able to undergo halogen bonding since the bromine atom at the *para*-position is missing. Interestingly, the crystal structure of *AthIspD* in complex with **4e** displays the phenyl moiety in both, *syn*- and *anti*-conformation. In *anti*, the metal chelation is abolished, whereas **4e** can interact with the backbone by the halogen atom in *ortho*-position.

My contribution to this publication was the performance of the NMR based activity assays and the crystallographic work. In addition, I was directly involved in writing the manuscript together with Prof. Dr. Michael Groll. On this publication, I am first author with equal contribution of Dr. Matthias Witschel.



## 5.2 Zusammenfassung

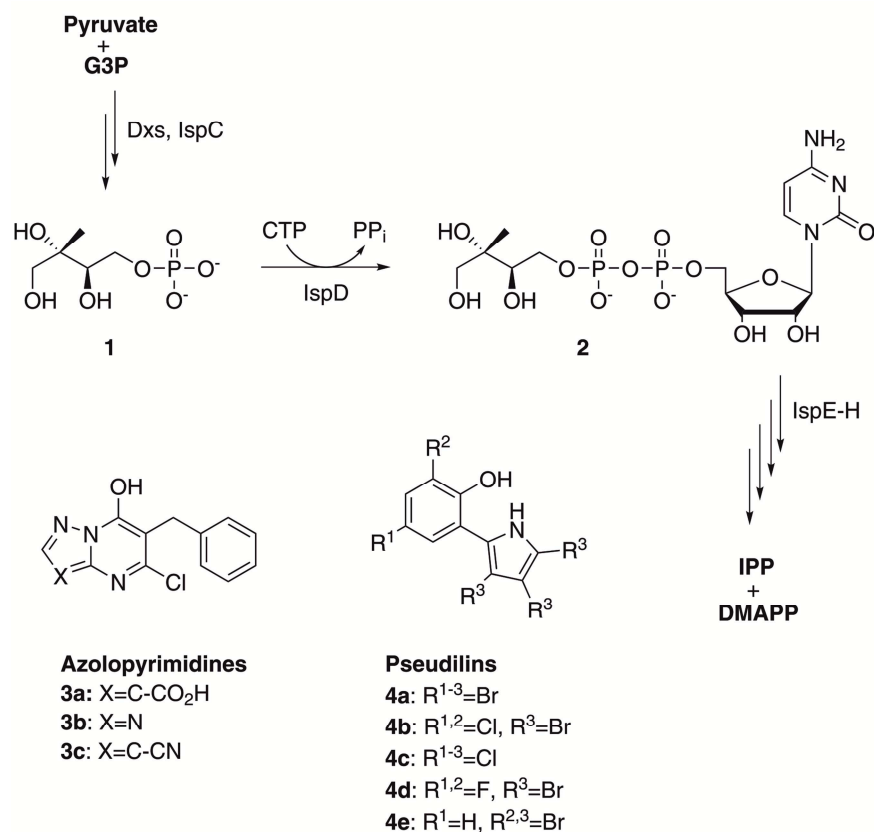
Heutzutage ist eine der schwierigsten Herausforderungen in der Behandlung von Infektionskrankheiten die Resistenzbildung gegen bekannte Antiinfectiva oder Herbizide. Deshalb sind neue Medikamente und folglich die Suche nach neuen Zielmolekülen im Fokus der Forschung. Pseudiline sind mehrfach halogenierte, marine Naturstoffe, welche das zweite Enzym des Mevalonat-unabhängigen Weges (IspD) durch eine allosterische Wirkungsweise mittels Halogenbindung und Metallkoordinierung inhibieren. Bemerkenswerterweise konnte den Verbindungen herbizide und antiplasmodiale Aktivität nachgewiesen werden. Ein Hochdurchsatzsuchverfahren einer Ligandenbibliothek gegen *AthIspD* führte zu zwei Pseudilinderivaten (Verbindungen **4a** und **4b**) mit potentiell herbizider Wirkung. Weitere photometrische sowie NMR-basierte Aktivitätsassays bestätigten die  $IC_{50}$  Werte im einstelligen mikromolaren Bereich. Zusätzliche Experimente mit Blutzelllinien von *P. falciparum* zeigten vielversprechende  $EC_{50}$  Werte im zweistelligen mikromolaren Bereich. Allerdings wurden in photometrischen Aktivitätsassays gegen *PvIspD* nur mäßige  $IC_{50}$  Werte im höheren mikromolaren Bereich gemessen. Kristallstrukturen von *AthIspD* mit den verschiedenen Pseudilinderivaten ermöglichten interessante Einblicke in den Bindungsmodus der Liganden. Dabei befinden sich die Pseudiline in einer allosterischen Tasche in der Nähe des aktiven Zentrums. Die Bildung dieser Tasche führt zu strukturellen Umlagerungen der umliegenden Seitenketten, was verhindert, dass das Kosubstrat CTP binden kann. Weiter nehmen die Liganden die *syn*-Konformation ein und chelatisieren dabei ein im Kristallisationspuffer enthaltenes  $Cd^{2+}$  durch die Hydroxylgruppe des Phenylrestes sowie durch den Pyrrolstickstoff. Zusätzlich bildet ein Halogenatom in *para*-Stellung eine Halogenbindung zum Enzymrückgrat aus. Verbindung **4e** scheint diese Bindung nicht eingehen zu können, da das Brom in *para*-Stellung fehlt. Die Kokristallstruktur mit *AthIspD* zeigte, dass **4e** in *syn*- als auch in *anti*-Konformation in der allosterischen Tasche gebunden vorliegt. In *anti*-Stellung geht zwar die Metallkoordinierung verloren, jedoch kann der Ligand dafür durch das Bromatom in *ortho*-Position eine Halogenbindung ausbilden.

Mein Beitrag zu dieser Arbeit war die Durchführung der NMR-basierten Aktivitätsassays sowie die kristallographische Arbeit. Zusätzlich habe ich zusammen mit Prof. Dr. Michael Groll das Manuskript verfasst. Bei dieser Publikation bin ich Erstautorin mit gleichwertigem Beitrag von Dr. Matthias Witschel.

### 5.3 Background

Two of the most urgent challenges for humanity are the fight against nutritional problems, and against infectious diseases, such as malaria<sup>[1-3]</sup> and tuberculosis.<sup>[4,5]</sup> Unfortunately, the key tools against those plagues, herbicides, which are essential for crop yields, and antiinfectives, suffer from rapid loss of efficacy due to increasing resistance of the targeted organisms. In an effort to cross-fertilize both fields, lead compounds from agro-chemistry research have been examined against infectious germs.<sup>[6]</sup> Whereas animals exclusively use the mevalonate pathway for the biosynthesis of the terpenoid precursors IPP and DMAPP,<sup>[7-9]</sup> plants and many human pathogens utilize the non-mevalonate pathway (also designated DXP pathway) discovered in the 1990s.<sup>[10-13]</sup> The seven enzymes of the non-mevalonate pathway (Scheme 5.1) are recognized drug targets.<sup>[14]</sup> Also, recent efforts in herbicide research have demonstrated the importance of this pathway to ensure food supply to a strongly increasing global population.<sup>[15,16]</sup> The commercial herbicide ketoclofazole inhibits Dxs, the first enzyme of the non-mevalonate pathway (for abbreviations see Scheme 5.1 and Supporting Information Figure 1SI).<sup>[17]</sup> The natural product fosmidomycin, which blocks IspC, has been favorably evaluated in clinical trials against malaria.<sup>[18]</sup> The third enzyme of the pathway, IspD, converts MEP (**1**) into CDP-ME (**2**). We recently showed that synthetic azolopyrimidine derivatives (**3a-c**) (Scheme 5.1) inhibit *AthIspD* with IC<sub>50</sub> values in the low nanomolar range, indicating that IspD is a potential target for drug development.<sup>[19]</sup>

Here, we report on the allosteric mode of action of pseudilin derivatives (Scheme 5.1), highly halogenated marine alkaloids<sup>[20,21]</sup> with herbicidal and antimalarial activity, against IspD. We determined the inhibitory potency in photometric and NMR-based activity assays by published procedures.<sup>[22]</sup> Moreover, these derivatives were analyzed *in vitro* for their efficacy against *P. falciparum*. The herbicidal activity of the pseudilins has already been described before,<sup>[6]</sup> and here, their allosteric binding properties were elucidated at the atomic level by crystallography of *AthIspD* complex structures, featuring effective protein-ligand halogen-bonding interaction.



**Scheme 5.1** IspD-catalyzed reaction and target compounds **3a-c** and **4a-e**. Compounds **4a-e** are shown in the *syn*-conformation. G3P, glyceraldehyde-3-phosphate; **1**, MEP; **2**, CDP-ME.

## 5.4 Results and discussion

### 5.4.1 *In vitro* activity assays

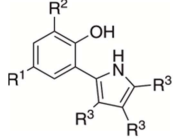
In order to discover new chemical entities as herbicidal drug leads against IspD, a library comprising of about 100,000 compounds with drug-like properties was screened using a photometrically monitored assay.<sup>[22,23]</sup> This approach allowed us to identify hits with IC<sub>50</sub> values in the low μM range (<25 μM) against *AthIspD* (Table 5.1), namely compounds **4a** and **4b**, which belong to the class of pseudilins that have been discovered in the 1960s and isolated from the marine bacterium *Pseudomonas bromoutilis*.<sup>[20,24-26]</sup> The chemical scaffold of the screening hits differs significantly from that of the previously published synthetic azolopyrimidines, suggesting that pseudilin derivatives might exhibit a new mode of action towards IspD.

To further investigate the pseudilin-type inhibitors, we synthesized **4a-e** using published procedures.<sup>[24-28]</sup> We started kinetic studies with the coupled assay using three supplementary enzymes and three cosubstrates in order to enable a photometric readout of the reaction

velocity (Table 5.1). The  $IC_{50}$  values for the auxiliary enzymes are summarized in Table 1SI. Under assay conditions utilizing 5 mM  $MgCl_2$  but no other divalent cations, **4a** had an apparent  $IC_{50}$  value of 13  $\mu M$ . As elucidated by the crystal structures described below, cadmium(II) is in a chelate complex with the pseudilin derivatives. Therefore,  $CdSO_4$  was added to the assay buffer to concentrations in the double-digit micromolar range, which was accompanied by a more than seven-fold increase in the inhibitory potential. Similar effects were noted with compounds **4b** and **4c**. In comparison to the other derivatives, **4e** exhibits a decreased inhibition profile in the photometric assay, which is in agreement with the structural results. As shown for compound **4b** (Table 2SI), the binding preference could also be increased two-fold by addition of other divalent cations ( $Ca^{2+}$ ,  $Cu^{2+}$ , or  $Zn^{2+}$ ) in a concentration of 20  $\mu M$ . We confirmed the photometrically monitored assay by quantitative  $^{31}P$  NMR spectroscopy that records simultaneously the concentrations of the IspD substrate **1** as well as the products **2** and diphosphate (Figure 5.5a). These experiments revealed that the equilibrium for the IspD-catalyzed reaction is not predominantly on the product side. Therefore, the overall free energy gradient of the catalyzed reaction was increased by the addition of inorganic diphosphatase in order to convert the reaction product diphosphate into orthophosphate (see chapter 5.5.7 for details on the assay). The  $IC_{50}$  values determined by the two distinct methods agreed within the limits of a factor of three ( $IC_{50}$  values are  $1.4 \pm 0.3 \mu M$  for compound **4a**,  $7.5 \pm 0.3 \mu M$  for compound **4e**), confirming that divalent metal ions are crucial components for the strong inhibition of IspD by pseudilin derivatives, except **4e**.

We also tested the pseudilin-type inhibitors against the blood stages of *P. falciparum*, the causative agent of malaria tropica, whose survival is dependent on the activity of the non-mevalonate pathway (Table 5.1).<sup>[29]</sup> The  $EC_{50}$  values of the cell-based assay were in 1-12  $\mu M$  range, suggesting that IspD might be the molecular target causing the antiplasmodial activity of pseudilins. Cytotoxicity of **4a** against mammalian (rat) cells was found to be 3.1  $\mu M$ . Hence, *PvIspD*<sup>[30,31]</sup> was tested in a photometric activity assay against the identified candidates. Compared to *AthIspD*, a weaker inhibition in the double-digit  $\mu M$  range was detected for the pseudilin derivatives studied in *PvIspD*. This, and the cytotoxicity seen in mammalian cells,<sup>[26]</sup> indicates that the inhibition of the *P. falciparum* blood stages by the pseudilin-type inhibitors most probably involves additional molecular targets other than IspD. We thus next investigated the inhibition mechanism of pseudilin derivatives causing the differences in IspD binding among species at the atomic level.

**Table 5.1**  $IC_{50}$  values of compounds **4a-e**, measured in the photometric assay against *AthIspD* and *PvlspD* with different concentrations of metal ions, and cell-based  $EC_{50}$  values against *P. falciparum*.

Ligand				$IC_{50}$ <i>AthIspD</i> <sup>[a]</sup> [ $\mu$ M]		$IC_{50}$ <i>PvlspD</i> <sup>[a]</sup> [ $\mu$ M]		$EC_{50}$ <i>Pf</i> cell <sup>[c]</sup> [ $\mu$ M]
	R <sup>1</sup>	R <sup>2</sup>	R <sup>3</sup>	w/o metal	40 $\mu$ M Cd <sup>2+</sup>	w/o metal	40 $\mu$ M Cd <sup>2+</sup>	
<b>4a</b>	Br	Br	Br	13 $\pm$ 2	1.4 $\pm$ 0.2	48 $\pm$ 9	57 $\pm$ 12	1.27
<b>4b</b>	Cl	Cl	Br	12 $\pm$ 1	2.2 $\pm$ 0.2	56 $\pm$ 8	41 $\pm$ 7	1.07
<b>4c</b>	Cl	Cl	Cl	19 $\pm$ 2	4.3 $\pm$ 0.8	46 $\pm$ 6	40 $\pm$ 7	n.d.
<b>4d</b>	F	F	Br	79 $\pm$ 6	13 $\pm$ 2	64 $\pm$ 15	51 $\pm$ 15	n.d.
<b>4e</b>	H	Br	Br	52 $\pm$ 6	19 $\pm$ 2	36 $\pm$ 10	24 $\pm$ 6	11.72

<sup>[a]</sup>Data sets have been treated with the program Dynafit<sup>[32]</sup> in order to calculate  $IC_{50}$  values. Values are the mean of three  $IC_{50}$  values obtained from independent measurements.

<sup>[b]</sup>*In vitro* activity on *P. falciparum* NF54 strain. Mean values of three independent experiments. n.d., not determined.

#### 5.4.2 Crystallization of *AthIspD* apo and in complex with ligands

We started the crystallographic work with the determination of the *AthIspD* apo structure at 1.5 Å resolution (PDB code 4NAI). *AthIspD* is physiologically present as a homo-dimer, and the subunit interface is mainly assembled over a linker region that points out of each monomer (Figure 5.1a). Notably, oligomerization is important for binding of the cosubstrate (CTP) and thus, for enzyme activity. A comparison of the overall structures of *AthIspD* apo and *EclspD* in complex with the reaction product **2** (PDB code 1INI)<sup>[33]</sup> showed that the residues involved in dimer formation as well as amino acids that coordinate the diphosphate moiety of CTP are conserved among species (Figures 5.1b, 5.1d, 2SI, and 3SI). For clarity, only the *AthIspD* numbering is used to describe the amino acid residues here. At the active site of *EclspD*, Asp179 interacts with and stabilizes both substrate **1** and product **2**. Binding of **1** and CTP is facilitated by only minor structural rearrangements, as depicted in the structural superposition (Figures 5.1b and 5.1d). Remarkably, the comparison of *EclspD* and *AthIspD* revealed that Arg157 and Asp262, both H-bonded near the active site, match perfectly, although Asp262 is a glutamate in case of *EclspD*. However, there is a major difference between the prokaryotic and eukaryotic IspD homologs: in the *E. coli* structure, Arg157 interacts with both, Asp179 and Glu262, hereby

stabilizing the active site cavity to facilitate substrate binding and turnover, whereas in AthIspD, Asp179 differs in its orientation, thus indicating that this position is species-specific.

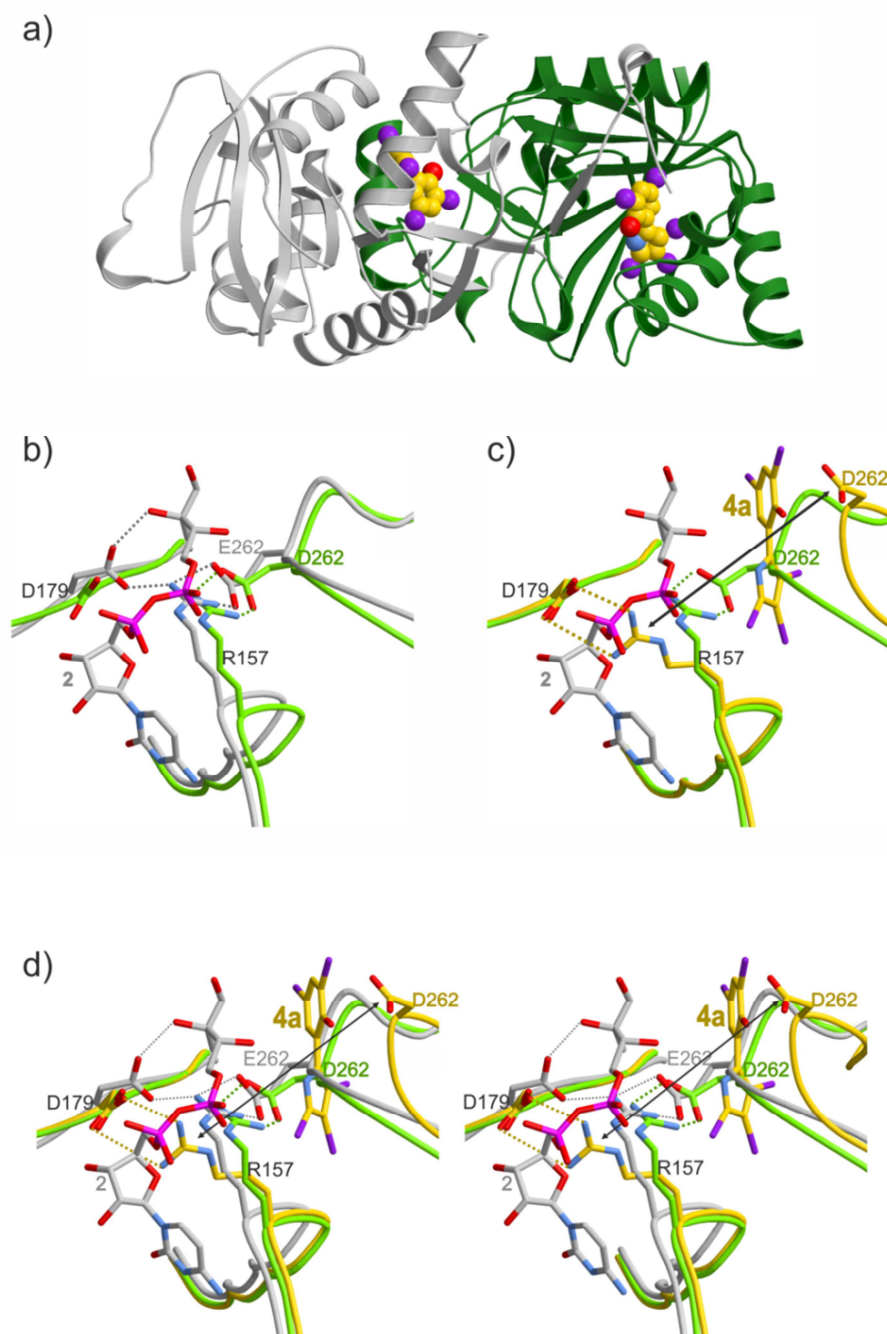


**Figure 5.1** a) Overall structure of the AthIspD dimer in complex with compound **4a** shown as secondary structure elements. **4a** is presented as balls and sticks. b) Structural superposition of the apo AthIspD structure (green) with the **2**:EclspD complex structure (gray; PDB code 1INI<sup>[33]</sup>). Interactions are indicated by dashed lines. Conserved amino acids are shown in black (AthIspD numbering), whereas the remaining residues are shown according to the color of the respective enzyme. c) Structural superposition of apo AthIspD with the **4a**:AthIspD complex structure (gold). Additionally, **2** from PDB code 1INI is presented in gray. d) Stereo view of the structural superposition of b) and c).

Next, we elucidated the crystal structures of *Ath*IspD in complex with **4a** (1.8 Å resolution, PDB code 4NAK), **4b** (1.8 Å resolution, PDB code 4NAL), and **4e** (1.8 Å resolution, PDB code 4NAN), resulting in well-defined electron density maps for each of the bound ligands (Figure 5.2). Interestingly, binding of the compounds occurs in a cavity located in close proximity to the active site and which is independent from the adjacent monomer. This pocket was already described in studies with azolopyrimidine-type inhibitors **3a-c**.<sup>[19]</sup> Nevertheless, the data presented here document a high degree of plasticity of this binding site, since the pseudilin derivatives differ in their molecular structure and mode of action compared to the azolopyrimidine ligands (Figure 5.3). With both, pseudilin- or azolopyrimidine-type inhibitors, there is a major conformational transition that affects predominantly amino acid residues Arg157 and Asp262. Notably, all reported crystal structures of apo IspD lack this characteristic cavity.<sup>[34-36]</sup> In the apo as well as the holo structures, Arg157 interacts with Asp262 and thereby keeps this ligand binding pocket locked. As shown in Figure 5.1c, binding of compound **4a** causes opening and hence accessibility into the cavity by major structural rearrangements. Asp262 becomes solvent exposed, and the interaction to Arg157 is abolished. Consequently, Arg157 moves into the CTP binding site, generating specific H-bonds with Asp179. This conformational twist prevents nucleotide binding by causing a clash with the ribose, and hence leads to enzyme inhibition. Thus, our results show that pseudilin derivatives act as allosteric inhibitors of IspD.



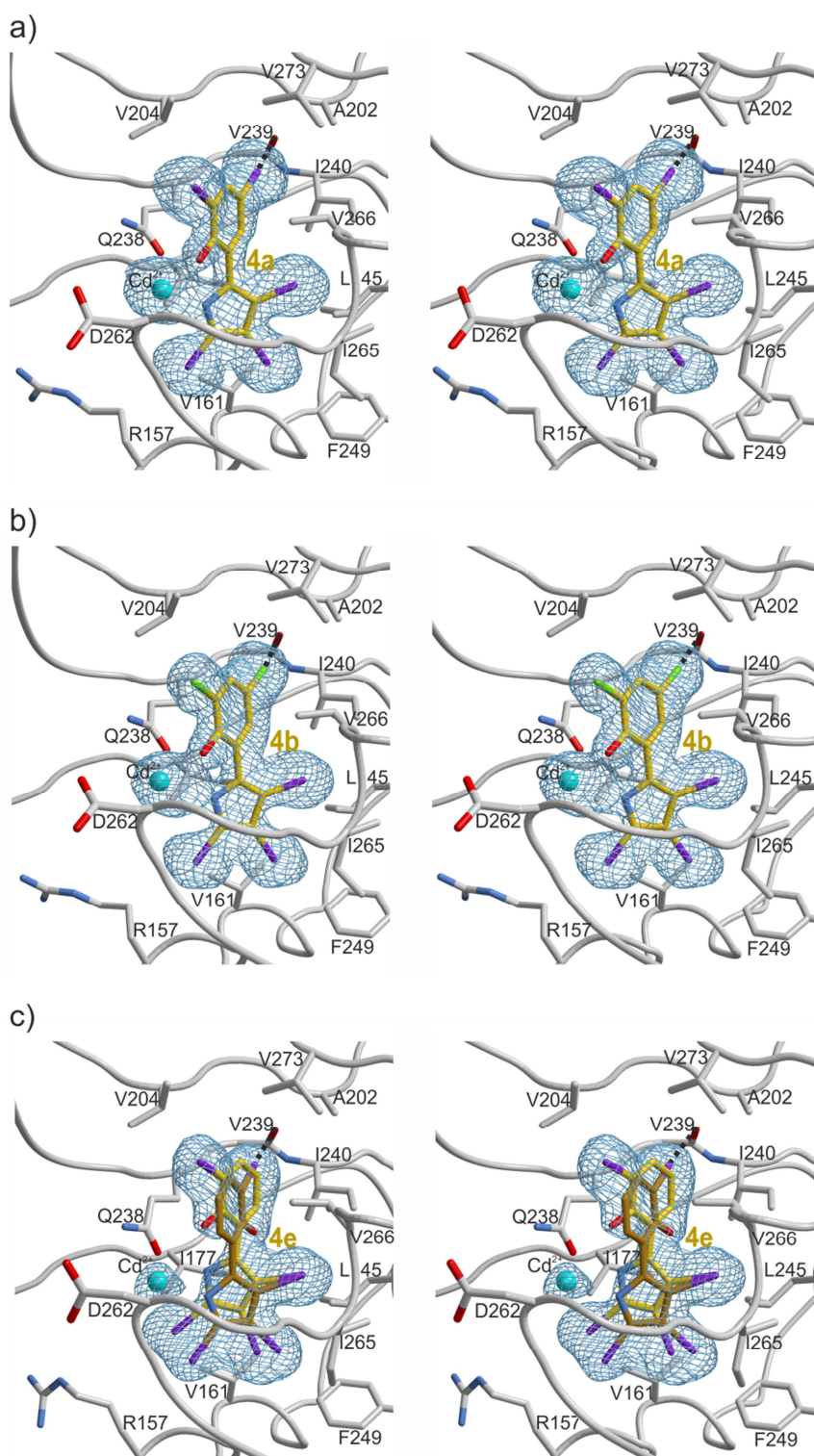


**Figure 5.2** Stereo view of the allosteric site of AthIspD in complex with a) compound **4a** (PDB code 4NAK, b) compound **4b** (PDB code 4NAL) and c) compound **4e** (PDB code 4NAN). **4e** is populated 7:3 as syn:anti-conformation. The  $2F_o - F_c$  electron density map (blue mesh) is contoured at  $1.0 \sigma$ . The ligand has been excluded prior phase calculation to avoid any model bias. The allosteric site residues and the ligands (gold) are presented as stick models,  $\text{Cd}^{2+}$  (cyan) is drawn as a sphere. The halogen bond between the ligand (bromine atom, purple; chlorine atom, green) and the backbone oxygen atom of Val239 is indicated as dashed line (for details on halogen bonding, see Figure 5.4). The orientation of the structure is according to Figure 5.1a.

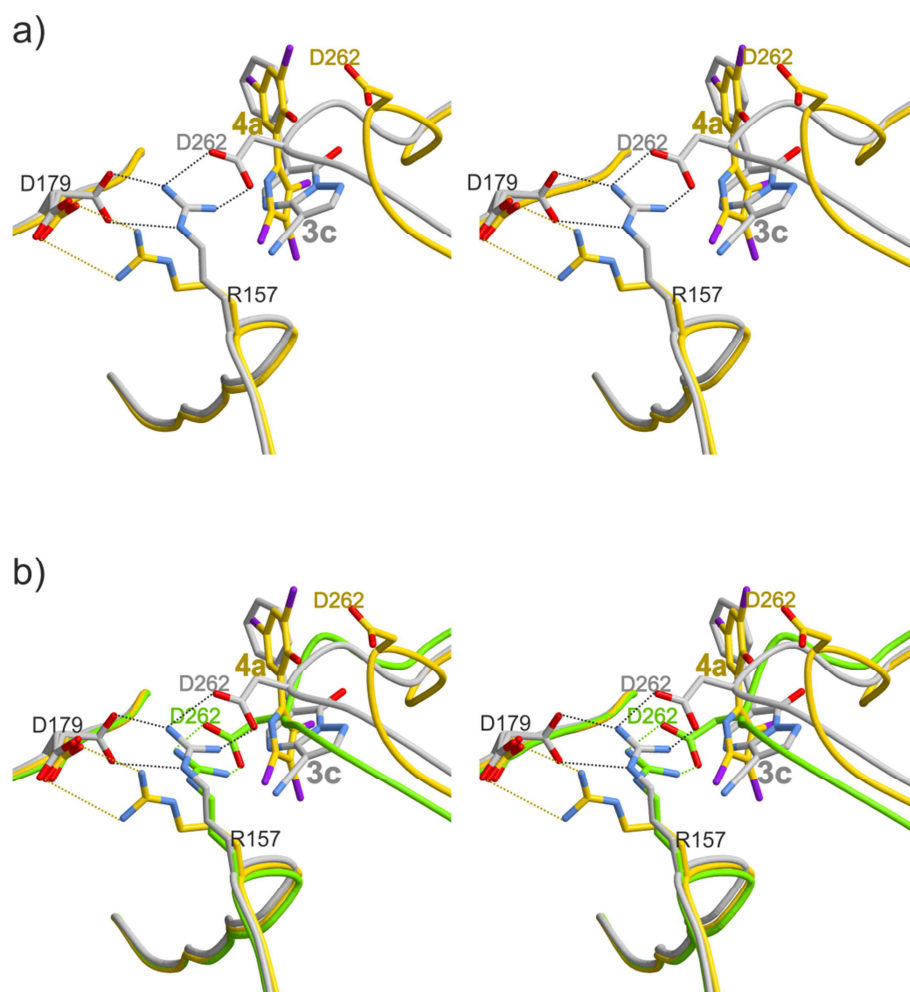


**Figure 5.3** a) Stereo view of the structural superposition of **4a**:AthlSpD (gold) with **3c**:AthlSpD (gray; PDB code 2YC5<sup>[19]</sup>). b) Stereo view of superposition of AthlSpD apo (green) with **4a**:AthlSpD and **3c**:AthlSpD. Interactions are indicated by dashed lines.

#### 5.4.3 Halogen bond interaction of the ligands with the enzyme backbone

The crystal structures of **4a** and **4b** in complex with AthlSpD reveal that the respective phenol and pyrrole rings of the ligands are in *syn*-conformation and are bound to a metal ion, which, based on the electron density map contour level and crystallization conditions, we propose corresponds to cadmium(II). Cd<sup>2+</sup> is tetrahedrally coordinated to the phenolic hydroxyl group and the pyrrole nitrogen of the inhibitors, the Gln238 side chain, and a water molecule with ion-to-ligand distances in the range of 2.2–3.7 Å (Figure 5.4). Besides this metal chelation, a chlorine and a bromine atom of the pseudilin derivatives (C–X) in the cocrystals of pseudilins **4a** and **4b** appear perfectly poised for halogen bonding with the backbone carbonyl oxygen of the enzyme (Val239; O–Y, Figure 5.4).<sup>[37–47]</sup> This interaction is characterized by the requirement for nearly collinear alignment of the halogen bond acceptor C–X with the halogen bond donor atom at sub-van der Waals distance, allowing the donor atom to orient its electron density into the  $\sigma$ -hole,

corresponding to the  $\sigma^*$ -orbital of the C-X bond. Typically, the distance between the halogen atom and the oxygen atom ( $X\cdots O$ ) is equal or less than the sum of their van der Waals radii<sup>[44-47]</sup> (3.27 Å for  $Cl\cdots O$ , 3.37 Å for  $Br\cdots O$ ), while the angles are  $\approx 165-180^\circ$  for  $C-X\cdots O$  and  $\approx 120^\circ$  for  $X\cdots O-Y$ .<sup>[44,48]</sup> The  $X\cdots O$  distance and the angles are 3.26 Å and  $164^\circ/112^\circ$  for compound **4a** and 3.25 Å and  $164^\circ/111^\circ$  for compound **4b**. The structural data thus show that halogen bonding with the enzyme adds to the metal ion coordination stabilization of the ligands, enhancing their inhibitory effect. We thus next determined the crystal structure of *Ath*IspD in complex with compound **4e** that lacks a halogen atom at the specific site in *para*-position to the phenolic OH. Interestingly, the X-ray data revealed that compound **4e** adopts two different conformations, 70% *syn* and 30% *anti* (Figures 5.2b, 5.4c), in the allosteric pocket of the enzyme. In the latter conformation, the molecule is unable to chelate with the phenolic OH-group to the  $Cd^{2+}$ , but with the *ortho*-bromine forms a halogen bond to the backbone oxygen of the protein ( $X\cdots O$  distance and angles 3.17 Å and  $170^\circ/113^\circ$ ). Additional van der Waals interactions ( $C\cdots C$  distances around 3.7 Å) between protein and pseudilin ligands are found in the four complexes, in particular van der Waals contacts below 4 Å with the amino acid side chains of Gln238 and Val266, which intercalate the phenolic ring of the ligand.

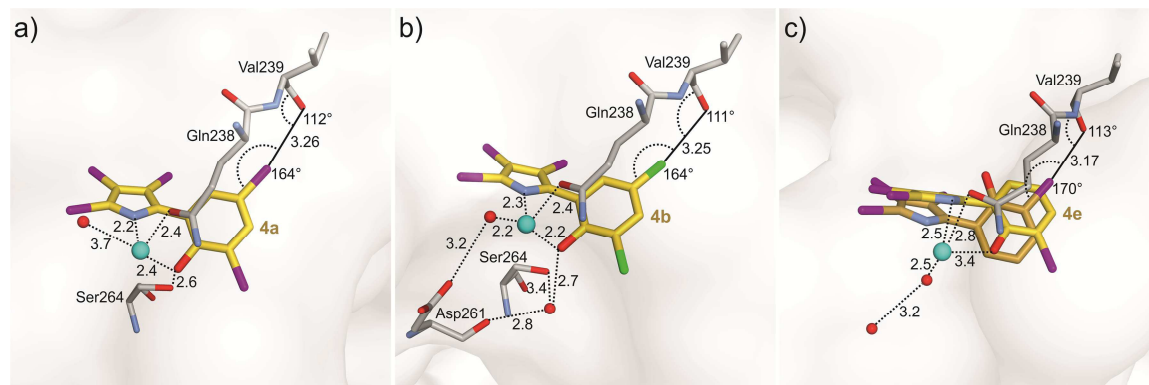


**Figure 5.4** Halogen bonding and metal ion interactions of compounds **4a**, **4b**, and **4e** (*syn*- and *anti*-conformation) with *Ath*IspD. Amino acid residues and compounds are presented as stick models, water (red) and  $Cd^{2+}$  as spheres (cyan). Distances are given in Å.

#### 5.4.4 Conclusion

As described in literature, there are other possible targets for pseudilin-type inhibitors: 12- and 15-lipoxygenases, nonspecific liver esterase, and myosin ATPases.<sup>[49]</sup> Since pseudilin derivatives may have more than one cellular target, it seems likely that the overall effect of this class of natural products on organisms can be highly dependent on the species, as shown e.g. by the altered  $IC_{50}$  values between the IspD enzyme of the plant *A. thaliana* and the protozoan *P. vivax*.

We consider the possibility that the IspD orthologs besides *A. thaliana* either lack the allosteric pocket or this loop region does not show the same flexibility compared to *AthIspD*. These questions have to be addressed by future mutational studies.

In conclusion, we demonstrate that halogenated marine alkaloids of the pseudilin-type bind into an allosteric pocket of *AthIspD*. They also inhibit *PvIspD* and are active against *P. falciparum* in cell-based assays. CTP binding by *AthIspD* is prevented by conformational changes, locking the catalytic active site. However, whether there also exists a common regulation of the non-mevalonate pathway at the allosteric site of IspD via endogenous feedback mechanisms still needs to be addressed. This site is exploited by the pseudilin derivatives, which block the formation of the essential precursors IPP and DMAPP for terpene biosynthesis. Since halogenated marine natural products are abundant,<sup>[50-52]</sup> their halogen atoms should be further investigated in biostructural work on different targets for active participation in the molecular recognition processes such as halogen bonding.

## 5.5 Experimental section

### 5.5.1 *In vitro* antimalarial activity and cytotoxicity

*P. falciparum* NF54 strains were cultivated in a variation of the medium previously described,<sup>[2]</sup> consisting of RPMI-1640 supplemented with 0.5% ALBUMAX® II, 25 mM HEPES, 25 mM NaHCO<sub>3</sub> buffer (pH 7.3), 0.36 mM hypoxanthine, and 100 µg mL<sup>-1</sup> neomycin. Human erythrocytes served as host cells. Cultures were maintained in an atmosphere of 3% O<sub>2</sub>, 4% CO<sub>2</sub>, and 93% N<sub>2</sub> in humidified modular chambers at 37 °C. Compounds were dissolved in DMSO (10 mg mL<sup>-1</sup>), diluted in hypoxanthine-free culture medium and titrated in duplicates over a 64-fold range in 96 well plates. Infected erythrocytes (1.25% final hematocrit and 0.3% final parasitemia) were added into the wells. After 48 h incubation, 0.25 µCi of [3H]hypoxanthine was added and plates were incubated for an additional 24 h. Parasites were harvested onto glass-fiber filters, and radioactivity was counted using a betaplate liquid scintillation counter (Wallac; Zurich, Switzerland). The results were recorded and expressed as a percentage of the untreated controls. Fifty percent effective concentrations (EC<sub>50</sub>) were estimated by linear interpolation.<sup>[3]</sup>

### **Determination of cytotoxicity data with cultured mammalian cells**

Rat skeletal myoblasts (L-6 cells) were used to investigate the cytotoxicity of the inhibitors in an Alamar Blue assay with podophyllotoxin as positive control. L-6 cells in RPMI-1640 medium with 10% fetal calf serum and 2 mM L-glutamine were added to each well of a 96-well microtiter plate and incubated at 37 °C under a 5% CO<sub>2</sub> atmosphere for 24 h. Compounds were added directly into the wells and subsequently serial drug dilutions were prepared covering a range from 100–0.002 μM. The plates were incubated for another 72 h. 10 μL of Alamar Blue (12.5 mg resazurin in 100 mL H<sub>2</sub>O) were added to each well, and incubation continued for further 1–4 h. The plates were read with a Spectramax Gemini XS microplate fluorimeter (Molecular Devices Cooperation; Sunnyvale, USA) using an excitation wavelength of 536 nm and an emission wavelength of 588 nm. Data were analyzed using the software Softmax Pro (Molecular Devices Cooperation; Sunnyvale, USA). The decrease of fluorescence (= inhibition) was expressed as percentage of the fluorescence of control cultures and plotted against the drug concentrations. From the sigmoidal inhibition curves, the IC<sub>50</sub> values were calculated. Assays were run in duplicate and at least repeated once.

### **5.5.2 Herbicidal activity of pseudilins**

The herbicidal activity of pseudilins against algae (*Scenedesmus acutus*), water fern (*Azolla filiculoides*), duckweed (*Lemna paucicostata*), and corn (*Zea mays*) cell cultures (for compounds **4b** and **4e**), as well as soybean (*Glycine max*) cell culture (for compound **4a**) has already been published.<sup>[6]</sup> The three compounds showed moderate to high activity in the tested assays. All experimental details can be found in reference 6.

### **5.5.3 Cloning and gene expression of *AthlspD* protein**

The cloning and transformation of the recombinant *E. coli* expression strain M15[pREP4]pNCO113YgbP\_ATH followed established protocols.<sup>[53]</sup> The cells were grown at 37 °C in LB-medium supplemented with ampicillin (180 mg mL<sup>-1</sup>) and kanamycin (50 mg mL<sup>-1</sup>) to an optical density at 600 nm of 0.6-0.7. The gene expression was induced with 1 mM IPTG, and the cell suspension was cultivated overnight at 30 °C under shaking (130 rpm). The cells were harvested by centrifugation at 5,100 rpm, 4 °C, resuspended in 0.9% NaCl-solution, and once more centrifuged. The cells were stored at -20 °C until further use.

#### **5.5.4 Purification of the recombinant *AthlspD* protein**

To disrupt the cells, they were resuspended in loading buffer (50 mM Tris-HCl (pH 8.1), containing 1 mM DTT) and passed through a cell disruption device (Basic Z Model; Constant Systems Limited; Northhamptonshire, UK) and afterwards centrifuged at 9,600 rpm, 4 °C. The supernatant was subjected to an anion exchange (Q Sepharose Fast Flow®, GE Healthcare Europe GmbH; Freiburg, Germany) column (50 mL) that had been pre-equilibrated with loading buffer. The column was flushed with 50 mM Tris-HCl (pH 8.1), containing 200 mM KCl, and 1 mM DTT and then developed with 50 mM Tris-HCl (pH 8.1), containing 300-400 mM KCl, and 1 mM DTT. *AthlspD* was obtained with approximately 85% purity, as estimated by SDS-PAGE. The fractions were combined and dialyzed overnight at 4 °C against 50 mM Tris-HCl (pH 8.0), containing 100 mM KCl, and 1 mM DTT. The protein was concentrated in an Amicon stirred cell® (Merck Chemicals GmbH; Schwalbach, Germany), 200 mL, with an ultrafiltration disc with 10 kDa molecular weight cut off. To further purify the protein, it was applied on a gelfiltration column (Superdex® 75 26/60; GE Healthcare Europe GmbH; Freiburg, Germany) and developed with 50 mM HCl (pH 8.0), containing 100 mM KCl, and 1 mM DTT. The *AthlspD* was obtained with >95% purity. For crystallization, the DTT was removed and the salt concentration decreased by dialysis overnight at 4 °C against 50 mM Tris-HCl (pH 8.0), containing 50 mM KCl and then concentrated to 15 mg mL<sup>-1</sup> with the Amicon stirred cell.

#### **5.5.5 Crystallization of *AthlspD***

*AthlspD* protein (diluted to 10 mg mL<sup>-1</sup>; 50 mM Tris-HCl (pH 8.0), containing 50 mM KCl) crystallized overnight at 20 °C using the sitting drop diffusion vapor method, where 30 µL of protein solution were mixed with 20 µL of reservoir buffer containing 50 mM HEPES-HCl (pH 7.5), containing 50 mM CdSO<sub>4</sub>, and 800 mM KOAc. The triangular prisms achieved their final size after 2 weeks of growth (dimensions approximately 100 x 100 x 300 µm<sup>3</sup>).

#### **Soaking of *AthlspD* with ligands**

To obtain the complex structures of *AthlspD* with the ligands **4a**, **4b**, and **4e**, the native crystals were soaked with a saturated solution of the ligand for 36 h. For this purpose, the compounds were dissolved in DMSO at room temperature. This solution was added to the enzyme crystals to give a final concentration of 5 mM. The crystal was then passed through a solution containing

reservoir buffer and 25% glycerol as cryoprotectant and flash-frozen in a stream of nitrogen gas at 100 K (Oxford Cryosystems Ltd; Oxfordshire, UK).

### 5.5.6 X-ray structure determination

For the apo *AthIspD* as well as the complex structures **4a**:*AthIspD*, **4b**:*AthIspD*, and **4e**:*AthIspD*, native data sets at 1.5 Å, 1.8 Å, 1.8 Å, and 1.8 Å, respectively, were collected using the synchrotron radiation at the X06SA beamline, Swiss Light Source (SLS), Villigen, Switzerland. Data were processed using the program package XDS,<sup>[54]</sup> and data reduction was performed with XSCALE. For details, see Table 5.2. Crystal structure analysis was carried out by molecular replacement using coordinates of *AthIspD* deposited at the PDB with the code 2YC5.<sup>[19]</sup> The anisotropy of diffraction was corrected by TLS-refinement using the program REFMAC5.<sup>[55]</sup> Electron density was improved by averaging and back transforming the reflections ten times over the two-fold non-crystallographic symmetry axis using the programs MAIN and COOT.<sup>[56]</sup> Crystallographic rigid body, positional, and temperature factor refinements were calculated using REFMAC5. The model was completed using the interactive three-dimensional program MAIN.<sup>[57]</sup> The atomic coordinates for *AthIspD* apo and in complex with the compounds **4a**, **4b**, and **4e** have been deposited at the PDB, Research Collaboratory for Structural Bioinformatics at Rutgers University under the accession codes 4NAI, 4NAK, 4NAL, and 4NAN, respectively.

**Table 5.2** Data collection and refinement statistics.

	<i>AthlspD</i> apo	<b>4a:</b> <i>AthlspD</i>	<b>4b:</b> <i>AthlspD</i>	<b>4e:</b> <i>AthlspD</i>
<b>Crystal parameter</b>				
Space group	H32	H32	H32	H32
Cell dimensions	a=b=73.64 Å, c=224.39 Å, γ=120 °	a=b=75.24 Å, c=224.14 Å, γ=120 °	a=b=74.46 Å, c=224.50 Å, γ=120 °	a=b=75.12 Å, c=224.13 Å, γ=120 °
Molecules per AU <sup>[a]</sup>	1	1	1	1
<b>Data collection</b>				
Beam line	SLS, X06SA	SLS, X06SA	SLS, X06SA	SLS, X06SA
Wavelength (Å)	1.0	1.0	1.0	1.0
Resolution range (Å) <sup>[b]</sup>	30-1.5 (1.6-1.5)	30-1.8 (1.9-1.8)	30-1.8 (1.9-1.8)	30-1.8 (1.9-1.8)
Observed / unique <sup>[c]</sup> reflections	201855 / 37895	110381 / 22147	216742 / 22692	176814 / 22879
Completeness (%) <sup>[b]</sup>	99.7 (99.9)	95.8 (97.3)	99.9 (99.6)	99.2 (98.8)
$R_{\text{merge}}$ (%) <sup>[b,d]</sup>	3.9 (56.7)	4.2 (53.6)	4.2 (62.5)	4.3 (61.2)
$I/\sigma(I)$ <sup>[b]</sup>	23.0 (3.8)	19.5 (3.3)	27.7 (4.0)	26.3 (3.6)
<b>Refinement</b>				
Resolution (Å)	10-1.5	10-1.8	10-1.8	15-1.8
$R_{\text{work}} / R_{\text{free}}$ <sup>[e]</sup>	17.7 / 19.4	19.1 / 21.8	20.5 / 24.6	20.7 / 24.7
No. atoms	1858	1737	1757	1766
Protein	1681	1631	1661	1634
Ligand	0	17	17	32
DTT	0	8	8	8
Cd <sup>2+</sup> / K <sup>+</sup> / Cl <sup>-</sup>	3 / 11 / 0	5 / 6 / 0	5 / 7 / 0	4 / 6 / 1
Water	163	70	59	81
<i>B</i> -factors	27.6	45.5	46.8	45.5
R.m.s. deviations <sup>[f]</sup>				
Bond lengths (Å)	0.027	0.005	0.005	0.018
Bond angles (°)	2.66	1.05	1.06	2.32
Ramachandran (%) <sup>[g]</sup>	98.6 / 1.4 / 0.0	99.0 / 1.0 / 0.0	98.6 / 1.4 / 0.0	97.5 / 2.5 / 0.0
PDB accession code	4NAI	4NAK	4NAL	4NAN

<sup>[a]</sup>Asymmetric unit.

<sup>[b]</sup>Values in parenthesis of resolution range, completeness,  $R_{\text{merge}}$  and  $I/\sigma(I)$  correspond to the last resolution shell.

<sup>[c]</sup>Friedel pairs were treated as identical reflections.

<sup>[d]</sup> $R_{\text{merge}}(I) = \frac{\sum_{\text{hkl}} \sum_j |I(\text{hkl})_j - \langle I(\text{hkl}) \rangle|}{\sum_{\text{hkl}} I(\text{hkl})}$ , where  $I(\text{hkl})_j$  is the measurement of the intensity of reflection hkl and  $\langle I(\text{hkl}) \rangle$  is the average intensity.

<sup>[e]</sup> $R = \frac{\sum_{\text{hkl}} | |F_{\text{obs}}| - |F_{\text{calc}}| |}{\sum_{\text{hkl}} |F_{\text{obs}}|}$ , where  $R_{\text{free}}$  is calculated without a sigma cut off for a randomly chosen 5% of reflections, which were not used for structure refinement, and  $R_{\text{work}}$  is calculated for the remaining reflections.

<sup>[f]</sup>Deviations from ideal bond lengths / angles.

<sup>[g]</sup>Number of residues in favored region / allowed region / outlier region.



### 5.5.7 $IC_{50}$ determination

#### **Photometric activity assay**

Assays were conducted in 96-well Nunc plates (Sigma-Aldrich; St. Louis, USA) with a transparent flat bottom. Assay mixtures (total volume: 200  $\mu$ L) contained 100 mM Tris-HCl (pH 7.6), 25 mM KCl, 5 mM  $MgCl_2$ , 5 mM DTT, 0.6 mM NADH, 1 mM ATP, 1 mM phosphoenolpyruvic acid, 0.5 mM CTP, 0.1 U of pyruvate kinase (PK), 0.1 U of lactate dehydrogenase (LDH), 0.1 U IspE from *E. coli* and 0.002 U of *Ath*IspD protein.<sup>[22]</sup> Dilution series (1:3) of inhibitors approximately covered the concentration range of 200  $\mu$ M to 0.01  $\mu$ M. The reaction was started by addition of **1** in 100 mM Tris-HCl (pH 7.6), to a final concentration of 0.5 mM. The reaction was monitored photometrically (rt) at 340 nm in a plate reader (SpectraMax5; Molecular Dynamics, Sunnyvale, USA). Initial rate values were evaluated with a nonlinear regression method using the program Dynafit.<sup>[32]</sup> Representative data curves are shown in Figure 6SI.

#### **NMR based activity assay**

Reaction mixtures (total volume: 800  $\mu$ L) containing 100 mM Tris-HCl (pH 8.0), 25 mM KCl, 5 mM  $MgCl_2$ , 250  $\mu$ M [1,3,4- $^{13}C$ ]-**1**, 500  $\mu$ M CTP, 40  $\mu$ M  $CdSO_4$ , 20 nM inorganic diphosphatase, 50 nM *Ath*IspD and varying concentrations of compounds **4a** and **4e**, respectively, were incubated at 30 °C for 1 h under shaking (900 rpm).<sup>[22]</sup> The reaction was stopped by addition of 10 mM EDTA. Samples were centrifuged at 13,000 rpm,  $D_2O$  was added to a final concentration of 10% (v/v).  $^1H$ -decoupled  $^{31}P$  NMR spectra were recorded using a Bruker AVANCE III 500 MHz spectrometer (Bruker; Billerica, USA) equipped with a cryo platform and a direct QNP ( $^{13}C/^{19}F/^{29}Si/^{31}P$ ) probe. The pulse width for  $^{31}P$  was 30°, the number of scans was 500. Prior to Fourier transformation, the FID was multiplied with a mild Gaussian function (lb=-1; gb=0.1). The phase and baseline were carefully corrected, and the  $^{31}P$  signals of [1,3,4- $^{13}C$ ]-**1** at 4.13 ppm and of inorganic phosphate at 2.33 ppm were integrated (Figure 5.5). Initial rate values of the conversion of **1** to  $P_i$  were evaluated with a nonlinear regression method using the program GraphPad Prism.<sup>[58]</sup>

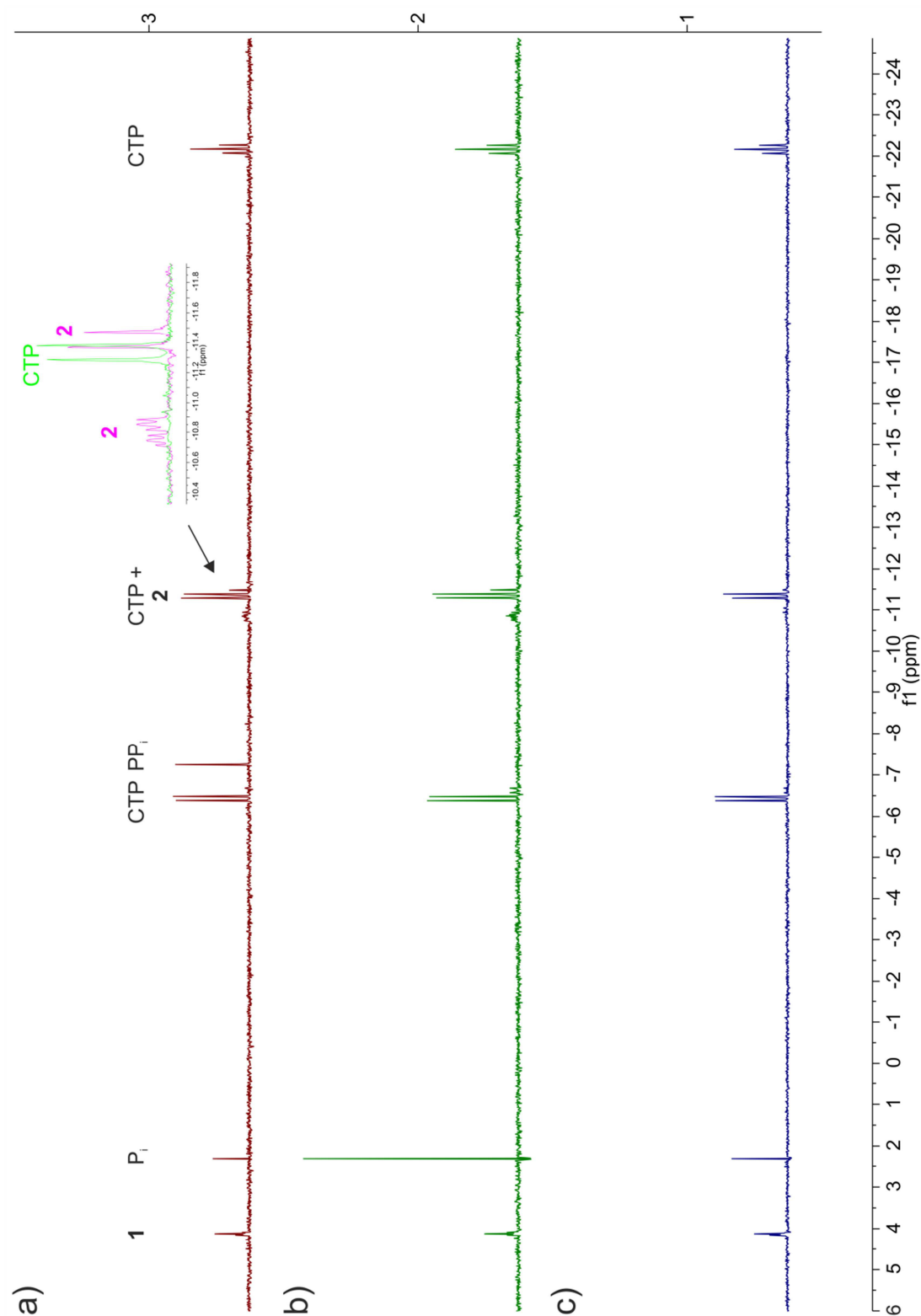


**Figure 5.5** Representative  $^1\text{H}$ -decoupled  $^{31}\text{P}$ -NMR assays of the IspD reaction. a) Assay with 1  $\mu\text{M}$  AthIspD without  $\text{CdSO}_4$  and diphosphatase: 18% turnover of MEP to  $\text{P}_i$ . b) Assay with 50 nM AthIspD including 40  $\mu\text{M}$   $\text{CdSO}_4$ , and 20 nM diphosphatase: 61% turnover.  $\text{PP}_i$  is completely converted to  $\text{P}_i$ . c) Assay with 50 nM AthIspD including 10  $\mu\text{M}$  **4b**, 40  $\mu\text{M}$   $\text{CdSO}_4$ , and 20 nM diphosphatase: 26% turnover.

### 5.5.8 Supporting Information

The Supporting Information, and the full article are available under DOI: 10.1002/anie.201309557 (English version) and 10.1002/ange.201309557 (German version).

### 5.6 References

- (1) Y. V. Ershov, *Appl. Biochem. Microbiol.* **2007**, *43*, 115-138.
- (2) P. Gao, Y. Yang, C. Xiao, Y. Liu, M. Gan, Y. Guan, X. Hao, J. Meng, S. Zhou, X. Chen, J. Cui, *Eur. J. Pharmacol.* **2012**, *694*, 45-52.
- (3) C. J. L. Murray, L. C. Rosenfeld, S. S. Lim, K. G. Andrews, K. J. Foreman, D. Haring, N. Fullman, M. Naghavi, R. Lozano, A. D. Lopez, *Lancet* **2012**, *379*, 413-431.
- (4) I. Abubakar, M. Zignol, D. Falzon, M. Raviglione, L. Ditiu, S. Masham, L. Adetifa, N. Ford, H. Cox, S. D. Lawn, B. J. Marais, T. D. McHugh, P. Mwaba, M. Bates, M. Lipman, L. Zijenah, S. Logan, R. McNerney, A. Zumla, K. Sarda, P. Nahid, M. Hoelscher, M. Pletschette, Z. A. Memish, P. Kim, R. Hafner, S. Cole, G. B. Migliori, M. Maeurer, M. Schito, A. Zumla, *Lancet Infect. Dis.* **2013**, *13*, 529-539.
- (5) A. Zumla, P. Nahid, S. T. Cole, *Nat. Rev. Drug Discovery* **2013**, *12*, 388-404.
- (6) M. Witschel, M. Rottmann, M. Kaiser, R. Brun, *PLoS Neglected Trop. Dis.* **2012**, *6*, e1805.
- (7) N. Qureshi, J. W. Porter, in *Biosynthesis of Isoprenoid Compounds*; J. W. Porter & S. L. Spurgeon: John Wiley & Sons, New York, **1981**; Vol. 1.
- (8) K. Bloch, *Steroids* **1992**, *57*, 378-383.
- (9) T. J. Bach, *Lipids* **1995**, *30*, 191-202.
- (10) M. Rohmer, *Nat. Prod. Rep.* **1999**, *16*, 565-574.
- (11) M. Rodriguez-Concepcion, A. Boronat, *Plant Physiol.* **2002**, *130*, 1079-1089.
- (12) W. Eisenreich, A. Bacher, D. Arigoni, F. Rohdich, *Cell. Mol. Life Sci.* **2004**, *61*, 1401-1426.
- (13) F. Rohdich, S. Lauw, J. Kaiser, R. Feicht, P. Koehler, A. Bacher, W. Eisenreich, *FEBS J.* **2006**, *273*, 4446-4458.
- (14) T. Masini, B. S. Kroezen, A. K. Hirsch, *Drug Discovery Today* **2013**, 1-7.
- (15) P. Mombelli, M. C. Witschel, A. W. van Zijl, J. G. Geist, M. Rottmann, C. Freymond, F. Roehl, M. Kaiser, V. Illarionova, M. Fischer, I. Siepe, W. B. Schweizer, R. Brun, F. Diederich, *ChemMedChem* **2012**, *7*, 151-158.

- (16) N. Scherr, K. Roeltgen, M. Witschel, G. Pluschke, *Antimicrob. Agents Chemother.* **2012**, *56*, 6410-6413.
- (17) Y. Matsue, H. Mizuno, T. Tomita, T. Asami, M. Nishiyama, T. Kuzuyama, *J. Antibiot.* **2010**, *63*, 583-588.
- (18) H. Jomaa, J. Wiesner, S. Sanderbrand, B. Altincicek, C. Weidemeyer, M. Hintz, I. Turbachova, M. Eberl, J. Zeidler, H. K. Lichtenthaler, D. Soldati, E. Beck, *Science* **1999**, *285*, 1573-1576.
- (19) M. C. Witschel, H. W. Höffken, M. Seet, L. Parra, T. Mietzner, F. Thater, R. Niggeweg, F. Roehl, B. Illarionov, F. Rohdich, J. Kaiser, M. Fischer, A. Bacher, F. Diederich, *Angew. Chem., Int. Ed.* **2011**, *50*, 7931-7935; *Angew. Chem.* **2011**, *123*, 8077-8081.
- (20) P. R. Burkhold, R. M. Pfister, F. H. Leitz, *Appl. Microbiol.* **1966**, *14*, 649-653.
- (21) R. J. Andersen, M. S. Wolfe, D. J. Faulkner, *Mar. Biol.* **1974**, *27*, 281-285.
- (22) V. Illarionova, J. Kaiser, E. Ostrozhenkova, A. Bacher, M. Fischer, W. Eisenreich, F. Rohdich, *J. Org. Chem.* **2006**, *71*, 8824-8834.
- (23) M. Witschel, F. Roehl, R. Niggeweg, T. Newton, *Pest Manage. Sci.* **2013**, *69*, 559-563.
- (24) H. Pudleiner, H. Laatsch, *Liebigs Ann. Chem.* **1990**, 423-432.
- (25) D. R. Baker, J. G. Fenyes, J. J. Steffens, *ACS Symp. Ser.* **1992**, *504*, 1-7.
- (26) H. Laatsch, B. Renneberg, U. Hanefeld, M. Kellner, H. Pudleiner, G. Hamprecht, H. P. Kraemer, H. Anke, *Chem. Pharm. Bull.* **1995**, *43*, 537-546.
- (27) R. Martin, A. Jaeger, M. Boehl, S. Richter, R. Fedorov, D. J. Manstein, H. O. Gutzeit, H.-J. Knoelker, *Angew. Chem., Int. Ed.* **2009**, *48*, 8042-8046; *Angew. Chem.* **2009**, *121*, 8186-8190.
- (28) M. Preller, K. Chinthalapudi, R. Martin, H.-J. Knoelker, D. J. Manstein, *J. Med. Chem.* **2011**, *54*, 3675-3685.
- (29) E. Yeh, J. L. DeRisi, *PloS Biol.* **2011**, *9*, e1001138.
- (30) Since *P. falciparum* IspD cannot be expressed in an active form, *PvIspD*, the causative agent of malaria tertiana, was used. Both genes were codon optimized.
- (31) M. Fischer, to be published elsewhere.
- (32) P. Kuzmic, *Anal. Biochem.* **1996**, *237*, 260-273.
- (33) S. B. Richard, M. E. Bowman, W. Kwiatkowski, I. Kang, C. Chow, A. M. Lillo, D. E. Cane, J. P. Noel, *Nat. Struct. Biol.* **2001**, *8*, 641-648.
- (34) L. E. Kemp, C. S. Bond, W. N. Hunter, *Acta Crystallogr., Sect. D: Biol. Crystallogr.* **2003**, *59*, 607-610.

- (35) J. Badger, J. M. Sauder, J. M. Adams, S. Antonysamy, K. Bain, M. G. Bergseid, S. G. Buchanan, M. D. Buchanan, Y. Batiyenko, J. A. Christopher, S. Emtage, A. Eroshkina, I. Feil, E. B. Furlong, K. S. Gajiwala, X. Gao, D. He, J. Hendle, A. Huber, K. Hoda, P. Kearins, C. Kissinger, B. Laubert, H. A. Lewis, J. Lin, K. Loomis, D. Lorimer, G. Louie, M. Maletic, C. D. Marsh, I. Miller, J. Molinari, H. J. Müller-Dieckmann, J. M. Newman, B. W. Noland, B. Pagarigan, F. Park, T. S. Peat, K. W. Post, S. Radojicic, A. Ramos, R. Romero, M. E. Rutter, W. E. Sanderson, K. D. Schwinn, J. Tresser, J. Winhoven, T. A. Wright, L. Wu, J. Xu, T. J. R. Harris, *Proteins: Struct. Funct. Bioinf.* **2005**, *60*, 787-796.
- (36) J. Behnen, H. Koester, G. Neudert, T. Craan, A. Heine, G. Klebe, *ChemMedChem* **2012**, *7*, 248-261.
- (37) O. Hassel, *Science* **1970**, *170*, 497-502.
- (38) P. Politzer, P. Lane, M. C. Concha, Y. Ma, J. S. Murray, *J. Mol. Model.* **2007**, *13*, 305-311.
- (39) T. Clark, M. Hennemann, J. S. Murray, P. Politzer, *J. Mol. Model.* **2007**, *13*, 291-296.
- (40) P. Metrangolo, F. Meyer, T. Pilati, G. Resnati, G. Terraneo, *Angew. Chem., Int. Ed.* **2008**, *47*, 6114-6127; *Angew. Chem.* **2008**, *120*, 6206-6220.
- (41) J. S. Murray, P. Lane, P. Politzer, *J. Mol. Model.* **2009**, *15*, 723-729.
- (42) Y. Lu, Y. Wang, W. Zhu, *Phys. Chem. Chem. Phys.* **2010**, *12*, 4543-4551.
- (43) T. M. Beale, M. G. Chudzinski, M. G. Sarwar, M. S. Taylor, *Chem. Soc. Rev.* **2013**, *42*, 1667-1680.
- (44) P. Auffinger, F. A. Hays, E. Westhof, P. S. Ho, *Proc. Natl. Acad. Sci. USA* **2004**, *101*, 16789-16794.
- (45) Y. Lu, T. Shi, Y. Wang, H. Yang, X. Yan, X. Luo, H. Jiang, W. Zhu, *J. Med. Chem.* **2009**, *52*, 2854-2862.
- (46) L. A. Hardegger, B. Kuhn, B. Spinnler, L. Anselm, R. Ecabert, M. Stihle, B. Gsell, R. Thoma, J. Diez, J. Benz, J.-M. Plancher, G. Hartmann, D. W. Banner, W. Haap, F. Diederich, *Angew. Chem., Int. Ed.* **2011**, *50*, 314-318; *Angew. Chem.* **2011**, *123*, 329-334.
- (47) L. A. Hardegger, B. Kuhn, B. Spinnler, L. Anselm, R. Ecabert, M. Stihle, B. Gsell, R. Thoma, J. Diez, J. Benz, J.-M. Plancher, G. Hartmann, Y. Isshiki, K. Morikami, N. Shimma, W. Haap, D. W. Banner, F. Diederich, *ChemMedChem* **2011**, *6*, 2048-2054.
- (48) A. Bondi, *J. Phys. Chem.* **1964**, *68*, 441-451.
- (49) B. Zhang, K. M. Watts, D. Hodge, L. M. Kemp, D. A. Hunstad, L. M. Hicks, A. R. Odoms, *Biochemistry* **2011**, *50*, 3570-3577.
- (50) M. T. Cabrita, C. Vale, A. P. Rauter, *Mar. Drugs* **2010**, *8*, 2301-2317.
- (51) T. S. Elliott, A. Slowey, Y. Ye, S. J. Conway, *MedChemComm* **2012**, *3*, 735-751.

- (52) G. W. Gribble, *In the Alkaloids*; Academic Press, Oxford, **2012**; Vol. 71.
- (53) F. Rohdich, J. Wungsintaweekul, M. Fellermeier, S. Sagner, S. Herz, K. Kis, W. Eisenreich, A. Bacher, M. H. Zenk, *Proc. Natl. Acad. Sci. USA* **1999**, *96*, 11758-11763.
- (54) W. Kabsch, *J. Appl. Crystallogr.* **1993**, *26*, 795-800.
- (55) G. N. Murshudov, A. A. Vagin, E. J. Dodson, *Acta Crystallogr., Sect. D: Biol. Crystallogr.* **1997**, *53*, 240-255.
- (56) P. Emsley, K. Cowtan, *Acta Crystallogr., Sect. D: Biol. Crystallogr.* **2004**, *60*, 2126-2132.
- (57) D. Turk, *PhD thesis*, Technische Universität München (Germany), **1992**.
- (58) H. Motulsky, A. Christopoulos, *Fitting Models to Biological Data using Linear and Nonlinear Regression. A Practical Guide to Curve Fitting.*; Oxford University Press, New York, **2004**.

## 6 ACKNOWLEDGMENTS

This thesis was realized at the Chair of Biochemistry at the Technische Universität München from December 2009 until December 2013.

Special thanks go to:

Prof. Dr. Michael Groll for the challenging projects and the possibility to perform my experimental studies in his group. Especially, I want to thank him for the introduction in crystallography and his enthusiasm in my projects.

Prof. Dr. Adelbert Bacher for the absolute support during the whole time of my thesis.

Prof. Dr. Thomas Kurz from the Heinrich-Heine Universität in Düsseldorf and his group members for the cooperation in the IspC project. Especially, many thanks go to Dr. Christoph T. Behrendt, Dr. Karin Brücher and Claudia Lienau for the pleasant teamwork.

Prof. Dr. François Diederich from the Eidgenössische Technische Hochschule in Zurich and his group members for the cooperation in the IspD project. Many thanks go to Dr. Michael Seet and Michael Harder for fun times at the group meetings.

Dr. Matthias Witschel and Dr. Wolfgang Höffken from the BASF SE in Ludwigshafen for the cooperation in the IspD project.

Prof. Dr. Markus Fischer from the Universität Hamburg and his group members for the cooperation in IspC and IspD projects. Especially, I would like to mention *in memoriam* Dr. Viktoriya Illarionova, Dr. Boris Illarionov and Dr. Tobias Gräwert.

Prof. Dr. Wolfgang Eisenreich and his group members for the introduction and support in NMR measurements. Especially, I want to thank Christine Schwarz.

Dr. Sabine Schneider for the support in crystallographic questions.

The members of the Groll group for a nice working environment. Especially, I want to thank the technicians Richard Feicht, Katrin Gärtner, Christoph Graßberger, Birgit Lange, Fritz Wendling and the secretary Ute Kashoa for their support and friendly help all the time.

All further cooperation partners not mentioned above.

Prof. Dr. Adelbert Bacher and Felix Quitterer for proofreading my thesis. Dr. Sebastian Walter for the help with the bureaucracy of cumulative dissertation writing.

My friends Veronika Flügel, Dr. Nerea Gallastegui, Dr. Nadine Gillmaier, Dr. Stephanie Grubmüller, Sabrina Harteis, Astrid König, Dr. Anja Löns, Dr. Ingrid Span, and Dr. Ursula Zinth.

Family Quitterer for being all ears for me and always giving me a place to recover.

My major gratitude goes to my parents Esther und Matheus, my sister Sandra and her family and Felix for their love and support. *Danka, dass iar nia ufghört hend an mi z'glauba...*